THE EFFECT OF SALINITY ON THE CONCENTRATIONS OF RADIUM AND THORIUM IN SEDIMENTS

Gary J. Hancock (BSc, University of Adelaide)

A thesis submitted for the degree of Master of Science of the Australian National University

Department of Geology

October 1993

Except where due acknowledgement is given, the contents of this thesis is all my own work.

Gary J. Hancock

Abstract

The effect of salinity on the sorption behaviour of radium and thorium has been studied with the aim of assessing the suitability of the $^{226}Ra/^{232}Th$ activity ratio (AR) as a tracer in saline waters. Radium has been reported in the literature as being highly mobile in saline water, and easily desorbed from sediments, whereas thorium is believed to remain tightly bound. Results of analyses of bed sediments from an inland river system with a record of past regimes of high dissolved salt concentrations were consistent with this behaviour. Radium-226 activity in the bed sediments was shown to be deficient with respect to its parent, ^{230}Th, indicating a loss of radium from the sediments.

A more detailed field study examined the extent of radium loss as a function of salinity in an estuary. Desorption of ^{226}Ra from freshwater suspended sediment increased to a maximum value (58% ±7 of the total sediment concentration) as the salinity of the estuary rose. Maximum radium desorption was reached in the 6-10 ppt salinity range. Net desorption then remained unchanged despite further rises in salinity.

Laboratory experiments indicated that the kinetics of radium desorption is rapid, with maximum desorption from river sediments reached within 1 h of contact with saline water. The net radium loss from freshwater sediment occurs as a result of the competition effects from other dissolved cations for ion-exchange sites on the sediment. Cation exchange is probably the dominant mechanism of radium release, although alpha recoil appears to be at least partly responsible for the higher losses of ^{224}Ra and ^{223}Ra by increasing their accessibility for ion-exchange reactions.

The effects of solid/liquid ratio and particle size of the sediment on radium sorption in saline water were also investigated. The results indicate that, when exposed to saline water, the greatest radium loss from freshwater sediments will occur from clay sized particles when they are present in the water column at low concentrations. Proportionally less radium is desorbed from coarse-grained bed sediments.

There was no evidence of any net loss of thorium from sediment as salinity is increased. In fact, laboratory experiments indicate that the transfer of dissolved or colloidal thorium onto sediment particles is enhanced in saline water. From the differing sorption behaviour of radium and thorium it is concluded that the $^{226}Ra/^{232}Th$ AR is not a suitable sediment tracer in saline water. However, the $^{230}Th/^{232}Th$ AR can provide a stable tracer of sediment movement in estuaries and is the preferred sediment tracer in saline rivers. In some circumstances the $^{228}Ra/^{226}Ra$ AR may also be useful.

The dissolved concentrations of all radium isotopes show strongly non-conservative increases in the Bega estuary. The shorter-lived isotopes, ^{224}Ra, ^{223}Ra and ^{228}Ra are particularly highly enriched. The most likely source of these isotopes is the pore water of bottom sediments. This work has shown that radium isotopes may give information on the rates and extent of surface-pore water mixing in an estuary.

Acknowledgements

I acknowledge the support given by CSIRO Division of Water Resources in terms of time and facilities.

I would like to thank my supervisors, Dr. A. Eggleton (Australian National University) and Dr. G. Taylor (University of Canberra) for their assistance throughout the study.

My colleagues at CSIRO, particularly Jon Olley and Dr. A. Murray provided constructive criticism of the work. Andrew Murray requires special thanks for suggesting the subject of research for this thesis, and for his willingness to provide helpful advice and ideas on the interpretation of the results.

Other staff at CSIRO also provided analytical support and help in the field. Rob Sageman performed AAS analyses and CEC determinations. Peter Wallbrink helped with gamma spectroscopy. Graeme Chiles aided with sample collection at the Loddon River region, and Gary Caitcheon operated the echo-sounder in the Bega River. Technical support was provided at the A.N.U. department of Geology by Robin Westcott, who performed XRD analyses.

Finally, I would like to thank my wife, Tricia, for her tolerance and support over the last two years.

Contents

1. Introduction 1
1.1 Uranium and Thorium Decay Series 1
1.2 Radionuclides as Sediment Tracers 2
1.3 Thesis Aims and Structure 3

2. Literature Review 4
2.1 Thorium Chemistry 4
2.2 Radium Chemistry 5
2.3 The Partitioning of Radium and Thorium Between Solid and Solution 6
2.4 Laboratory Sorption Studies 7
2.5 Estuarine Studies 11
2.6 Summary 13

3. Analytical Techniques 15
3.1 Alpha Spectrometry 15
3.2 Gamma Spectrometry 17
3.3 Liquid Scintillation 18
3.4 Atomic Adsorption Spectrophotometry 19
3.5 Sedimentation Analysis 19
3.6 Cation Exchange Capacity 20
3.7 X-Ray Diffraction Analysis 20

4. Sediment Tracing in a Saline Inland River System 21
4.1 The Loddon River-Barr Creek Confluence 21
4.2 Methods 22
4.3 Results and Discussion 22

5. The Behaviour of Radium and Thorium in an Estuary 28
5.1 Introduction 28
5.2 The Bega River Catchment 30
5.3 Sample Collection and Analyses 32
5.4 Water Quality Parameters 34
5.5 Dissolved Radionuclides 38
5.6 Radionuclides in Suspended Sediment 40
5.7 Bottom Sediments 50
5.8 Sources of Dissolved Radium to the Water Column 54
5.9 Summary 59

6. Laboratory Experiments 61
6.1 Introduction 61
6.2 Methods 63
6.3 Adsorption Experiments - Results and Discussion 67
6.4 Desorption Experiments - Results and Discussion 72
6.5 The Effect of Solid/Liquid Ratio 79
6.6 The Fraction of Sediment-bound Radium Available for Exchange 80
6.7 Summary 83

7. Discussion and Conclusions 85
7.1 The Behaviour of Thorium in Saline Water 85
7.2 The Behaviour of Radium in Saline Water 85
7.3 Other Factors Influencing Radium Desorption 87
7.4 Implications for Sediment Tracing 90
7.5 Radium Isotopes as Tracers of Water Movement in an Estuary 91
7.6 Conclusions 92

8. References 93

List of Figures

1.1 The ^{238}U decay series 2

1.2 The ^{232}Th decay series 2

3.1 A typical thorium alpha-particle spectrum (sediment sample). 17

3.2 (a) Count rate as a function of ^{226}Ra activity and (b) its deviation from linearity. 20

3.3 The effect of salinity on the ^{226}Ra count rate. 20

4.1 The Loddon-Barr Creek confluence, showing the location of sampling sites. 22

5.1 The Bega River catchment. 31

5.2 The Bega River estuary, showing the location of sampling sites. 31

5.3 A depth profile of the Bega River estuary. 32

5.4 Dissolved silicon and salinity in the Bega River estuary. 37

5.5 Dissolved ^{226}Ra concentrations as a function of salinity in the Bega River estuary. 37

5.6 Estuarine suspended sediment concentrations of ^{232}Th as a function of salinity. 44

5.7 The $^{230}Th/^{232}Th$ activity ratio of suspended sediment plotted against salinity. 44

5.8 The suspended sediment $^{228}Th/^{232}Th$ activity ratio and salinity (November data only). 44

5.9 The suspended sediment $^{226}Ra/^{232}Th$ activity ratio and salinity. 46

5.10 The $^{228}Ra/^{226}Ra$ activity ratio and salinity. 46

5.11 The dissolved concentrations of all radium isotopes. 57

5.12 The dissolved $^{228}Ra/^{226}Ra$ activity ratio of samples collected in September and November 1991. 59

5.13 The dissolved $^{224}Ra/^{223}Ra$ activity ratio of surface water samples collected in November 1991. 59

List of Figures (contd.)

6.1 ^{228}Th distribution coefficient (K_d) as a function of salinity in adsorption experiments. 69

6.2 Radium distribution coefficient (K_d) as a function of salinity in adsorption experiments. 71

6.3 (a) Ra_F (see section 6.3.3) as a function of salinity. (b) An expansion of (a). 71

6.4 Desorption of radium isotopes and their activity ratios as a function of time. 74

6.5 Desorption of radium isotopes and their activity ratios as a function of salinity. 77

6.6 The desorption of ^{226}Ra as a function of salinity from two different size fractions of Bega River sediment. 77

6.7 ^{226}Ra desorption (%) at 7 ppt salinity from <63 μm Bega River sediment plotted against the inverse of sediment concentration. 81

6.8 The effect of repeated leaching on the % ^{226}Ra desorbed from <63μm Bega River sediment. 81

7.1 An expansion of Figure 5.9, illustrating the approximate linearity between the $^{226}Ra/^{232}Th$ activity ratio and salinity in the salinity range 0.2-4.4 ppt. 88

List of Tables

4.1 Flow, conductivity and suspended sediment data for the Loddon River and Barr Creek on the date of sample collection. 23

4.2 Thorium and radium isotope concentrations of suspended sediment and bed sediment samples collected from the Loddon River and Barr creek. 25

5.1 Water quality parameters of water samples collected from the Bega River estuary. 35

5.2 Dissolved cation and anion concentrations in the Bega River estuary. 35

5.3 Dissolved thorium concentrations in the Bega River estuary. 38

5.4 Dissolved radium isotope concentrations and activity ratios in the Bega River estuary. 41

5.5 Thorium and radium isotope concentrations and activity ratios in CFC sediments, Bega River. 42

5.6 Comparison of thorium and radium isotope concentrations and activity ratios in particulates and CFC sediment, Bega River. 49

5.7 Thorium and radium isotope concentrations and activity ratios in particle size fractions of bed sediments, Bega River. 52

6.1 ^{228}Th adsorption as a function of salinity. 67

6.2 Results of ^{226}Ra adsorption experiments. 70

6.3 Radium isotope concentrations and CECs of sediments used in desorption experiments. 73

6.4 The effect of equilibration time on the desorption of radium isotopes. 73

6.5 The effect of equilibration time on the desorption of radium isotopes. 76

6.6 The effect of solid/liquid (S/L) ratio on the desorption of ^{226}Ra from <63 μm Bega River sediment. 79

6.7 Sequential leaching of radium from Bega River sediment. 81

1. Introduction

Determining the source of transported sediments using tracers offers a direct method of targeting soil conservation works by spatially identifying the source of erosion. To be successful, a sediment tracer needs to have a high degree of spatial variability throughout the landscape so that it has a high probability of providing a characteristic label for sediment from a particular area. In general, source areas cannot be distinguished using sediment properties such as mineralogy, colour, and major element content (Walling and Kane 1984). However, it has been demonstrated that lithospheric radionuclides can be used successfully as sediment tracers (Murray et al. 1990, 1991). In particular, thorium and radium concentrations in sediments transported by freshwater rivers and streams have been used to identify the sources of the sediment, and the relative contributions of each source quantified.

The main objective of this thesis is to determine the relative stability of radium and thorium concentrations of transported sediment in saline water, and so assess whether these tracing techniques can be extended to river systems where the total dissolved salt (TDS) concentration is variable.

1.1 Uranium and Thorium Decay Series

The two most abundant lithospheric radionuclides are thorium (^{232}Th) and uranium (^{238}U). Both these radionuclides undergo radioactive decay to form their own decay series (Figures 1.1 and 1.2). In rock-forming minerals which remain geochemically undisturbed, all nuclides in these series will eventually reach a state known as secular equilibrium. In this state the activity concentrations of all members of a series are equal, and the activity ratio (AR) of any two members of the series is equal to one. However, because of the different chemistries of the nuclides in each series, perturbations from secular equilibrium are common in nature (Ivanovich and Harmon 1982). Geochemical processes, such as the preferential dissolution or precipitation of a radionuclide can give rise to an enhancement or reduction of the activity of that nuclide relative to other nuclides in the series.

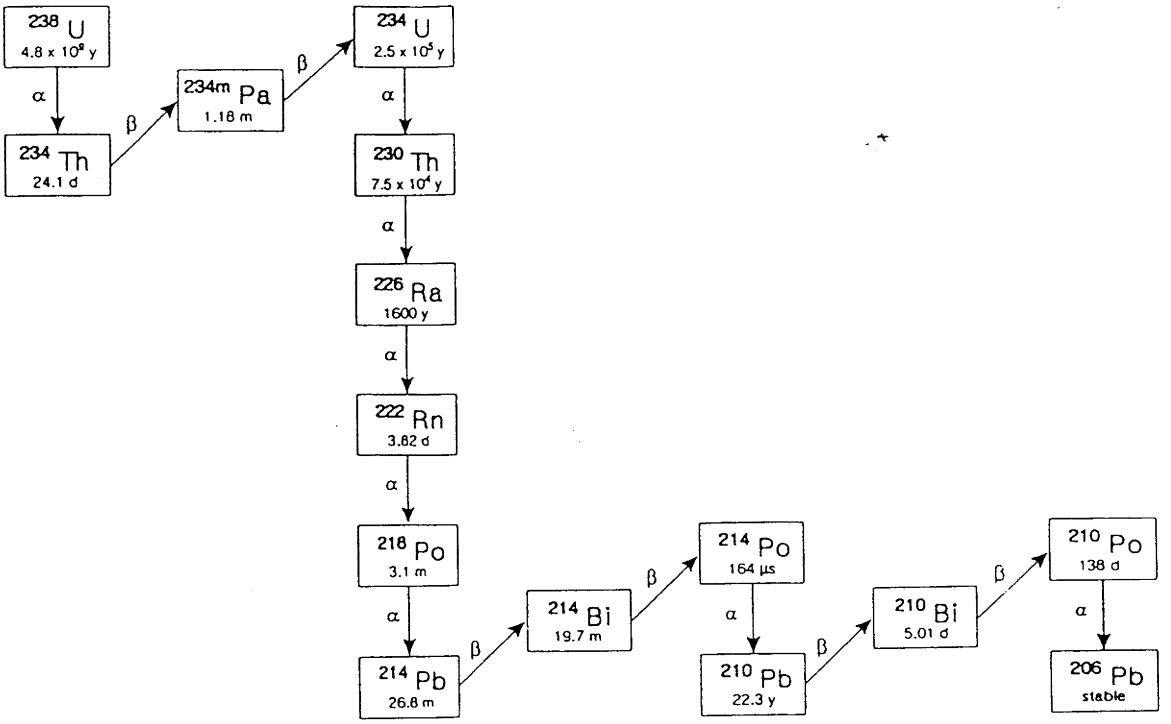

Figure 1.1 The ^{238}U decay series

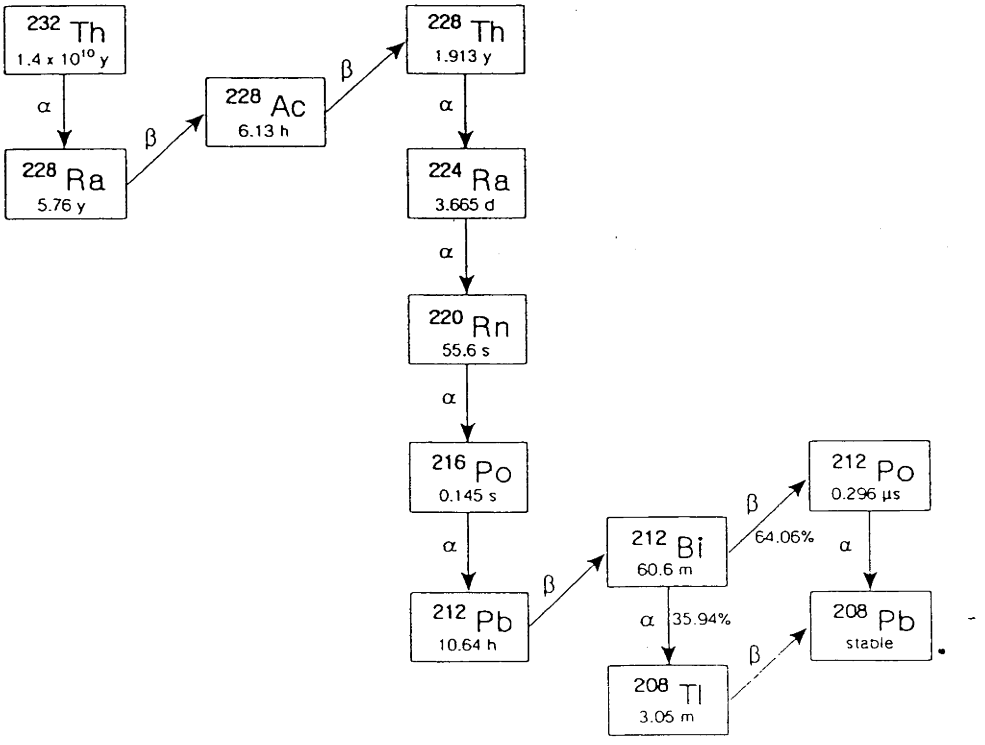

Figure 1.2 The ^{232}Th decay series

The conversion from thorium (an actinide element) to radium (an alkaline earth element) is an important parent-daughter relationship, as this decay step involves a marked change in chemical behaviour (Molinari and Snodgrass 1990). The different geochemical behaviour of radium and thorium during soil formation can lead to Ra/Th activity ratios in soils which are spatially highly variable. Where the radium and thorium isotopes are from different decay series, spatial variability is further enhanced by the natural variability of the U/Th ratio in the source rocks. Consequently, the activity ratio of ^{226}Ra, a member of the ^{238}U decay series, to that of ^{232}Th has been found to have distinctive values in soils from different areas, and can be used to 'fingerprint' soils from that area.

1.2 Radionuclides as Sediment Tracers

Correlations between ^{226}Ra and ^{232}Th concentrations of sediments transported from their source have been used to identify the spatial source of that sediment, where each source has a unique $^{226}Ra/^{232}Th$ AR (Murray et al. 1990, 1992b; Olley et al. 1993). Where more than one source is identified, an estimate of the relative sediment flux from each of these sources has been derived. For a tracer to be of general value it must not only show spatial variability, but it must also be conservative, i.e. the sediment concentrations of ^{226}Ra and ^{232}Th should be constant with respect to time and distance of transport of the sediment (Murray et al. 1991). If the sediment concentration of either radium or thorium should change during transport, the source signal is lost.

So far these tracing techniques have been successfully applied to a number of freshwater systems. In freshwater, radium and thorium are believed to be tightly bound to the sediment particles (Moore and Edmond 1984; Murray et al. 1992a), and so the $^{226}Ra/^{232}Th$ AR is likely to provide a reliable label of that sediment. However, the effects of variable water composition on the stability of sediment signal have not been investigated. One parameter which varies significantly in many Australian rivers is the TDS concentration. The salt content of rivers in some areas of inland Australia is high, and the estuaries of coastal rivers exhibit a range of salinities as river and ocean water mix. It is important therefore to establish whether the use of radium and thorium isotopes as sediment tracers can be extended to river systems of varying salt content.

Where the TDS concentration of a river changes, preferential adsorption or desorption of either radium or thorium from the suspended sediment may alter the tracer signal.

1.3 Thesis Aims and Structure

The aim of this thesis is to determine the effect of the TDS concentration of river water on the concentrations of radium and thorium isotopes in the suspended sediment and bed load compartments in rivers. This is done by studying their relative sorption behaviour in fresh and saline waters. An assessment is then made of the suitability of radium and thorium isotope AR's as sediment tracers in saline river systems.

The following chapter is a literature review of the factors likely to affect the sorption of radium and thorium. Particular emphasis is placed on sediment-solution interactions, and the behaviour of radium and thorium in saline waters. Chapter 3 describes the principal analytical techniques employed in the study.

The problems associated with sediment tracing using Ra/Th AR's in a saline inland river system are illustrated in chapter 4, and potential alternative tracers highlighted. The changes in radium and thorium isotope concentrations in suspended sediment and solution with discrete increases in TDS concentration (salinity[1]) are then investigated in more detail by studying their behaviour in an estuary (chapter 5). The suitability of some radium and thorium isotope activity ratios as potential sediment tracers in saline waters are assessed.

Laboratory experiments are then used to examine more closely radium and thorium sorption as a function of salinity and solid/liquid ratio (chapter 6). The extent of radium loss from the sediment, and the mechanisms of release are discussed.

A summary of the results of this study, and the implications for sediment tracing in saline waters are presented in chapter 7.

[1] The term 'salinity' is used in this thesis in the oceanographic sense only, i.e. its use is restricted to marine or coastal waters where the salt content is dominated by seawater, and major ion ratios are constant.

2. Literature Review

This chapter reviews what is known of the environmental chemistry of thorium and radium, with particular reference to the effects of ionic strength (TDS concentration) on sediment/solution interactions.

2.1 Thorium Chemistry

All thorium isotopes are radioactive. The most abundant naturally-occurring isotope, ^{232}Th, has a half-life ($t_{1/2}$) of 1.4 x 10^{10} y, and is the parent of a decay series which includes ^{228}Th ($t_{1/2}$ = 1.9 y) (Figure 1.2). The other common thorium isotope is ^{230}Th which forms part of the ^{238}U decay series (Figure 1.1).

In nature thorium exists as a small highly charged cation, Th^{4+}. It has an ionic radius of 0.99 angstrom. Between pH 2-3 thorium undergoes extensive interaction with one or more OH^- ligands in aqueous solutions to form a range of hydrolysis products (Baes and Mesmer 1976). It is generally believed that the species $Th(OH)^{\circ}_4$ is the predominant species above pH 5 (Ames and Rai 1978; Langmuir and Herman 1980; LaFlamme and Murray 1987; Hunter et al. 1987), although Harmsen and deHaan (1980) consider $Th(OH)_2^{2+}$ to be the major species in soil solutions above pH 4. Above 5, pH does not affect the solution concentration of hydrolysed thorium (Ames and Rai 1978).

The calculated solubility of thorianite (ThO_2) in pure water is 10^{-5} ppb (Langmuir and Herman 1980). The presence of inorganic ions such as sulphate and phosphate can significantly increase thorium solubility at pH <6. Between pH 6-8 the strong thorium complexes formed with the organic ligands often present in surface waters are considered to dominate, increasing thorium solubility by many orders of magnitude.

2.1.1 The distribution of thorium in the environment

Thorium is usually found in trace amounts in geological materials, although its content can vary considerably in rocks and soils. Its concentration is typically in the range 0.03-50 ppm (Ames and Rai 1978).

Thorium is generally assumed to be immobile in surface waters, based on its low solubility at pH 6-8, and its high particle reactivity, i.e. its ability to sorb onto and remain fixed to clays and soil colloids. Soluble thorium in surface waters is primarily present as complexed or colloidal species. Concentrations often exceed 0.01 ppb, which is at least three orders of magnitude higher than the computed solubility of ThO_2 (Langmuir and Herman 1980). These elevated concentrations are attributed to organic ligands present in most surface waters. Humic substances associated with soils and organic matter dissolve to form humic and fulvic acids capable of forming colloidal complexes with thorium (Harmsen and de Haan 1980; Choppin 1988). Wahlgren and Orlandini (1982) observed a correlation between soluble thorium and dissolved organic matter in a series of lakes.

The low concentrations of thorium in seawater (less than 10^{-4} ppb), are probably due to the lack of dissolved organic species (Knauss et al. 1978). The dissolved salts present in seawater tend to flocculate colloidal and suspended material which subsequently aggregate to form larger particles (Scott 1982; Gibbs and Konwar 1986). Li et al. (1984) suggested that this was the dominant mechanism by which metals are removed from the open ocean.

2.2 Radium Chemistry

There are four naturally-occurring isotopes of radium, all of which are radioactive. The longest-lived of these, ^{226}Ra, has a half-life of 1600 y, and occurs as part of the ^{238}U series (Figure 1.1). ^{228}Ra ($t_{1/2}$ = 5.8 y) and ^{224}Ra ($t_{1/2}$ = 3.7 d) occur as part of the thorium decay series (Figure 1.2). Radium-223 ($t_{1/2}$ = 11.3 d) occurs as part of the ^{235}U decay series.

The outer electronic configuration of radium is $7s^2$, and its ion has a +2 charge. Radium is situated in Group IIA of the Periodic Table, together with Be, Mg, Ca, Sr and Ba. Collectively these elements are known as the alkaline earth elements. Radium shares similar chemical properties with the other alkaline earths, particularly strontium and barium. The geochemistry of these elements is dominated by their ease of oxidation, the ionic nature of their metal-oxygen bonds and the insolubility of their sulphate and carbonate salts (Molinari and Snodgrass 1990).

The thermodynamic properties of radium have been evaluated recently by Langmuir and Riese (1985), and the speciation of radium in aqueous solutions has been studied by Benes et al. (1982). Of the aqueous species, Ra^{2+} and the ion-pair $(RaSO_4)^o$ are likely to have the most significance in the environment, although Benes (1982) suggested that dissolved organic species were capable of complexing radium.

2.2.1 The distribution of radium in the environment

The radium content of various igneous and sedimentary rocks has been summarised by Ames and Rai (1978), and range from 0.01-1.4 x 10^{-6} ppm. Concentrations of radium in surface waters are usually less than 10^{-13}M, and probably never reach saturation. Instead, radium concentrations in solution are limited by adsorption and/or solid solution formation (co-precipitation) processes (Langmiur and Riese, 1985).

In the pH range of most natural waters containing low TDS concentrations (pH 6-8), Ra^{2+} is strongly adsorbed by clay minerals (Benes 1985, 1986a). However in saline groundwaters (Dickson 1990) and estuaries (section 2.5 below) elevated concentrations of radium have been found.

2.3 The Partitioning of Radium and Thorium Between Solid and Solution

2.3.1 Radium/thorium disequilibrium

The different chemical behaviour of radium and thorium in the environment is best illustrated by the degree of their radioactive disequilibrium. Although all radium isotopes are formed as a result of the decay of their parent thorium isotopes, deviations from secular equilibrium for the thorium-parent/radium-daughter relationship in the biosphere are common, (Molinari and Snodgrass 1990). Geochemical sorting processes, such as solution and precipitation can result in disequilibrium where one daughter is more mobile than the other (Osmond and Cowart 1982). This is likely to be the case in river systems, and $^{226}Ra/^{230}Th$ activity ratios (AR's) differing significantly from unity have been reported in the dissolved and particulate phases of a freshwater creek (Murray et al. 1992a) and estuarine river sediments (Li et al. 1977, Elsinger and Moore 1980).

2.3.2 The distribution coefficient (K_d)

A common concept used to indicate the degree of partitioning between the solid and solution phases is that of the distribution coefficient or K_d, given by

$$K_d(mL/g) = \frac{\text{concentration of cation in the solid phase}}{\text{concentration of cation in solution}}$$

Because the K_d incorporates both the solution and solid concentrations, small changes in the adsorption of an ion may result in large changes in the K_d. The behaviour of radionuclides in natural systems depends on numerous factors, and so the absolute K_d values derived for a particular system cannot in general be extended to other natural environments. The main advantage of the K_d concept lies in its ability to indicate the fate of dissolved species involved in solid-solution interactions (Li et al. 1984).

2.4 Laboratory Sorption Studies

2.4.1 Thorium

Results of laboratory studies on thorium adsorption have been summarised by Ames and Rai (1978). Thorium was found to be strongly adsorbed to clay sized particles, and concentrations decreased with increasing soil particle size (Nishiwaki et al. 1972). However, organic complexing agents such as calcium citrate are capable of removing sorbed thorium from clay minerals (Bondietti 1974). Hunter et al. (1987) noticed reduced adsorption of thorium from seawater by δMnO_2 in the presence of the competing ligands EDTA and CDTA.

Thorium adsorption onto clay minerals increases with increasing pH, and is practically complete at pH 6.5 (Bondietti 1974). Experiments by LaFlamme and Murray (1987) and Hunter et al. (1987) showed that adsorption of thorium onto hydrous iron and manganese oxides is strongly dependent on pH in the range 2 to 5. Adsorption is essentially complete above pH 6. The latter study was performed using marine electrolytes of varying major

ion composition. The authors concluded that changes in the concentrations of the major cations Ca^{++} and Mg^{++} did not affect thorium adsorption, but the presence of SO_4^{2-} decreased adsorption at pH <6 due to the formation of ion pairs.

LaFlamme and Murray (1987) concluded that above pH 9 thorium adsorption onto goethite decreased with increasing carbonate alkalinity. Experimental variations of ionic strength at pH 8.9 did not have any influence on adsorption. Nishiwaki et al. (1972) also did not observe any effect of salinity on thorium adsorption on fine sand and silt-clay suspensions spiked with ^{232}Th.

2.4.2 Radium

Laboratory studies on the sorption properties of radium have been undertaken utilizing radiotracers (Havlik et al. 1967; Ames and Rai 1978; Barney 1984; Benes et al. 1984, 1985, 1986). These studies indicate that the equilibration of radium between solid and solution occurs primarily by ion-exchange (Ames and Rai 1978; Barney 1984; Benes 1990). In a detailed summary of papers dealing with the sorption properties of radium, Benes (1990) found that the distribution of radium between water and sediments was influenced by the time of contact, suspended solids concentration (solid/liquid ratio), composition of the water and composition of the sediment. The effects of each of these factors is summarised below.

Contact time

In general, surface adsorption of radionuclides which appear to be controlled by ion-exchange occur rapidly (Serne and Relyea 1981). Havlik et al. (1967) reported that desorbed radium reached ion-exchange equilibrium within 15 min. Benes (1990) concluded that the radium adsorbed onto model solids did not change from 1 h to 17 h of contact. Over longer periods (days-months) however, Dickson (1985) observed a decrease in the amount of radium released into saline water from crushed ore. He postulated that this decrease may be due to mineralogical alteration in the ore, or slow radium sorption processes.

Li et al. (1984) observed that the adsorption rate constant in seawater for a number of elements, including barium, depended on the suspended sediment concentration. They suggested that these reactions took place as surface processes involving isotopic exchange and/or coagulation of colloids which subsequently adsorbed onto surface sites of clays.

Solid/liquid (S/L) ratio

Laboratory studies with radiotracers have generally shown that adsorption of a cation from solution increases as the S/L ratio increases, and is due to the greater number of available adsorption sites (Balistrieri and Murray 1984). However K_d values for many species tend to be higher at low S/L ratios; i.e. the extent to which they are adsorbed per unit mass of the solid phase is greater at low concentrations of the solid phase (O'Connor and Connolly 1980). This trend has also been observed for radium (Benes et al. 1984, 1985, 1986a), barium (Li et al. 1984) and strontium (Schell and Sibley 1982). Li et al. (1984) considered that soluble metal ions may form colloids which subsequently coagulate onto larger particles. This process would only be significant at low suspended solid concentrations, as it would be masked by surface adsorption processes at high concentrations. In addition, the higher degree of particle aggregation associated with high suspended solid concentrations may decrease the effective surface area for adsorption. Both these processes would tend to the lower K_d value as the suspended solid concentration increased.

Water composition

a) Ionic strength

Adsorption of radium from solution decreases with increasing ionic strength of the solution (Serne and Relyea 1981; Benes et al. 1984, 1985, 1986a, 1986b). This effect is ascribed to the competing effects of the other cations in solution for the same ion-exchange sites on the surface of the solid phase (Barney 1984). Sayles and Mangelsdorf (1977) concluded that on introduction to seawater, fluvial clays give up their exchangeable Ca^{2+} for Na^{+}. Inasmuch as Na^{+} may also replace Ra^{2+} on exchange sites, the result will be an overall net desorption of radium as freshwater sediment is exposed to increasing salinity.

Results of laboratory desorption experiments performed on freshwater river sediments (Elsinger and Moore 1984) and crushed ore (Dickson 1985) showed that a positive correlation exists between soluble radium concentration and dissolved salt concentration. Elsinger and Moore used seawater to desorb radium, and found that radium desorption reached a maximum at about 18 parts per thousand (ppt) salinity.

Havlik et al. (1967) studied the effect of different cations on radium release from ore and sediments. They found that KCL and NaCl leached the most radium, and $SrCl_2$ and $BaCl_2$ leached the least. However, Benes (1982) noted that the desorption effects of monovalent and bivalent cations varied considerably, suggesting that differences in sediment type and in the nature of the radium bond were responsible.

The sulphate anion can enhance the retention of radium by solids by suppressing the dissolution of barite and other sulphate minerals containing radium (Benes 1990). Dickson (1985) found that the addition of up to 10 g/L of sulphate decreased the leaching of radium by a NaCl solution. He considered that this decrease may be due to the formation of $RaSO_4$ complexes which were unable to diffuse from the rock matrix.

b) pH

For most minerals adsorption of radium increases with rising pH in the range 2-9. The same effect was noted for barium adsorption onto interfacial sediments in seawater (Balistrieri and Murray 1984). This pH dependence can be explained by the competition of H^+ ions with radium for ion-exchange sites, and by the possible decomposition of some minerals at pH <3. Also, soil colliods and crystalline solids carry a net negative charge which increases with rising pH, giving rise to an increased cation exchange capacity (CEC) (Ames and Rai 1978).

Havlik et al. (1967) found that for typical surface waters pH did not play a major role in releasing radium from sediments. However (Benes et al. 1984, 1985, 1986a) found that in the pH range 6-8 the adsorption behaviour of radium may depend on the mineralogical composition of the solid. Adsorption of radium by ferric hydroxide, quartz, and to lesser extent

kaolinite showed a significant dependence on pH in this range.

Sediment properties

a) Particle size

In general, the fine fraction of sediments and soils contains more radium than the coarser fractions (Scott 1968; Megumi and Mamuro 1977; Benes 1990). Megumi and Mamuro (1977) suggested that this relationship is due to the fact that surface area plays an important role in the enrichment of radionuclides on the surfaces of soil particles, and that the surface area per unit mass of soil particles increases with decreasing particle size.

b) Mineralogical composition

Ames at al. (1983) studied the adsorption of radium onto a range of secondary minerals, and found that clinoptilolite, illite and nontrite were the most efficient adsorbers of radium. They also observed a general correlation between radium adsorption and the CEC of the substrate.

Benes et al. (1984, 1985, 1986a) found that the adsorption ability towards radium in the pH range 7.4-8.1 followed the sequence: muscovite > albite > montmorillonite > kaolinite > quartz. They concluded that the extent of radium adsorption by each mineral depends on the nature of the bond formed, and the structure of the mineral. However the results of subsequent experiments using freshwater river sediments were contradictory (Benes et al. 1986b), and the authors concluded that they could not easily relate radium sorption behaviour to the composition of the sediments.

2.5 Estuarine Studies

As mentioned above, changes in the salinity of the water may significantly affect the behaviour of soluble metals. Where river and ocean waters mix a salinity gradient is formed resulting in the coagulation and adsorption of some cations, and the progressive desorption of others, including radium, from the river-borne particulates.

The behaviour of radium in estuarine systems has been extensively studied (Li et al. 1977; Li and Chan 1979; Moore 1981; Elsinger and Moore 1980, 1983, 1984; Key et al. 1985; Moore and Scott 1986). In all these studies, radium exhibited non-conservative behaviour. Li and Chan (1979) estimated that desorption increases the total river flux of radium to the ocean by 9 to 22 times that of freshwater input alone. They suggested that this flux is due to desorption from river sediments. Elsinger and Moore (1980) showed that the increase in dissolved ^{226}Ra concentrations with rising salinity in Winyah Bay was accompanied by a corresponding decrease in the suspended sediment ^{226}Ra concentrations. Moore and Scott (1986) compared the desorption curves of dissolved ^{226}Ra for three river estuaries. They found that the desorption maximum occurred at a different salinity for each river, and that this salinity was determined by the characteristics of the water, sediment and hydrography of the river.

Measurements of other radium isotopes, particularly ^{228}Ra (Moore 1981; Elsinger and Moore 1984; Key et al. 1985) have shown that bottom sediments are an additional source of radium to the estuary. The enrichment of dissolved ^{228}Ra is greater than ^{226}Ra, and is probably due to diffusion of radium from bottom sediments where, because of its much shorter half-life, the rate of re-generation of ^{228}Ra activity far exceeds that of ^{226}Ra.

Diffusive losses of radium from bottom marine sediments are often reflected by radioactive disequilibria in these sediments. Because thorium is not mobilized, a $^{226}Ra/^{230}Th$ AR <1 in bottom sediments will normally indicate a loss of radium to the water column. A deficiency of ^{226}Ra with respect to its parent ^{230}Th was observed in Winyah Bay (Elsinger and Moore 1980), and in acid leachates of surface sediments in Hudson Bay (Li et al. 1977).

Dissolved thorium in river water which mixes with saline water in an estuary is rapidly removed onto precipitated iron and manganese oxyhydroxides and flocculated organic colloids. Consequently, thorium removal by particulate matter in seawater is expected to be rapid (e.g. Bacon and Anderson 1982, Nozaki et al. 1981). Its removal rate in marine systems has also been found to be correlated with the particulate matter concentration in the water column (Sanstchi et al. 1979; McKee et al. 1986).

2.6 Summary

Broadly, water and sediment composition are the two factors which govern the sorption behaviour of radium and thorium in surface waters. Salinity is the major factor influencing the behaviour of radium. As salinity increases, radium is released from freshwater sediments. Radium is probably replaced on ion-exchange sites on the sediment by major cations present in solution. Other factors such as the S/L ratio of sediment suspensions, and contact time may also affect radium sorption. The extent to which pH effects radium sorption appears to depend on the sediment composition.

Thorium is strongly adsorbed onto sediments in the pH range of most surface waters (6-8). The presence of organic colloids in freshwater may increase the mobility of thorium, but in saline water thorium is likely to retain its particle reactive nature due to the flocculation of colloidal material.

Given the difficulty in relating the sorption behaviour of radium for individual minerals to sediments as a whole, it is appropriate that this study focus on the effects of variable salinity on radium and thorium sorption using a typical river sediment at a typical pH range for surface waters. Furthermore, if the suitability of the $^{226}Ra/^{232}Th$ AR as a sediment tracer in saline surface waters is to be properly assessed, the following points need particular attention;

- the relative sorption behaviour of both radium and thorium isotopes in suspended sediment over a wide salinity range. The behaviour of radium as a function of TDS concentration is well documented, but data for thorium is sparse, particularly at low salt concentrations. None of the previous studies have studied the behaviour of the isotopes of both of these elements in the same material with changing TDS concentration.

- the response of radium and thorium sorbed onto freshwater sediment to small increases in TDS concentration, such as those which often occur in Australian inland water. At what salt concentration will changes in the sediment $^{226}Ra/^{232}Th$ AR become significant?

- the effect of S/L ratio on radium loss in saline waters. If radium K_d's in saline waters vary with S/L ratio, losses of radium from suspended sediment may differ from that of bottom sediments.

3. Analytical Techniques

3.1 Alpha Spectrometry

Alpha-particle spectrometry following radiochemical separation is the most sensitive method of analysis of radium and thorium isotopes, particularly for environmental samples where activities are low, and sample size is limited. The procedures used in this work have been described in detail by Hancock and Martin (1991) and Martin and Hancock (1992). A brief summary follows.

3.1.1 Sample dissolution and radiochemical separation

Water samples: The tracer solution used was a calibrated ^{229}Th ($t_{1/2}$ = 7340 y) solution (Amersham, ±1%) containing ^{225}Ra ($t_{1/2}$ = 14.8 d) in secular equilibrium. After addition of a known quantity of the tracer nuclides to 2-5 L of acidified filtrate, radium and thorium isotopes were concentrated by co-precipitation with manganese dioxide at pH 10. This precipitate was recovered by filtration, dissolved in a HCl/H_2O_2 solution and evaporated to dryness. The residue was dissolved in 0.1 M HCl and radium and thorium isotopes co-precipitated with lead sulphate. After decanting the supernatant and washing, the precipitate was dissolved in an ammoniacal EDTA solution. This solution was poured onto an anion exchange column. Thorium was retained on the column, whereas radium passed through and was collected for further purification (see below). The column was then washed with 8 M HNO_3 solution and thorium eluted with 9 M HCl. This eluate was evaporated to dryness and electrodeposited onto a stainless steel disc (20 mm diameter) from a sulphate electrolyte. The active area of the disc was approximately 250 mm^2.

The radium fraction (above) was further purified using a cation exchange column. Alkaline earth cations were sequentially eluted from the column by washing with 1.5 M ammonium acetate and 2.5 M HCl solutions. Radium was finally eluted with 6 M HNO_3. After evaporation to dryness, radium was electrodeposited onto a stainless steel disc from an aqueous/ethanol solution at pH 2.

Sediment samples: The tracer isotope was added to 0.5-1 g of dry sediment in a platinum dish, 2-3 mL each of nitric and hydrofluoric acids were added and the slurry evaporated to dryness. The residue was then solubilised by fusion with potassium fluoride, followed by transposition to a pyro-sulphate cake. This cake was then dissolved in 0.1 M HCl and the thorium and radium isotopes separated from the sample matrix by co-precipitation with lead sulphate. Analysis then proceeded as described for water samples.

Virtually all chemical yields for both radium and thorium determinations were in the range 60-90%.

3.1.2 Spectrometry

Electrodeposited discs were counted using an Ortec silicon surface barrier detector (active area 450 mm^2) connected to a Canberra Multi-Channel Analyser. The duration of counting varied from 1-4 days depending on the activity of the source.

The unit of activity used in this work is the Bequerel (Bq). One Bq is equal to 1 disintegration/sec. The detection limits for the determination of radium and thorium isotopes by alpha-particle spectrometry are dependent on the count time and background count rates, but are typically in the range 0.4-1.0 mBq per sample.

Thorium

A typical thorium spectrum produced from a source prepared from a sediment sample is shown in Figure 3.1. The positions of the three naturally-occurring thorium isotopes, ^{232}Th, ^{230}Th and ^{228}Th are shown, together with the ^{229}Th tracer. The concentration of each isotope in the sample can be calculated by integrating the counts for that isotope over its energy region, and deducting the calculated number of counts present in this region due to interfering peaks and background activity. The net count of each isotope is then compared to the net tracer peak count, and the isotope activity derived from the known activity of the tracer.

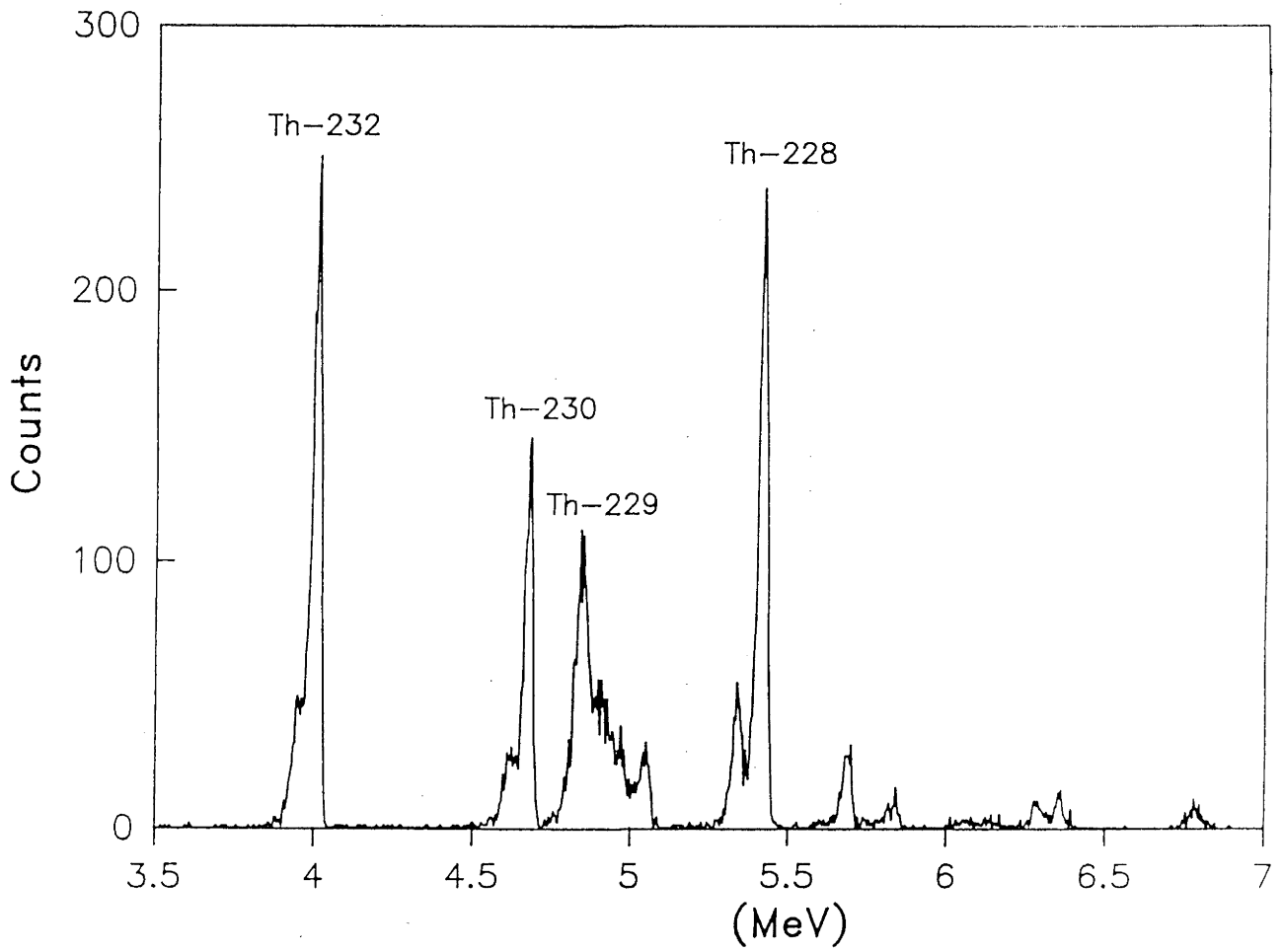

Figure 3.1 A typical thorium alpha-particle spectrum (sediment sample).

Radium

The activities of the four naturally-occurring radium isotopes were obtained from three different counting periods of the same source. An initial count within two days of electrodeposition enabled the determination of the ratio of the short-lived radium isotopes (^{223}Ra and ^{224}Ra) to that of ^{226}Ra. A second count 2-3 weeks later enabled the recovery of the ^{225}Ra tracer to be calculated via ingrowth of its alpha-emitting daughters, and the absolute concentration of ^{226}Ra in the sample determined. Using the ratios determined in the first count, the activities of ^{223}Ra and ^{224}Ra could then be calculated. A third count 6-12 months later enabled a measurement of ^{228}Ra by determining the ingrowth of ^{228}Th.

3.1.3 Calculation of errors

The accuracy of measurements by alpha spectrometry is usually limited by counting statistics. The standard deviation (σ) of N random counts is given by

$$\sigma = N^{1/2}$$

and the uncertainty of analysis, at the 67% confidence limit, is given by $\pm\sigma$. This calculation has also been used for the determination of counting errors for determinations by gamma spectrometry and liquid scintillation counting (sections 3.2 and 3.3 below). Unless otherwise stated, the quoted uncertainty of all determinations using counting techniques in this thesis will be $\pm\sigma$. The other major source of analysis error is the uncertainty in the activity of the standards used, usually less than ±1%.

3.2 Gamma Spectrometry

Where sufficient sample was available (>40 g ash weight), sediment samples were analysed by gamma spectrometry. The procedure is discussed in detail by Murray et al. (1987), and involves the forming of solid samples, previously ashed at 450°C, into a reproducible geometry by casting them in polyester resin. The samples were then counted on a high resolution, low background germanium detector. The resin allows complete retention of

^{222}Rn gas, and ^{226}Ra can be determined with high sensitivity after a suitable ingrowth period (3 weeks) for ^{222}Rn and daughters. The other radionuclides determined by this technique were ^{228}Th and ^{228}Ra. Detection limits for a 40 g sample counted for 24 h are typically 200 mBq for ^{226}Ra, and 1 Bq for ^{228}Ra and ^{228}Th. Although this technique is less sensitive than alpha spectrometry, it is less labour intensive, and there is no delay in the measurement of ^{228}Ra.

3.3 Liquid Scintillation

This method is insufficiently sensitive for the analysis of ^{226}Ra in environmental water samples in this study, but is rapid and has application in the laboratory studies (chapter 6). The method used here is based on that of Cooper and Wilkes (1981). In summary, a weighed amount (~7 g) of filtered water sample and 15 mL scintillant (5 g PBBO, 400 g napthalene in 1 L toluene) were added to a glass scintillation vial, and the vial capped and shaken. All vials were stored for at least 3 weeks to allow ^{222}Rn and daughters (^{214}Po and ^{218}Po) to grow into secular equilibrium with ^{226}Ra. The vials were stored in an inverted position to limit radon loss through the cap.

Samples were counted using a photomultiplier (PM) tube. The base of the vial was optically coupled to the face of the PM tube, and a matt white reflector placed around the vial. Pulses from the PM tube were recorded using a multi-channel analyser with a conversion gain of approximately 17 channels/MeV. The observed counts were integrated in the energy region 3.8-10.5 MeV. The background count rate in this region for a vial containing only demineralised water and scintillant was ~1 count/sec. For all determinations a minimum of 5000 counts were accumulated.

^{226}Ra standards were prepared from the stock solution in triplicate over a range of salinities. In general the standard error on the mean of each triplicate set of standards was greater than the error (at the 1σ level) due counting statistics. Williams (1985) noted that losses of radon through the foil-lined caps of scintillation vials was the major factor causing variability in the determination of ^{226}Ra by this method. He claimed that 'viton' discs inserted in the cap virtually eliminated radon loss. Unfortunately, viton discs were not acquired until after the

completion of the laboratory analyses. Nevertheless, tests were run to compare the activity of the ^{226}Ra standards in vials containing viton seals with those using the foil-lined cap. In general, the mean of standards in vials containing foil-lined caps were 5% ±3 lower in activity than the those containing viton. This suggests that the variability in the activity of standards described above was due to variable radon loss.

A plot of the observed count rate against the amount of ^{226}Ra added to each vial was found to be linear ($r^2 = 0.99$) in the concentration range of the solutions measured in these experiments (Figure 3.2.a). Deviations from the line of best fit show no trend with increasing ^{226}Ra concentration (Figure 3.2.b). However, count rates were found to be depressed at salinities greater than 3.5 ppt (Figure 3.3), probably as a result of quenching by the chloride ion (M. Cooper, pers. comm.). Quenching refers to losses that can occur during energy transfer from the radioactive particle to the light detecting surface (Williams 1985). Consequently the ^{226}Ra content of all samples were referenced to the mean value of standards of the same salinity.

3.4 Atomic Adsorption Spectrophotometry

Flame atomic adsorption spectrophotometry was used to determine concentrations of the major cations, Na, Ca, Mg, K, Fe and Mn in filtered water. An air-acetylene flame was used, and the samples were aspirated directly into the flame. The high salt content of some samples was found to give spurious results for Fe. Consequently, Fe standards were prepared in solutions containing a range of NaCl concentrations, and a series of calibration curves generated. The Fe concentration of each sample was then obtained by relating its absorbance to the calibration curve of closest salinity.

3.5 Sedimentation Analysis

Sedimentation techniques were used to fractionate sediment particles in the <63μm size range. The method used was similiar to the pipette method described by Gee and Bauder (1986), with the exception that the sediment pre-treatment consisted of ultrasonic rather than chemical dispersion.

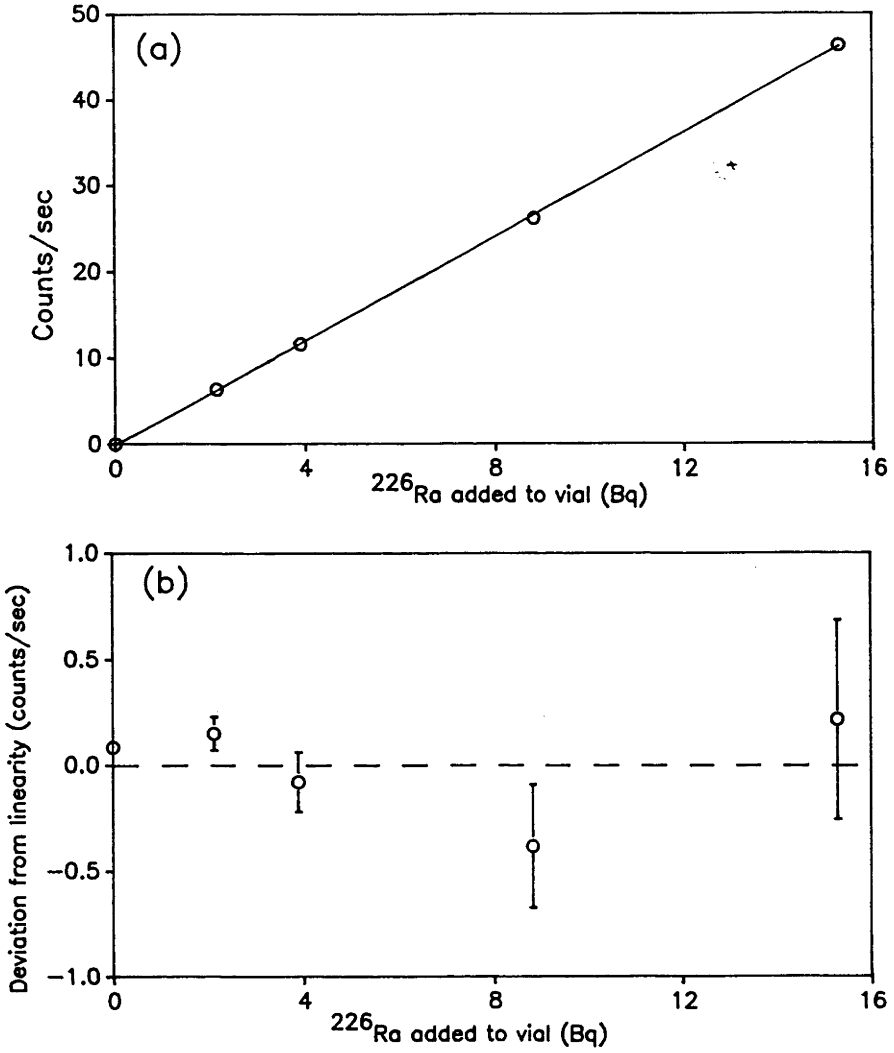

Figure 3.2 (a) Count rate as a function of ^{226}Ra activity and (b) its deviation from linearity.

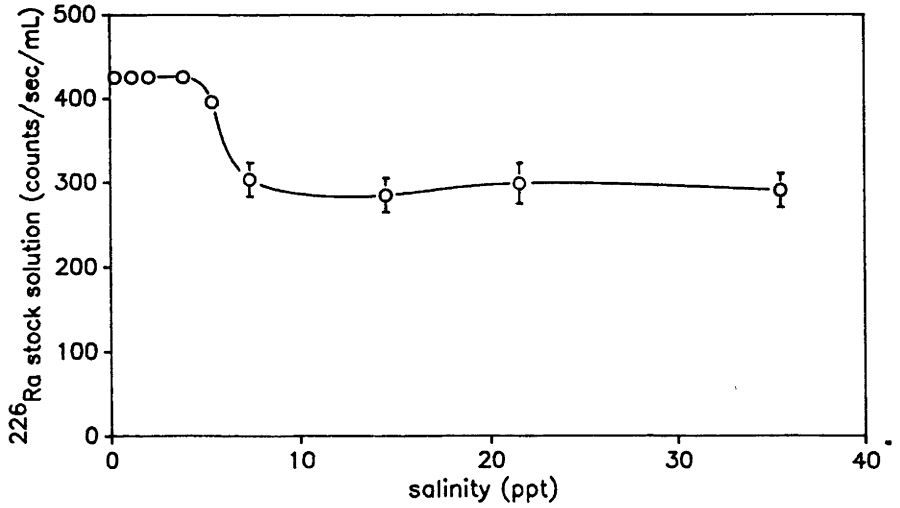

Figure 3.3 The effect of salinity on the ^{226}Ra count rate.

3.6 Cation Exchange Capacity (CEC)

Sediment CECs were determined using the compulsive exchange method described by Gillman (1979). The sediment was first saturated with Ba^{2+}, equilibrated with $BaCl_2$ solution equivalent in ionic strength to the sediment solution, and then reacted with $MgSO_4$ to replace Ba with Mg. The amount of Mg adsorbed is determined from the loss the $MgSO_4$ solution, and is equivalent to the CEC of the sediment.

3.7 X-Ray Diffraction (XRD) Analysis

XRD analyses were carried out with a Siemens D-501 automated θ:2θ goniometer using Cu Kα radiation and a graphite monochromater at 50 kV and 30 mA. Scans were made from 4-60° 2θ with 1° divergence and scatter slits. Sediment samples were initially run air-dried, and then with ethylene glycol in order to detect smectite minerals.

4. Sediment Tracing in a Saline Inland River System

The objective of this field study was to assess empirically whether the $^{226}Ra/^{232}Th$ AR could provide a reliable tracer signal for sediment transported through an inland river system which was known to carry high concentrations of total dissolved salts (TDS). A simple system was chosen, involving the transport and mixing of sediment from two known sediment sources. The system consisted of the confluence of a river containing water with a low salt content, and its tributary containing water with a relatively high salt content. Downstream of their confluence the TDS concentration of the river water had risen significantly. The radium and thorium concentrations of suspended and bed sediment samples from the two upstream arms were examined, and compared with sediments downstream of their confluence.

4.1 The Loddon River-Barr Creek Confluence

A section of the Loddon River downstream of Kerang in Victoria, and its tributary Barr Creek was selected as the study site (Figure 4.1). The Loddon River is a tributary of the Murray River, entering it near Swan Hill. Barr Creek joins the Loddon River about 20 km north of Kerang. The Kerang region is a groundwater discharge zone, and is responsible for increases in the TDS concentration of the Murray River. Barr Creek receives highly saline groundwater outseepage and is the largest single point source of soluble salts to the Murray River (Macumber 1991).

Water quality monitoring of Barr Creek has shown that periods of high electrical conductivity (EC), up to 34,900 μS/cm, have occurred between 1978 and 1986 (Mackay et al. 1988). This EC corresponds to about 21,000 mg/L TDS (c.f. seawater ~45,000 μS/cm, or 35,500 mg/L TDS). The mean conductivity over the same period was 8,495 μS/cm. By contrast, the EC of the Loddon River was lower by about an order of magnitude. At Kerang, upstream of its confluence with Barr Creek, the Loddon had a mean EC of 760 μS/cm, and a maximum recorded EC of 3800 μS/cm. The Loddon River downstream of its confluence with Barr Creek does not appear to have been monitored. However Mackay et al. 1988 report flow data for both Barr Creek and the Loddon River, together with their total salt load. This data

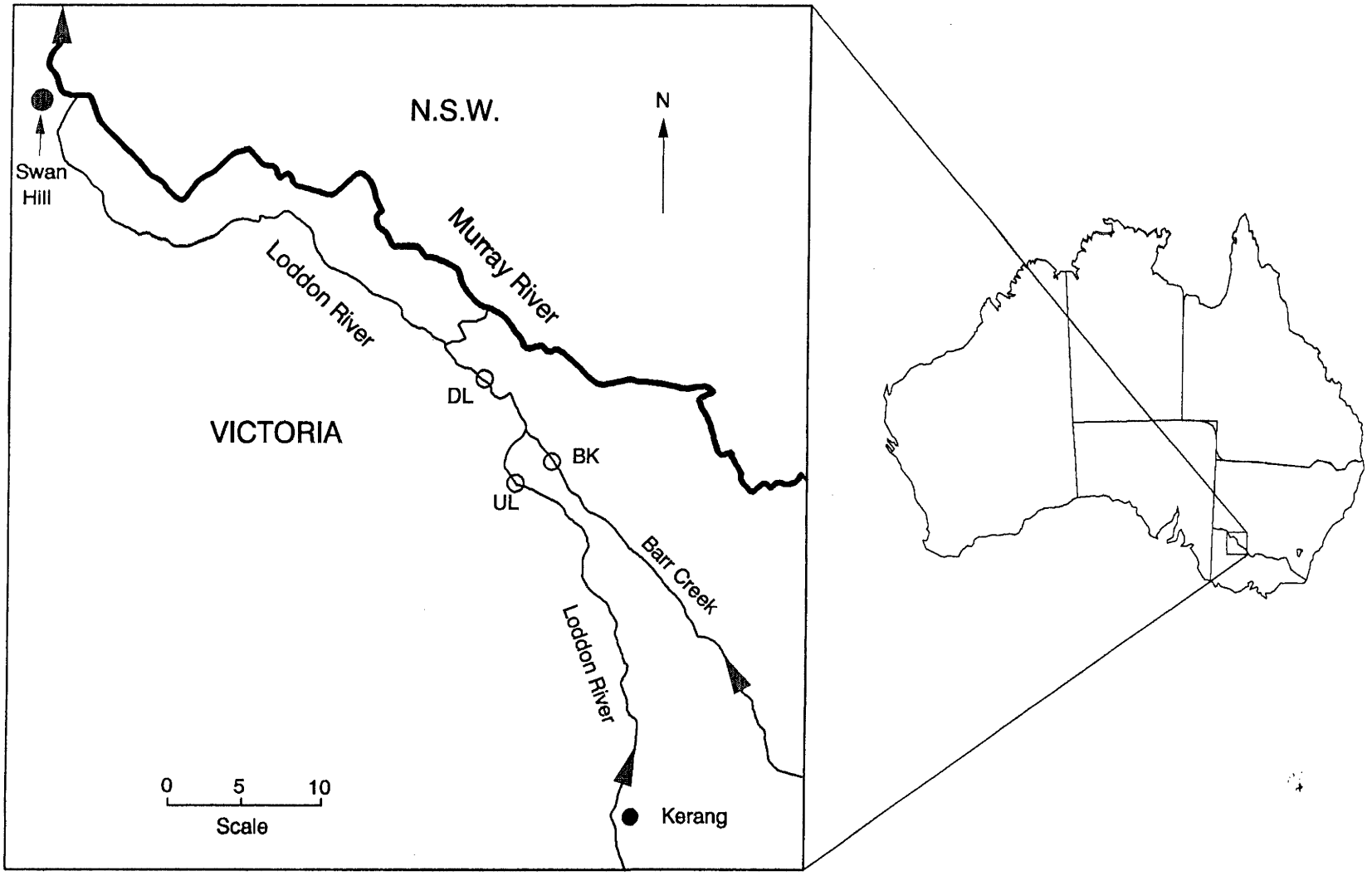

Figure 4.1 The Loddon River-Barr Creek confluence, showing the location of sampling sites (O)

indicates that the TDS concentration of the Loddon River more than doubles downstream of its junction with Barr Creek.

4.2. Methods

4.2.1 Sample collection and analysis

Sediment and water samples were collected in May 1992 from three sites; the Loddon River (site UL) and Barr Creek (BK), 3 and 5 km respectively upstream of their confluence, and the Loddon River 6 km downstream of its confluence with Barr Creek (DL). The locality of the sites are shown in Figure 4.1. Three river bed sediment samples were collected from each site along a 1 km reach of the river using an Eckman grab sampler. A 20 L water sample was also collected from each site, and its EC measured (μS/cm @ 25°C). The suspended sediment in each water sample was allowed to settle over a period of 3 days, and the water decanted. The sediment was recovered, dried and the concentrations of radium and thorium isotopes determined by alpha spectroscopy. Radium and thorium isotope concentrations of bed sediment samples were determined by gamma and alpha spectrometry respectively.

4.3 Results and Discussion

4.3.1 Suspended sediment

Table 4.1 gives the EC and suspended sediment concentrations of the water samples. The EC of both the Loddon River and Barr Creek were well below their recorded maxima (section 4.1) at the time of sampling, probably due to the recent heavy rains and high river flows in the region. Flow data for the date of sampling (also included in Table 4.1) was available for the Loddon River at Kerang, and for Barr Creek about 15 km upstream of site BK (Rural Water Authority of Victoria). No flow data are available for the Loddon River downstream of the confluence, but if it is assumed that there is no other significant contribution to the flow of either arm between the point of monitoring and site DL, these data indicate that Barr Creek contributed 75% of the total flow downstream of the confluence. This calculation is supported by both EC and suspended sediment measurements. Using a simple two-component mixing model, the downstream value of a

conservative parameter can be calculated using the relationship

$$Ax + By = C \qquad (1)$$

where x and y are the relative contributions of the two sources, so that $x + y = 1$, and A and B are the upstream, and C the downstream values of the parameter. Using the flow data to quantify the contributions of the Loddon River and Barr Creek (x and y in equation (1)), the measured EC at site DL (1960 μS/cm) corresponds well with the calculated EC (1870 μS/cm). Likewise, the suspended sediment concentration at site DL (76.5 mg/L) is also close to its calculated value (72.7 mg/L). The fraction of the total suspended sediment load at site DL carried by arm B can be calculated from

$$By/(Ax + By)$$

For Barr Creek this fraction is 0.67, and by difference the fraction contributed by the Loddon River upstream of the confluence is 0.33.

Table 4.1 Flow, EC and suspended sediment data for the Loddon River and Barr Creek on the date of sample collection (19/5/92).

site	flow* (ML/day)	EC (μS/cm)	suspended sediment (mg/L)
BK	1504	2310	79.5
UL	952	1182	62.2
DL	n/a	1959	76.5

* flow monitored 30 km and 15 km upstream of sampling sites UL and BK
n/a not available

Radium and thorium isotope concentrations and AR's are presented in Tables 4.2 and 4.3. The $^{226}Ra/^{232}Th$ AR of the suspended sediment of the Loddon River at site UL (AR_{UL} = 0.745 ±0.033) is significantly different to that of Barr Creek at site BK (AR_{BK} = 0.597 ±0.025). As expected the AR at

site DL, downstream of their junction lies between the values of the two arms (AR_{DL} = 0.660 ±0.030). Using these AR's, the fraction of Barr Creek suspended sediment at site DL can be calculated from

$$(AR_{BK} - AR_{DL})/(AR_{UL} - AR_{BK})$$

The calculated value is 0.57 ±0.24, within error of the value derived above using suspended sediment and flow data.

4.3.2 Bed sediments

The radium and thorium concentrations of the bed sediment samples are also presented in Table 4.2. The concentrations of bed sediment nuclides, particularly those of Barr Creek, are significantly higher than the suspended sediments. This relationship is opposite to that expected in rivers, given that suspended sediments usually contain a higher proportion of fine clay particles than do bed sediments, and that clay particles usually have higher radionuclide concentrations than coarse particles (Megumi and Mamuro 1997). The bed sediments of both the Loddon River and Barr Creek contained a high proportion of silt and clay particles. The relativley low radionuclide concentration of the suspended sediment could be due to the high flow conditions at the time of sampling. The higher energy of the river would allow it to carry a greater amount of relatively coarse low activity material, such as sand, reducing the radionuclide concentrations of the total suspended sediment.

The bed sediment radionuclide AR's are presented in Table 4.3, and have been expressed as the mean of the three samples collected at each site. The associated uncertainty is the standard error of the mean. The Loddon River bed sediment $^{226}Ra/^{232}Th$ AR's at sites UL and DL are significantly lower than the suspended sediment AR at the same site. These differences would normally suggest that the suspended sediment in the Loddon River at the time of sampling had a source different to its bed sediments.

Table 4.2 Thorium and radium isotope concentrations of suspended sediment and bed sediment samples collected from the Loddon River and Barr Creek.

site	^{232}Th	^{230}Th	^{228}Th	^{226}Ra	^{228}Ra
		(mBq/g dry wt.)			
Suspended sediment					
BK	37.5 ±0.8	24.0 ±0.6	39.2 ±0.9	22.4 ±0.8	38.6 ±1.7
UL	53.3 ±1.4	37.3 ±1.1	59.4 ±1.5	39.7 ±1.4	60.8 ±2.8
DL	40.9 ±1.1	27.2 ±1.5	43.2 ±1.1	27.0 ±1.0	44.7 ±2.9
Bed sediment					
BK1	55.3 ±1.8	34.4 ±1.2	60.1 ±1.1	33.7 ±0.6	60.1 ±1.5
BK2	64.0 ±2.0	42.2 ±1.5	66.9 ±1.3	36.8 ±0.6	63.7 ±1.6
BK3	63.9 ±2.0	41.8 ±1.5	69.6 ±1.1	39.1 ±0.6	67.3 ±1.5
UL1	62.1 ±2.1	40.6 ±1.6	61.2 ±0.6	38.3 ±0.4	62.9 ±0.7
UL2	61.9 ±2.5	40.6 ±1.8	59.4 ±1.1	37.9 ±0.5	60.1 ±1.3
UL3	63.3 ±3.1	42.8 ±2.3	61.2 ±0.9	37.5 ±0.4	63.3 ±1.1
DL1	68.8 ±1.2	49.1 ±0.9	71.7 ±1.2	44.4 ±0.7	69.1 ±1.6
DL2	67.3 ±2.8	43.5 ±2.1	66.3 ±1.2	36.8 ±0.6	58.7 ±1.5
DL3	60.7 ±2.2	39.3 ±1.5	62.9 ±1.1	37.0 ±0.6	60.1 ±1.5

Table 4.3 Thorium and radium isotope activity ratios in suspended sediment and bed sediment samples collected from the Loddon River and Barr Creek.

site	$^{226}Ra/^{232}Th$	$^{226}Ra/^{230}Th$	$^{228}Ra/^{226}Ra$	$^{230}Th/^{232}Th$
Suspended sediment				
BK	0.597 ±0.025	0.933 ±0.046	1.727 ±0.063	0.641 ±0.019
UL	0.745 ±0.033	1.064 ±0.055	1.534 ±0.058	0.700 ±0.022
DL	0.660 ±0.030	0.993 ±0.056	1.656 ±0.081	0.664 ±0.022
Bed sediment*				
BK	0.600 ±0.010	0.916 ±0.018	1.739 ±0.009	0.644 ±0.010
UL	0.607 ±0.006	0.917 ±0.017	1.597 ±0.033	0.662 ±0.006
DL	0.601 ±0.024	0.897 ±0.022	1.629 ±0.029	0.670 ±0.018

* the bed sediment ARs are the mean of three values from each site; the corresponding uncertainty is the standard error of the mean.

However, it is also possible that the lower bed sediment $^{226}Ra/^{232}Th$ AR's may reflect loss of radium incurred by many years of periodic flushing with highly saline water. By contrast, suspended sediment may have only been recently transported, and its radium content of the suspended sediment may therefore only reflect the EC (TDS concentration) of the river water at the time of sampling. On this sampling occasion the EC's of both the Loddon River (1180 μS/cm) and Barr Creek (2310 μS/cm) were relatively low, indicating that there may have only been a relatively small amount of radium desorbed from the suspended sediment. In these circumstances a difference in the $^{226}Ra/^{232}Th$ AR's of suspended and bed sediments could have arisen, even though both had been transported from a common source.

Evidence for mobilisation of radium from bed sediments can be obtained by examination of $^{226}Ra/^{230}Th$ AR's. Thorium-230 and ^{226}Ra are parent and daughter nuclides in the ^{238}U decay series (Figure 1.1). In soils where neither radium or thorium has been mobilised, these nuclides would be expected to be in secular equilibrium, i.e. the $^{226}Ra/^{230}Th$ AR should be equal to one. The $^{226}Ra/^{230}Th$ AR of the suspended sediment from sites UL and DL both have values within error of, or slightly greater than one. This is in contrast to the mean bed sediments AR's which show a deficiency of ^{226}Ra with respect to ^{230}Th of 8-12%. Thorium is generally not considered to be mobile in surface waters (chapter 2), and so the deficiency of ^{226}Ra activity is likely to be due to a net loss of ^{226}Ra from the sediment.

Only Barr Creek shows a suspended sediment $^{226}Ra/^{230}Th$ AR which is close to its bed sediment values. The low value of the suspended sediment AR suggests that the TDS concentration of Barr Creek at the time of sampling may have been high enough to release radium from the suspended sediments during transport. Alternatively, the suspended sediments may have been transported from a region previously exposed to high levels of dissolved salts. Whatever the reason, the depletion of radium activity with respect to thorium indicates that radium has been lost from the sediments. This loss is probably associated with the salt content of these rivers.

4.3.3 The effect of radium loss on the ability to source sediments

If a finite but unknown loss of radium relative to thorium has occurred from sediments in the Loddon River-Barr Creek system, Ra/Th AR's cannot be reliably used as tracers of transported sediment. On this occasion the use of $^{226}Ra/^{232}Th$ AR's yielded a Barr Creek suspended sediment contribution at site DL which was consistent with the expected value. However, application of the same method to bed sediments could give an incorrect result due to the fact the $^{226}Ra/^{232}Th$ AR of bed sediments may depend more on the maximum TDS concentrations they have encountered, than their original values prior to transport. Alteration of the sediment signal during or after transport may not only indicate an incorrect source, but may also introduce an error in the derivation of the relative contribution of each sediment source.

4.3.4 Other potential tracers

The chemical behaviour of isotopes of the same element is identical, and so interactions between sediment and solution should affect all isotopes of that element to the same extent. In a system where radium or thorium is preferentially mobilised, the use of AR's of isotopes of the same element as sediment tracers may overcome the problems associated with Ra/Th AR's (section 4.3.3).

Table 4.3 shows that the values of both the $^{228}Ra/^{226}Ra$ and $^{230}Th/^{232}Th$ AR's in the suspended sediment are within error of the corresponding mean bed sediment AR's at all sites. This relationship may be coincidental, but it may also indicate a common source for both suspended and bed sediments. Both of these tracers are potentially useful in rivers containing high levels of TDS, however a more detailed study of their behaviour over a range of TDS concentrations is required before they can be used with confidence.

5. The Behaviour of Radium and Thorium in an Estuary

The Loddon River system data suggest that increases in the TDS concentration of river water reduces the reliability of the $^{226}Ra/^{232}Th$ AR as a sediment tracer. Accordingly, the effects of TDS concentration on the behaviour of radium and thorium in a natural system were investigated in more detail in the Bega River estuary. These effects are most readily observed in an estuary because it approximates a simple two-component mixing system exhibiting a continual and wide ranging salinity gradient. In most cases the two end-members are well defined, with the major input of suspended sediment originating from the freshwater end. The effects of salinity on this sediment can then be studied as it is exposed to progressively more saline water.

5.1 Introduction

The aims of this field study were;

- to determine the extent to which the radium and thorium concentrations in both the suspended sediment and dissolved phases change as a function of salinity;
- define the salinity range over which these changes occur;
- assess the stability of the $^{226}Ra/^{232}Th$ AR in suspended sediments under saline conditions in a natural system;
- assess the potential of other radium or thorium AR's as sediment tracers in saline waters.

Most of the previous publications describing the behaviour of radium in saline surface waters have dealt with estuarine systems, and these have been mainly concerned with dissolved radium isotopes. The studies have shown that dissolved ^{226}Ra initially increases in concentration as the salinity of the estuary rises. This increase has been mainly attributed to desorption from suspended sediments carried in by the river, and diffusion from estuarine bottom sediments (Li et al. 1977; Elsinger and Moore 1980, 1984; Moore 1981; Key et al. 1985; Moore and Scott 1986). Yet very few publications have presented data showing the corresponding radium

concentrations in both the dissolved and suspended sediment phases over a range of salinities. Key et al. (1985) noticed a decrease in the concentrations of ^{226}Ra and ^{228}Ra in four samples of suspended solids from the Amazon River estuary. An extensive set of suspended sediment data has been presented by Elsinger and Moore (1980). They observed a decrease in ^{226}Ra suspended sediment concentrations in the Pee Dee River-Winyah Bay estuary which corresponded well with increases in dissolved ^{226}Ra.

Data illustrating the behaviour of thorium as a function of salinity is also mostly confined to estuarine studies. Because of its particle-reactive nature, the dissolved concentrations of the long-lived thorium isotopes (^{232}Th and ^{230}Th) in surface waters are usually extremely low. Estuarine studies have therefore usually focussed on the shorter-lived isotopes, ^{234}Th and ^{228}Th, whose activities are higher. Santschi et al. (1979) reported particulate and dissolved concentrations of thorium isotopes in a narrow range of high salinities in Narragansett Bay. McKee et al. (1986) did not observe any systematic relationship between the ^{234}Th distribution coefficient and salinity in samples from the Amazon shelf. Sholkovitz et al. (1978) showed that dissolved iron and humic acids carried into an estuary by river water coagulate at salinities <5 ppt. These substrates can efficiently scavenge dissolved or colloidal particle-reactive species such as thorium (Scott 1982; Choppin 1988). Even though the dissolved river water concentrations of ^{232}Th and ^{230}Th may be low, this process could still result in a significant change in the suspended sediment concentrations of these isotopes if the suspended sediment concentrations are low.

This field study encompassed the analysis of radium and thorium isotope activities in both the dissolved and suspended sediment phases in water samples of varying salinity collected along the length of an estuary. Emphasis was placed on the measurement of suspended rather than bottom sediments. Due to fluctuations in river flow together with the ebb and flood of the tide, bottom sediments are likely to be exposed the range of salinities. The radium content of the sediments may therefore reflect the effects of the highest salinity water they have contacted, rather than the salinity at the time of sampling. By contrast, suspended sediments should, in the main, move conservatively with river and tidal flow. Although

settling of heavier particles and resuspension of bottom sediments may occur, suspended sediments should more accurately reflect equilibrium cation concentrations at a known salinity.

5.2 The Bega River Catchment

The Bega River estuary was selected as the field site primarily because of its close proximity to the CSIRO Canberra laboratory. The site had the advantage that there are no major tributaries to the river within the river-seawater mixing zone. Apart from run-off during and after rainfall, the section of the river below the tidal limit contained little or no water or sediment inputs other than from the fresh and seawater end-members.

5.2.1 Location and topography

The Bega River Basin is located in south-east N.S.W. (Figure 5.1) and has a total catchment of approximately 2000 km^2. The river is fed by three major tributaries. Two of these, the Bemboka River and Tantawangalo Creek, together with a number of minor tributaries converge to form the Bega River west of the town of Bega. The third, the Brogo River, enters at Bega town. All the major tributaries originate in mountains comprising part of the Great Dividing Range approximately 40 km to the west and north-west. The topography here is rugged and the slopes are mostly uncleared. Closer to the coast the catchments of all tributaries consist mainly of cleared farm-land, predominantly supporting dairying with some agriculture.

The Bega River estuary is located approximately 15 km east of the town of Bega. It comprises an 11 km stretch of the river from just upstream of the tidal limit, to where the river enters the Tasman Sea (Mogareka Inlet) (Figure 5.2). Apart from Jellat Jellat Creek, which enters the river about 300 m downstream of the tidal limit, there are no permanently flowing tributaries to the estuary. However, numerous ephemeral channels drain steep hill slopes along the upper region of the estuary. These channels only flow after significant rainfall.

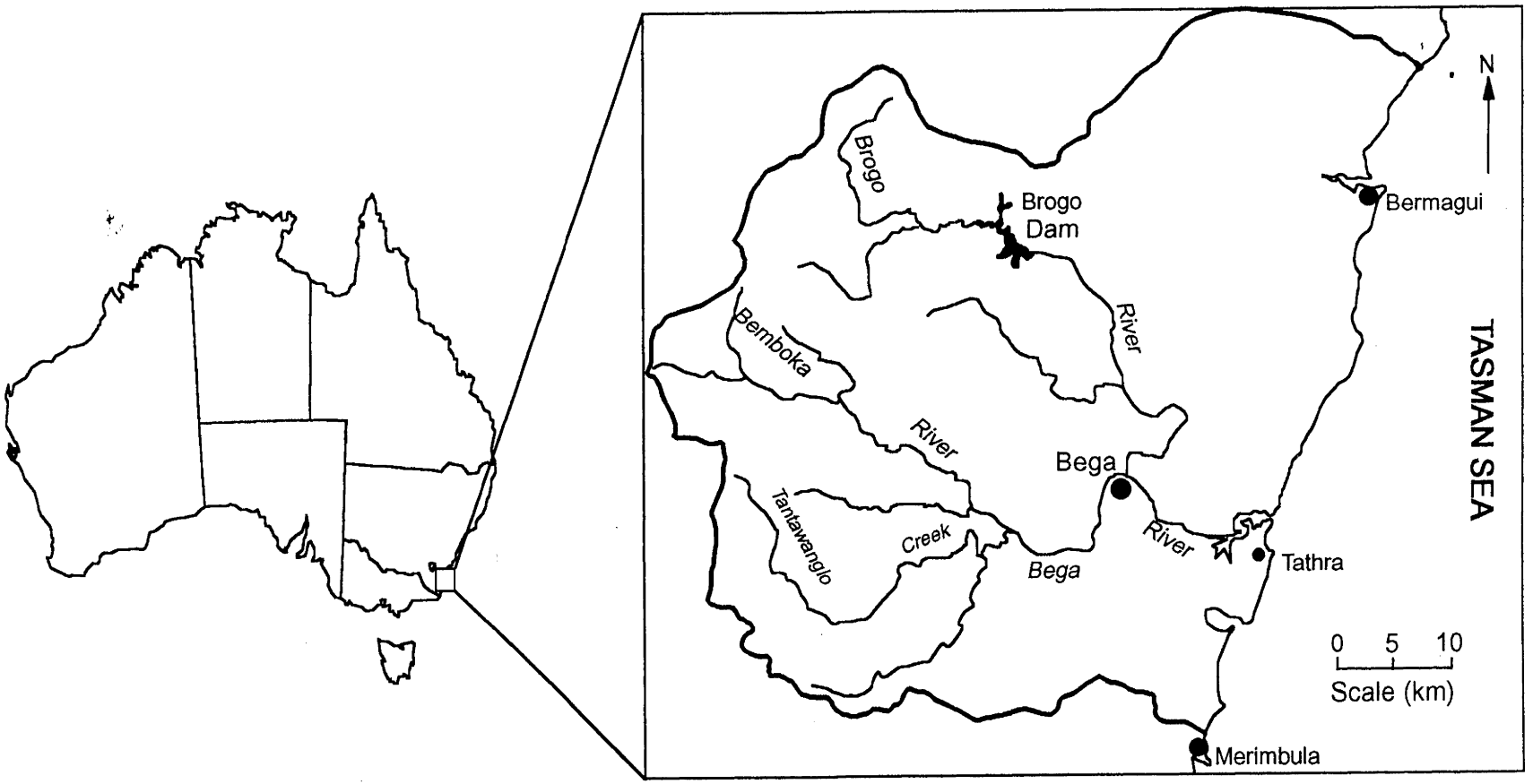

Figure 5.1 The Bega River catchment

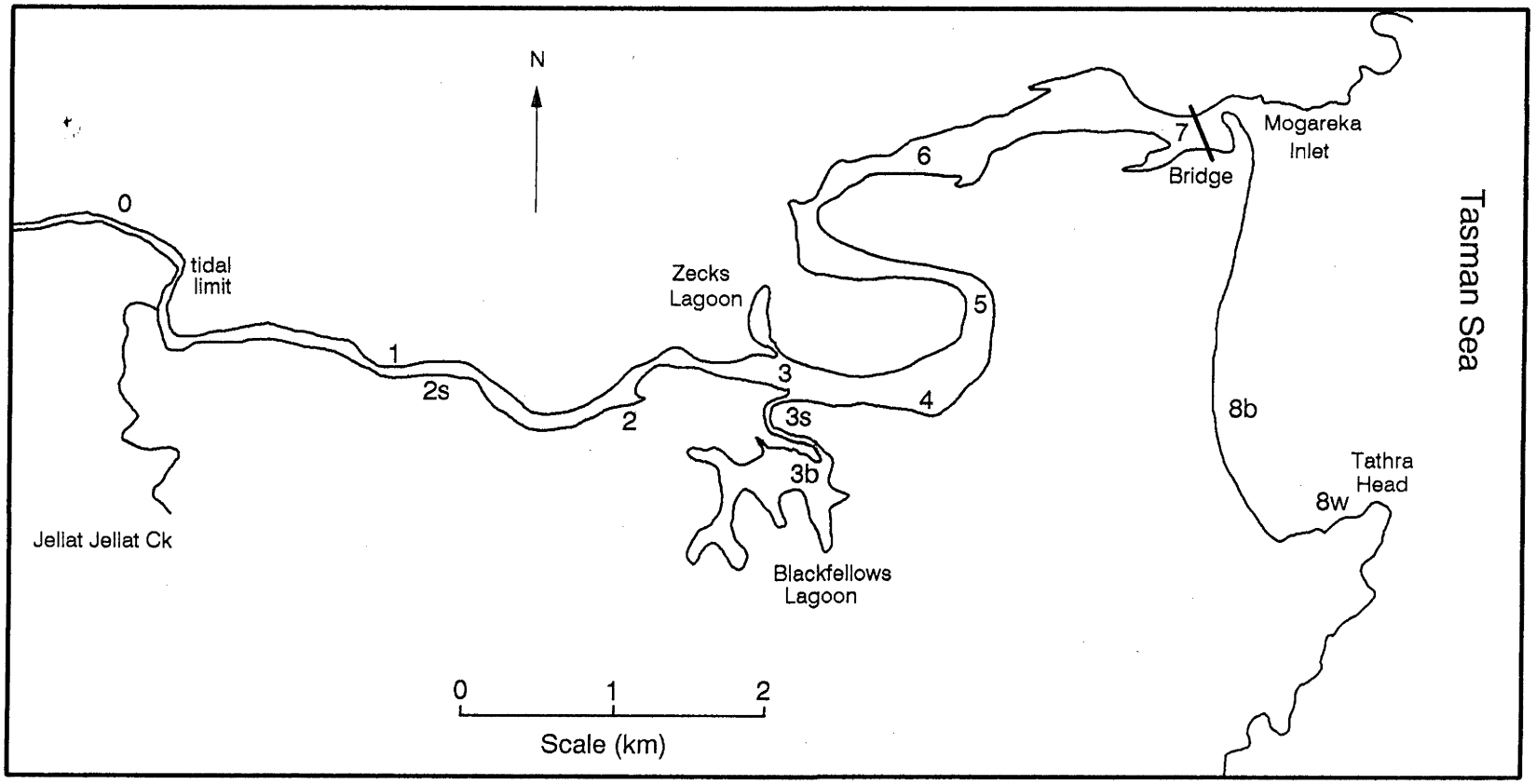

Figure 5.2 The Bega River estuary, showing the location of sampling sites.

There is a general increase in the depth of the river towards its mouth. A longitudinal depth profile of the lower 8 km of the estuary, taken at high tide, is shown in Figure 5.3. The depth readings were taken using an echo sounder, and the profile was obtained by taking depth traces of continuous diagonal crossings of the river. Each point in Figure 5.3 represents the approximate average depth of the river of each crossing at a distance downstream of the tidal limit defined by the mid-point of that crossing. The average depth of the river at high tide was ~2.5 m in the main channel in the upper region of the estuary, increasing to 3-4 m nearer its mouth. Localised areas up to 14 m deep were found about 2.5 km upstream of the mouth. There are at least two back-flow lagoons in the estuary. The largest of these, Blackfellows Lagoon, is shallow with an average depth of about 1 m.

At its mouth, water flow in and out of the estuary is restricted by a sand-bar, the position of which is largely governed by the flow of the river. At the time of sampling low flow conditions prevailed, and the width of the mouth was only about 50 m. During periods of low flow, the movement of water in the estuary is greatly influenced by the level of the tides.

5.2.2 Regional geology

The geology of the catchment of the Bega River and its tributaries is dominated by the Bega Batholith. This granite is the most easterly of the meridionally trending batholiths of the Lachlan Fold Belt, and is of Late Silurian to Early Devonian age. It comprises a series of plutons intruding a sequence of folded quartz rich greywackes and slates of probable Ordovician age. The geology and geochemistry of these plutons has been described in detail by Lesh (1975). The upper catchment of the Brogo River west of Mt. Murrabrine contains Upper Devonian sediments of the Merimbula Group. Nearer the coast the river course is confined by recent Tertiary gravels, sands and clays.

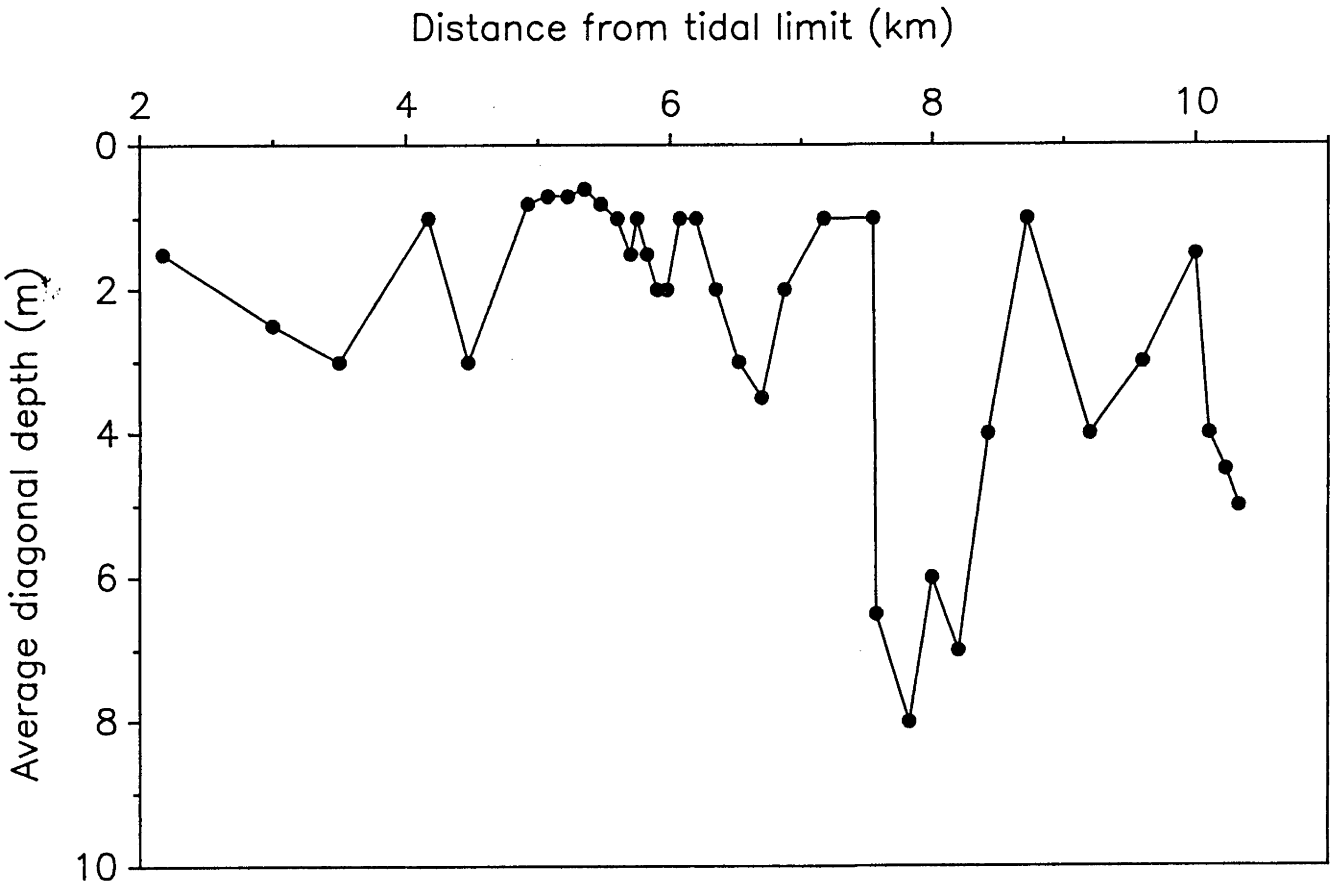

Figure 5.3 A depth profile of the Bega River estuary.

5.3 Sample Collection and Analyses

5.3.1 Sampling program

Water and suspended samples were collected from sites along the estuary on two occasions: 11-13 September and 19-20 November 1991. During September sampling was land-based and was undertaken from the bank of the river. Due to the inaccessibility of some sections of the river, only five sites were sampled. To improve access to the estuary, a boat was chartered in November for one day, enabling the collection of a more complete set of samples at desired salinities. Seven sites were sampled downstream of the tidal limit on this occasion, and spanned an 8 h period of rising and falling tide. An additional site upstream of the tidal limit was sampled on the following day. A 40 L seawater sample was collected from Tathra Wharf (site 8w) about 3 km south of Mogareka Inlet. Sediment grab samples were taken from the river bed at sites 0 and 5, and Blackfellows Lagoon (site 3b) using an Eckman Grab sampler. Beach sand grab samples were also taken approximately 2 km north and south of Mogareka Inlet; at Tathra beach (site 8b), and Nelsons Beach (site 8n). All sites except site 8n are located in Figure 5.2.

5.3.2 Sampling methods

Water was pumped from the river at a depth of about 0.3 m using a Mono pump through plastic hose into a continuous flow centrifuge (CFC) (Alpha-Laval, model no. MAB103b). During centrifugation the water was drawn out by a second pump, resulting in a continuous flow of water through the CFC. Suspended sediment greater than approximately 1 μm was retained in the centrifuge (Murkes 1967). The flow rate was about 10 L/min, and was maintained by adjustment of an inlet water by-pass valve. The pH and electrical conductivity (EC) of the inlet water was monitored during sampling and ten 400 mL samples of inlet water were collected at regular intervals and poured into a plastic bottle. A sub-sample was taken to determine the average pH and EC of the water during sampling. The centrifuged sediment was quantitatively washed into a 2 L plastic bottle with river water.

5.3.3 Laboratory analyses

Water samples: The inlet water samples were filtered through pre-washed, pre-weighed 0.45 μm membrane filters. These filters were dried at 50°C overnight, allowed to cool in a dessicator and re-weighed. After correction for losses using blank filter determinations, the suspended solids concentration for each sample was calculated. These filters were retained for possible radiochemical analysis.

The filtrate from each sample was collected and 60 mL retained for analysis of major cations and anions by AAS (section 3.4). The remaining 3-4 L was acidified with 1 mL HCl per litre and stored for determination of radium and thorium activities by alpha spectrometry.

CFC samples: The CFC sediment-water suspension was centrifuged at approximately 3000 rpm for 10 min using a laboratory centrifuge and the supernatant decanted. After washing with demineralised water and centrifuging again, the sediment cake was transferred into an open plastic container and placed in a drying cabinet overnight at 50°C. The weight of dry sediment was recorded, and a portion (0.1-0.2 g) retained for X-Ray Diffraction (XRD) analysis. The remainder was weighed, ashed at 450°C for 4 h, and re-weighed after cooling in a dessicator to determine the loss on ignition (LOI). This portion was retained for radionuclide and major cation analysis.

Bed Sediments: The bed sediment samples were wet-sieved to obtain a series of particle size fractions. The <2 um and <20 μm size fractions (classified as the clay, and fine-medium silt and clay fractions by the Standards Association of Australia classification system) were separated from the finest wet-sieved fraction (<63 μm) using suspension settling techniques (section 3.5). The size fractions were then dried at 50°C.

5.3.4 Radiochemical analysis

Water and dried sediment samples were analysed for radium and thorium isotopes using radiochemical separation techniques and alpha-particle spectrometry (chapter 3). Where appropriate, the nuclide activities were

corrected for decay or ingrowth between collection and analysis, so that the reported activities refer to the time of collection.

5.4 Water Quality Parameters

Results for various parameters measured in water samples from all sites are given in Table 5.1. Concentrations of major cations and anions are shown in Table 5.2. In accordance with common practice, all ions present in the filtrate are referred to as dissolved ions.

5.4.1 Salinity and pH

The total salt concentration of water is commonly expressed in two ways; as EC units (μS/cm), or as parts per thousand (ppt) dissolved salts. The former was measured in all water samples in the laboratory, whereas the latter units were calculated by summing all major cation and anion concentrations of samples collected in November only. Major ion concentrations were not determined on the September samples, and their salinity values (as ppt) were derived from the EC-salinity relationship of the November data. Both units are listed in Table 5.1, although future reference to 'salinity' in this thesis will be in units of ppt derived from EC measurements. The term 'salinity' is used here in the oceanographic sense (see footnote, section 1.3), as the salt content of the Bega estuary is dominated by the contibution of seawater.

Water salinity increased along the length of the estuary from a low of 0.1 ppt (EC = 224 μS/cm) at site 0, to 27 ppt (33,800 μS/cm) at site 7. The EC of water 7 km upstream of site 0 (229 μS/cm) was virtually the same as site 0. This indicates that the water at site 0, upstream of the section of the river denoted as the tidal limit (Topographic Map Bega 8824-I-S, Central Mapping Authority, N.S.W.) was uncontaminated by seawater at the time of sampling, and can be considered representative of the freshwater input to the estuary. If the salinity of a seawater sample collected from Tathra wharf (35 ppt) is assumed to represent the salinity of coastal seawater in the vicinity of the Bega estuary, the seawater component of the estuarine samples ranged from about 2% at site 1, to 75% at site 7.

Table 5.1 Water quality parameters of water samples collected from the Bega River in September and November 1991.

site no.	distance from tidal limit (km)	EC (uS/cm)	salinity (ppt)	% sea water	pH	suspended sediment LOI[a] (%)	suspended sediment conc.[b] (mg/L dry wt.)
September 12-13							
1	2.1	297	0.1	0	7.30	18.2	1.6
2s	2.3	2020	1.6	1.4	7.42	18.9	1.6
3s	4.9	14840	9.6	26.8	7.72	18.9	3.7
5	7.1	22900	16.0	44.7	7.86	21.2	4.5
7	11.0	33400	26.3	73.9	8.06	20.4	4.5
November 19-20							
0	-0.3	224	0.1	0	7.25	18.1	1.7
1	2.1	1447	0.8	1.9	7.57	17.4	2.0
2	3.6	4010	2.2	5.9	7.69	33.7[c]	3.2
3	4.8	7660	4.4	12.2	7.83	17.4	3.1
4	5.7	15590	10.0	28.0	7.96	16.1	5.2
5	7.0	21400	14.9	41.7	8.00	18.4	3.8
6	9.3	27400	20.0	56.1	8.03	23.4	2.9
7	11.0	33800	26.7	74.8	8.05	28.4	1.8
8k	14.0	44800	35.6	100	8.03	n.d.	0.7

[a] Loss on ignition obtained from CFC sediment.
[b] Concentration of suspended particulates >0.45μm.
[c] High LOI probably due to high algal content.
n.d. not determined due to insufficient mass.

Table 5.2 Dissolved cation and anion concentrations in the Bega River estuary, November collection.

site	salinity (ppt)	Na	K	Ca	Mg	Fe	Mn	Al	Si	Cl	SO_4
						(mg/L)					
0	0.1	22	2	11	6	<0.02	<0.05	<1	7.54	34	5
1	0.8	230	11	19	31	<0.02	<0.05	<1	6.82	410	56
2	2.2	660	30	35	82	<0.02	<0.05	<1	6.45	1200	170
3	4.4	1340	60	58	161	<0.05	<0.05	<1	5.95	2440	331
4	10.0	3090	140	130	375	<0.1	<0.05	<1	4.80	5760	555
5	14.9	4580	200	179	542	<0.1	<0.05	<1	3.88	8250	1160
6	20.0	6180	280	258	751	<0.2	<0.05	<1	2.63	11300	1560
7	26.7	8170	370	321	1020	<0.3	<0.05	<1	1.51	15000	1770
8	35.6	11100	460	444	1260	<0.4	<0.05	<1	0.05	20300	1970

The pH of the river also increased along the length of the estuary, ranging from a freshwater value of about 7.3 to the seawater value of 8.03 at the mouth.

5.4.2 Dissolved silicon

Dissolved silicon concentrations are listed in Table 5.2. Figure 5.4 shows the silica-salinity plot to be linear with a negative slope. A linear relationship between concentration and salinity is typical of conservative behaviour of an element in an estuary (Moore 1990), and indicates that there has been little or no net gain or loss of that element from the water column. On this basis it would appear that processes such as the dissolution of minerals and/or biological precipitation of silica are not of major importance. The probability that these two opposing processes would exactly compensate each other to produce a linear plot is low.

5.4.3 Suspended sediment

A comparison of the XRD analyses of the November collection of CFC sediment from sites 0 and 7 indicated that there was no observable change in clay mineralogy along the length of the estuary. The presence of a peak with a 'd' spacing of 10 angstroms indicated the presence of the layered silicates, mica and/or illite. Given the particle size of the suspended sediment is likely to be <20 μm, the mineral is probably illite. The presence of the clay mineral kaolinite and possibly halloysite are also indicated, together with quartz and feldspars. The CEC of the suspended sediment at site 0 was found to be 28 meq/100 g.

The suspended sediment concentrations >0.45 μm at each site are listed in Table 5.1, together with the % LOI for the corresponding CFC sediment. Suspended sediment concentrations were extremely low throughout the estuary (maximum 5.2 mg/L at site 4), and are indicative of the low flow conditions prior to and during both sampling periods. There had been no significant rain in the Bega Basin for at least a month prior to sampling in September and November. High concentrations of suspended sediment typically occur during high river flows, stimulated by rainfall run-off within the

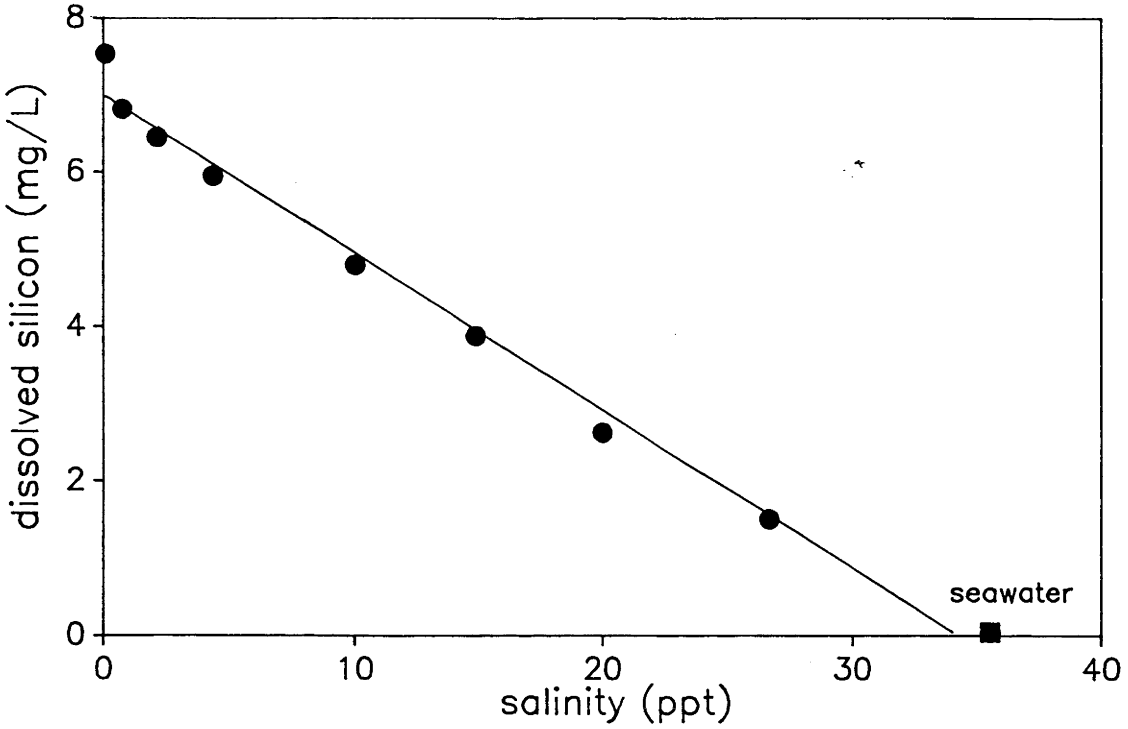

Figure 5.4 A plot of dissolved silicon and salinity, illustrating the conservative mixing of the river and seawater end-members.

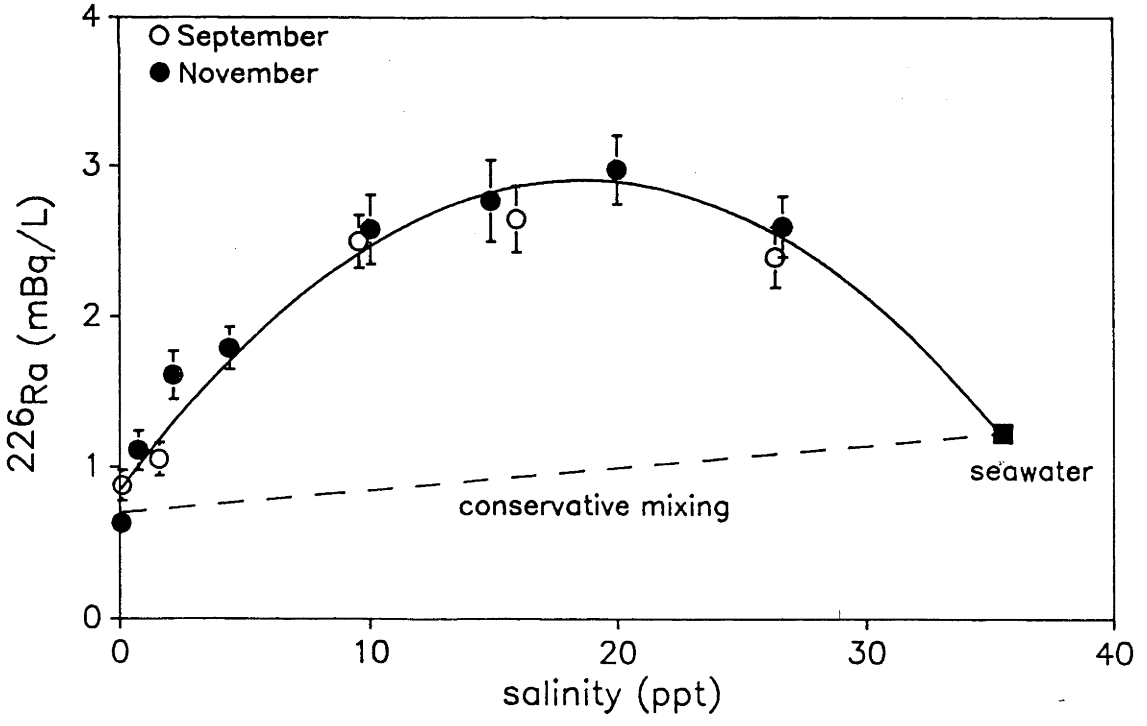

Figure 5.5 Dissolved ^{226}Ra concentrations as a function of salinity. The dashed line is the concentration expected from the conservative mixing of the river and seawater end-members. The fact that the estuarine values are greater than either end-member indicates an additional source of ^{226}Ra.

catchment of the river and its tributaries. The concentrations from both collection periods show a general increase towards the middle of the estuary. The November concentrations then decline towards the mouth, probably as a result of dilution by seawater containing low particulate concentrations (0.7 mg/L). The maximum concentrations are well above the values measured for both end-members, indicating that some suspended material (~3 mg/L) has been added to the water column. Possible sources of this additional material include flocculated colloids, and/or resuspended bottom sediments.

As discussed in section 5.1, colloids <0.45 μm in size which are present in freshwater, such as complexes of iron, manganese, and organic species, may flocculate when mixed with saline water, increasing the concentration of suspended material >0.45 μm. Dissolved iron and manganese concentrations at site 0 (Table 5.2) are <0.02 and <0.05 mg/L respectively. Even if their combined dissolved concentrations were as high as 0.10 mg/L and they completely precipitated as hydroxides, dissolved iron and manganese could not have contributed more than about 0.2 mg/L (dry wt) to the suspended solids concentration of the estuary. Concentrations of dissolved organics were not determined, but if flocculation of significant quantities of organic colloids were responsible for the increase in suspended sediment, this should be reflected by an increase in their LOI values. Apart from an anomalously high value at site 2 which had a suspected high algal content, there is no observable LOI increase in the salinity range 0-15 ppt. This is well above the salinity range (0-5 ppt) in which the greatest removal of dissolved humic acids were observed by Sholkovitz et al. (1978). Although flocculation of colloids <0.45 μm may be occurring in this estuary, it is not likely that this process can account for the observed increase in the suspended sediments.

A more likely explanation, discussed in detail in sections 5.6.1 and 5.7.3 below, is the resuspension of bottom sediments. This was probably due to wind and tidal effects, although disturbance of bottom sediments by the boat's propeller during sampling cannot be completely ruled out. Particular care was taken, however, to avoid this possibility. The boat was flat-bottomed and sites were chosen which were at least 2 m in depth. Water was pumped from a depth of no more than 0.3 m. Moreover, the river

became deeper and wider in the region of the estuary where the highest suspended sediment concentrations were measured, indicating that the higher values were not an artifact of sampling.

5.5 Dissolved Radionuclides

5.5.1 Thorium isotopes

Dissolved thorium isotope concentrations are given in Table 5.3. There is no detectable ^{232}Th at any site, with all values less than 0.08 mBq/L at the 1 sigma (67% confidence) level. Thorium-230 activities are also below detection, with the possible exceptions of site 5 in September, and site 4 in November. Due to spectral interferences, the standard errors of ^{230}Th determinations are higher than ^{232}Th. Thorium-228 activities are also low; only in the November collection from site 5 (0.14 ±0.06 mBq/L) is there

Table 5.3 Dissolved thorium isotope concentrations in Bega River water.

site	salinity (ppt)	^{232}Th	^{230}Th (mBq/L)	^{228}Th*
September 11-13				
1	0.1	0.05 ±0.03	0.03 ±0.03	0.06 ±0.05
2s	1.6	0.04 ±0.04	0.05 ±0.05	0.14 ±0.09
3s	9.6	0.04 ±0.04	0.05 ±0.05	0.11 ±0.09
5	16.0	0.01 ±0.02	0.08 ±0.03	0.01 ±0.05
7	26.3	0.02 ±0.02	0.05 ±0.03	0.08 ±0.05
November 18-20				
0	0.1	0.02 ±0.02	0.03 ±0.03	0.06 ±0.05
1	0.8	0.02 ±0.02	0.03 ±0.03	0.06 ±0.05
2	2.2	0.02 ±0.03	0.09 ±0.05	0.05 ±0.06
3	4.4	0.02 ±0.02	0.04 ±0.03	0.01 ±0.04
4	10.0	0.01 ±0.03	0.14 ±0.06	0.11 ±0.06
5	14.9	0.03 ±0.02	0.06 ±0.04	0.14 ±0.06
6	20.0	-0.02 ±0.02	0.04 ±0.03	0.02 ±0.04
7	26.7	0.00 ±0.02	0.02 ±0.03	0.01 ±0.04
8w	35.6	-0.02 ±0.02	0.00 ±0.04	0.05 ±0.07

* ^{228}Th activities corrected to date of collection to allow for ingrowth from ^{228}Ra

possibly any detectable activity. Any dissolved ^{228}Th activity is almost certainly due to 'in situ' ingrowth from its dissolved parent, ^{228}Ra (Moore 1967), the concentration of which increases rapidly as the water becomes more saline (section 5.8.2 below). Sanstchi et al. (1979) concluded that the removal rate of dissolved and colloidal thorium isotopes was quite rapid, and increased at higher particulate concentrations. Even though suspended sediment concentrations in the Bega River are low, the ^{228}Th concentrations also remain low in the estuary, even near the mouth of the estuary (sites 6 and 7) where ^{228}Ra concentrations are close to their maximum (see section 5.8.2 below). This suggests that dissolved ^{228}Th produced in the water column is being continually scavenged by suspended sediment.

5.5.2 Dissolved Radium

Dissolved radium isotope concentrations are shown in Table 5.4, together with ratios of the shorter-lived isotopes (^{224}Ra, ^{223}Ra, ^{228}Ra) to that of ^{226}Ra. The behaviour and origins of the short-lived isotopes are discussed separately in section 5.8.2.

The non-conservative behaviour of ^{226}Ra in the estuary is illustrated by a plot of concentration versus salinity (Figure 5.5). Both the September and November collections data sets show a similar trend; an increase in concentration from the freshwater end of the river to a maximum at a salinity value of 20 ppt (site 6, November). There is a slight decrease in ^{226}Ra at site 7 towards the seawater value, represented by the sample collected from site 8w.

If radium was behaving conservatively in the estuary, as was the case for silicon, the dissolved ^{226}Ra concentrations should lie on the straight line joining the two end-members (dashed line, Figure 5.5). The fact that ^{226}Ra concentrations within the mixing zone lie well above this line is evidence that there is an additional source of dissolved radium within the estuary. As discussed in section 5.1, previous studies have identified these sources as river-borne suspended sediments and estuarine bottom sediments.

5.6 Radionuclides in Suspended Sediment

This section presents and discusses the radionuclide concentrations of the CFC sediment in September and November 1991. The thorium and radium isotope concentrations and their AR's are given in Table 5.5.

5.6.1 Thorium isotopes

The November data show an increase in the activities of all thorium isotopes towards the middle of the estuary. Figure 5.6 shows a plot of the ^{232}Th suspended sediment concentration against salinity. Some of this increase could be due to adsorption of dissolved thorium by newly flocculated colloids, formed as a result of increasing salinity. If an upper estimate of 0.04 mBq/L is taken for the freshwater ^{232}Th concentration (Table 5.3, site 0), and all this activity was subsequently incorporated into the suspended sediment (average concentration 3 mg/L), an increase of about 13 mBq/g would be observed in the ^{232}Th concentration of the suspended sediment. This is 50% of the maximum observed increase of 26 ±4 mBq/g at sites 4 and 5.

Alternatively the concentration increase could be due to an increase in the proportion of clay minerals in the suspended sediment. Clay sized particles typically have higher concentrations of radionuclides than larger particles (Scott 1968; Megumi and Mamuro 1977). An increase in the fraction of suspended clays in the water column could occur either by the settling of coarse particles, or the resuspension flocculated clay particles in bottom sediments. As discussed below, the latter is the most likely explanation.

Although the absolute thorium concentrations in the suspended sediment vary, a plot of $^{230}Th/^{232}Th$ against salinity (Figure 5.7) indicates that this ratio remains constant within statistical error, along the length of the estuary. Ten of the 13 values are within their quoted uncertainties (1 standard deviation, 67% confidence limit) of the weighted mean (0.716 ±0.008), represented by the horizontal line in Figure 5.7. Twelve of the 13 values are within 2 standard deviations (95% confidence limit).

Table 5.4 Dissolved radium isotope concentrations and activity ratios in Bega River water.

site	salinity (ppt)	^{226}Ra	^{228}Ra[a]	^{223}Ra[a]	^{224}Ra[a]
			mBq/L		
September 11-13					
1	0.1	0.88 ±0.10	1.7 ±0.3		
2s	1.6	1.06 ±0.11	2.5 ±0.4		
3s	9.6	2.50 ±0.17	8.7 ±0.9		
5	16.0	2.65 ±0.22	8.9 ±0.9		
7	26.3	2.40 ±0.20	6.2 ±0.8		
November 18-20					
0	0.1	0.63 ±0.08	1.3 ±0.2	0.03 ±0.02	1.1 ±0.4
1	0.8	1.11 ±0.13	3.7 ±0.6	0.12 ±0.06	4.0 ±0.9
2	2.2	1.61 ±0.16	5.8 ±0.9	0.23 ±0.11	7.9 ±1.8
3	4.4	1.79 ±0.14	6.7 ±0.8	0.50 ±0.14	9.4 ±1.8
4	10.0	2.58 ±0.23	11.4 ±1.4	0.98 ±0.27	20.2 ±3.1
5	14.9	2.77 ±0.27	13.9 ±1.8	1.33 ±0.27	21.1 ±2.9
6	20.0	2.98 ±0.23	14.4 ±1.5	1.06 ±0.23	24.9 ±3.1
7	26.7	2.60 ±0.20	12.9 ±1.5	1.29 ±0.23	28.2 ±3.2
8w	35.8	1.30 ±0.08	0.7 ±0.1	0.21 ±0.04	3.07 ±0.34
5[b]	14.4	3.08 ±0.21	17.2 ±1.9	2.63 ±0.39	72.7 ±7.6

site	salinity (ppt)	$^{228}Ra/^{226}Ra$	$^{224}Ra/^{226}Ra$	$^{223}Ra/^{226}Ra$	$^{224}Ra/^{223}Ra$
September 11-13					
1	0.1	1.94 ±0.30			
2s	1.6	2.39 ±0.32			
3s	9.6	3.47 ±0.28			
5	16.0	3.35 ±0.19			
7	26.3	2.59 ±0.23			
November 18-20					
0	0.1	2.03 ±0.28	1.7 ±0.5	0.05 ±0.03	34 ± 22
1	0.8	3.37 ±0.37	3.6 ±0.7	0.11 ±0.05	34 ± 15
2	2.2	3.63 ±0.41	4.9 ±1.1	0.14 ±0.07	35 ± 17
3	4.4	3.75 ±0.32	5.2 ±0.6	0.28 ±0.06	19 ± 4
4	10.0	4.42 ±0.37	7.8 ±1.0	0.38 ±0.10	21 ± 5
5	14.9	5.02 ±0.44	7.6 ±0.8	0.48 ±0.09	16 ± 3
6	20.0	4.83 ±0.34	8.4 ±0.8	0.36 ±0.07	23 ± 5
7	26.7	4.98 ±0.43	10.9 ±0.9	0.50 ±0.08	22 ± 4
8w	35.8	0.57 ±0.05	2.4 ±0.2	0.17 ±0.03	14 ± 4
5[b]	14.4	5.57 ±0.47	23.6 ±1.9	0.86 ±0.11	28 ± 3

[a] ^{228}Ra, ^{223}Ra and ^{224}Ra activities corrected to the time of collection
[b] pore water sample collected ~100m downstream of site 5 in July 1992

Table 5.5 Thorium and radium isotope concentrations and activity ratios in suspended (CFC) sediment, Bega River.

site	salinity (ppt)	^{232}Th	^{230}Th	^{228}Th	^{226}Ra	^{228}Ra
			mBq/g dry wt.			
September 11-13						
1	0.1	64.4 ±2.4	46.3 ±2.0	79.6 ±2.8	52.8 ±2.5	88.9 ±6.9
2s	1.6	60.4 ±2.3	43.0 ±1.9	73.0 ±2.7	38.4 ±2.1	65.0 ±5.5
3s	9.6	64.9 ±2.2	46.1 ±1.7	61.4 ±2.1	32.2 ±1.3	48.4 ±3.9
5	16.0	61.2 ±2.2	48.0 ±1.9	70.2 ±2.4	26.5 ±1.0	38.2 ±3.0
7	26.3	55.5 ±2.2	40.4 ±1.8	60.3 ±2.4	23.8 ±1.6	31.9 ±3.4
November 18-20						
0	0.1	65.9 ±2.0	49.2 ±1.6	84.6 ±2.3	64.3 ±3.1	106.7 ±7.2
1	0.8	65.2 ±2.1	44.1 ±1.6	83.0 ±2.5	60.7 ±2.5	117.1 ±7.8
2	2.2	60.0 ±2.2	43.4 ±1.8	76.5 ±2.6	43.8 ±2.2	84.9 ±5.8
3	4.4	76.7 ±3.0	57.0 ±2.4	89.6 ±3.3	43.6 ±1.6	89.5 ±5.7
4	10.0	91.8 ±3.4	63.0 ±2.6	79.8 ±3.0	39.0 ±1.8	63.2 ±5.0
5	14.9	91.6 ±3.4	62.3 ±2.6	83.7 ±3.1	36.1 ±1.9	59.6 ±5.2
6	20.0	74.7 ±3.0	54.1 ±2.4	71.6 ±2.9	32.2 ±1.8	53.8 ±4.9
7	26.7	72.3 ±2.3	51.4 ±2.1	68.3 ±2.5	29.2 ±1.6	50.8 ±4.5
8w[a]	35.6	9.0 ±1.6	9.9 ±1.8	16.1 ±2.3	11.4 ±1.9	11.2 ±2.7

site	salinity (ppt)	$^{226}Ra/^{232}Th$	$^{230}Th/^{232}Th$	$^{228}Ra/^{226}Ra$	$^{228}Th/^{232}Th$
September 11-13					
1	0.1	0.820 ±0.049	0.719 ±0.033	1.68 ±0.10	1.24 ±0.05
2s	1.6	0.636 ±0.042	0.713 ±0.034	1.69 ±0.11	1.21 ±0.05
3s	9.6	0.496 ±0.026	0.711 ±0.028	1.50 ±0.10	0.95 ±0.03
5	16.0	0.433 ±0.023	0.774 ±0.032	1.44 ±0.10	1.13 ±0.04
7	26.3	0.429 ±0.033	0.729 ±0.036	1.34 ±0.11	1.09 ±0.05
November 18-20					
0	0.1	0.976 ±0.056	0.746 ±0.026	1.66 ±0.06	1.28 ±0.04
1	0.8	0.931 ±0.049	0.676 ±0.026	1.93 ±0.10	1.27 ±0.04
2	2.2	0.730 ±0.045	0.723 ±0.031	1.94 ±0.09	1.28 ±0.05
3	4.4	0.568 ±0.030	0.743 ±0.031	2.14 ±0.11	1.17 ±0.04
4	10.0	0.425 ±0.025	0.686 ±0.027	1.62 ±0.06	0.87 ±0.03
5	14.9	0.394 ±0.025	0.680 ±0.028	1.65 ±0.11	0.91 ±0.03
6	20.0	0.431 ±0.030	0.724 ±0.034	1.67 ±0.12	0.96 ±0.04
7	26.7	0.404 ±0.026	0.711 ±0.030	1.74 ±0.13	0.95 ±0.04
8w[a]	35.6	1.27 ± 0.31	1.10 ± 0.27	0.96 ±0.19	1.79 ±0.39

[a] seawater particulates >0.45 μm.

The $^{228}Th/^{232}Th$ AR however is not constant along the length of the estuary. Figure 5.8 shows that this ratio remains relatively stable at a value of about 1.28 ±0.05 for the first three sites, then decreases rapidly to a minimum value at site 4 (0.87 ±0.03), before slowly increasing again. Although both ^{232}Th and its daughter ^{228}Th are usually in secular equilibrium in rocks and dry soils with an age of more than a few decades, this is often not the case in aqueous systems. Suspended sediment having a $^{228}Th/^{232}Th$ AR greater than one is common in surface waters (e.g. Murray et. al. 1992a), and is attributed to the decay of dissolved ^{228}Ra to produce ^{228}Th, which subsequently sorbs. The continued production of ^{228}Th in solution coupled with its relatively short half-life can result in an increase in the sediment ^{228}Th activity relative to ^{232}Th. It is interesting to note that the suspended sediment activity of ^{228}Ra at site 0 is in excess of its daughter ^{228}Th by 27% ±9, and in excess of its parent ^{232}Th by 63% ±12 (see Table 5.5). This excess has been attributed by J. Olley (pers. comm.) to sorption of radium isotopes in the oxidizing zone in soils, possibly in association with iron precipitation. This process would also lead to a higher $^{228}Th/^{232}Th$ AR, as the ^{228}Th activity in the suspended sediment will grow towards that of ^{228}Ra.

Both the above processes will have contributed towards the suspended sediment $^{228}Th/^{232}Th$ AR attaining a value >1 at site 0. The subsequent decrease to values <1 at sites of higher salinity is almost certainly due to decay of ^{228}Th towards an equilibrium activity with its parent ^{228}Ra, which in turn has decreased due to desorption losses in the estuary (Table 5.5, section 5.6.3 below). If this is the case, the magnitude of the decrease of the $^{228}Th/^{232}Th$ AR should be related to the period of time the sediment has remained in the estuary. Because a considerable fraction of ^{228}Th ($t_{1/2}$ = 1.9 y) activity in the suspended sediment has decayed towards the ^{228}Ra activity, it would appear that the suspended sediment in the mid-estuary region of the Bega estuary has a mean 'estuarine age' of at least 1-2 ^{228}Th half-lives (2-4 y). The flushing time of water in the estuary is expected to be no longer than a few weeks at most (I. Webster, pers. comm.), and so older sediments must have been added to the water column from another source. Given the observed increases in the suspended sediment concentration in the same region of the estuary, the most likely

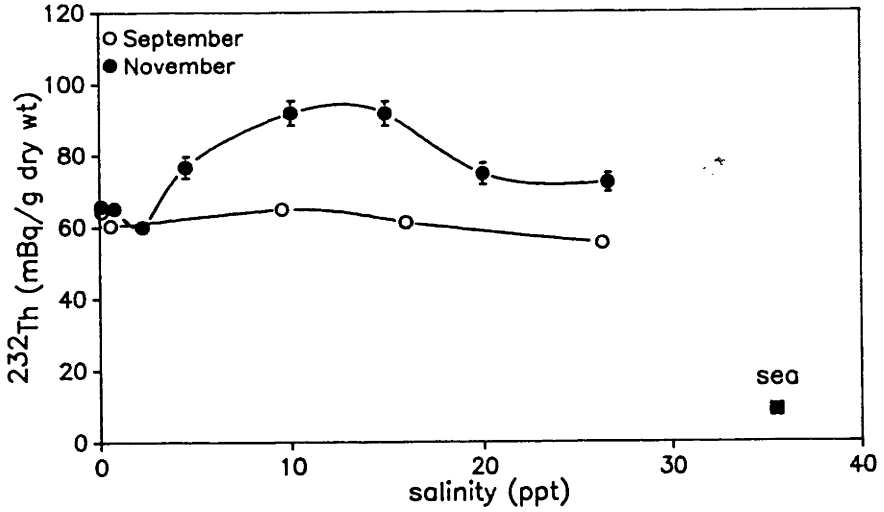

Figure 5.6 Suspended sediment concentrations of ^{232}Th as a function of salinity.

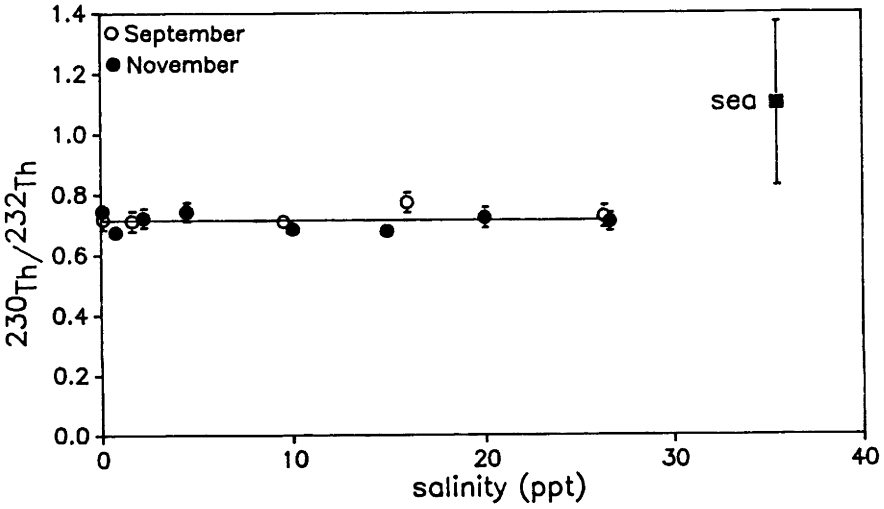

Figure 5.7 The ^{230}Th/^{232}Th activity ratio of suspended sediment plotted against salinity. The solid line represents the weighted mean of all Bega River suspended sediment samples.

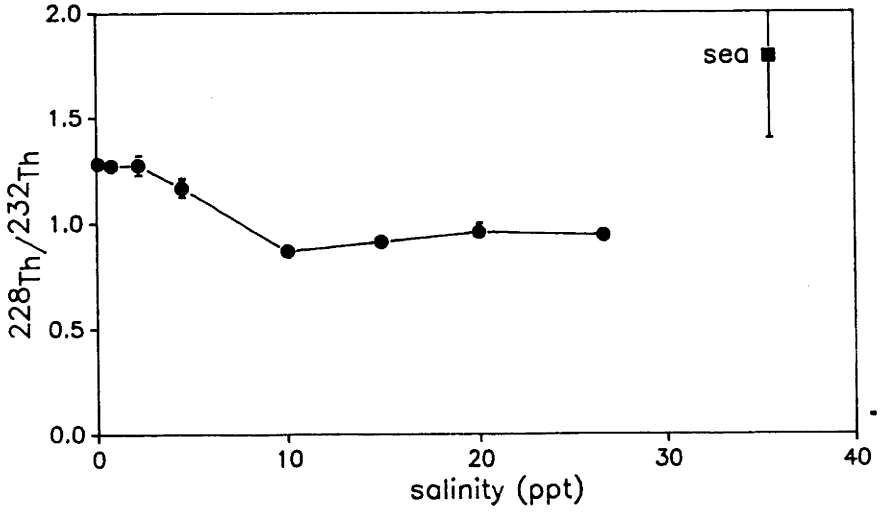

Figure 5.8 The suspended sediment ^{228}Th/^{232}Th activity ratio and salinity (November data only).

source is resuspended bottom sediments. The exact location of this source is considered in section 5.7.3.

5.6.2 Extent of ^{226}Ra desorption

Table 5.5 shows that the ^{226}Ra concentrations of suspended sediment decrease with increasing salinity from the freshwater end of the river to minimum value at site 7. This is opposite to the trend observed for dissolved radium (section 5.5.2), and supports the conclusion reached in previous studies (chapter 2) that ^{226}Ra is increasingly desorbed from sediments as salinity rises. The concentration all radium and thorium isotopes in the suspended material in seawater are much lower than the estuarine suspended sediment, probably because it contains a large component of low activity marine derived particulates.

Any attempt to quantify the loss of radium from the suspended sediment on a dry weight basis is complicated by fluctuations in the sediment ^{226}Ra concentration caused by changes in the particle size and organic content of the sediment, and by dilution of low activity suspended sediment carried in by seawater. Helz et al. (1985) suggested that normalisation of ^{226}Ra concentrations to aluminium may help eliminate the effects of particle size variation. Thorium-232 has also been used in this way (Olley et al. 1990). If sorption of ^{232}Th by suspended sediment in the estuary is negligible, which appears to be the case, the fraction of ^{226}Ra lost from the suspended sediment should be directly related to decreases in the $^{226}Ra/^{232}Th$ AR.

When plotted against salinity, the $^{226}Ra/^{232}Th$ AR in the suspended sediment initially decreases (Figure 5.9), in agreement with the expected desorptive behaviour of radium relative to thorium (section 5.1). The ratio reaches a minimum at a salinity of about 10 ppt (site 4), and remains relatively unchanged at higher salinities in the estuary. This behaviour is similar to that observed by Elsinger and Moore (1980) for the Pee Dee River-Winyah Bay estuary, where the ^{226}Ra suspended sediment concentration reached a minimum at 8 ppt salinity.

For the November data, the $^{226}Ra/^{232}Th$ AR decreases from 0.98 ±0.06 at site 0, to an average value of about 0.41 ±0.01 (weighted mean of

sites 4-7). This decrease represents a loss of 58% ±7 of ^{226}Ra (38 ±3 mBq/g) from the freshwater suspended sediment. The corresponding value for the September data is 50% ±7 (26 ±4 mBq/g). These losses are comparable with results from the Pee-Dee River (Elsinger and Moore 1980) and the Mississippi River (Moore and Scott 1986), but higher than the ~36% ^{226}Ra desorption estimated by Key et al. (1985) for the Amazon River. Moore and Scott (1986) suggested that the high desorption of ^{226}Ra from the Mississippi River suspended sediment was due to its high CEC (54 meq/100 g), which in turn was attributed to the presence of montmorillonite. However this is not a likely explanation for the high loss of ^{226}Ra from the Bega River suspended sediment. XRD analysis of this sediment (section 5.4.3) did not yield any evidence for smectitic clay minerals such as montmorillonite. Although its CEC (28 meq/100 g) is somewhat higher than that expected solely from illite/kaolinite mineralogy, it is still well below the Mississippi value.

Losses of ^{226}Ra (25% ±2) from the suspended sediment have certainly occurred at a salinity of at least 2.2 ppt (site 2). Smaller losses may have occurred at a salinity as low as 0.8 ppt (site 1). However the uncertaintities of the ^{226}Ra/^{232}Th AR determinations for site 0 and site 1 do not allow any decrease in this region to be stated unequivocably.

5.6.3 Relative behaviour of ^{226}Ra and ^{228}Ra

Suspended sediment ^{228}Ra concentrations also show a general decrease with salinity (Table 5.5). However a plot of the ^{228}Ra/^{226}Ra AR against salinity (Figure 5.10) indicates that for the November collection at least, the fraction of each isotope lost from the suspended sediment is not equal. The ratio initially increases as the suspended sediment contacts increasingly saline water, reaching a maximum at site 3 (4.4 ppt) before decreasing to a constant value (within error) at sites 4 to 7. The higher values at low salinities may be due to increases in the dissolved ^{228}Ra/^{226}Ra AR in the water column (Table 5.4, see also section 5.8.2 below). If radium in ion-exchange sites of the suspended sediment is in ion-exchange equilibrium with dissolved radium, the ^{228}Ra/^{226}Ra AR's in the dissolved and ion-exchangeable sediment phases should be the same. This is because all radium isotopes are chemically identical. Consequently,

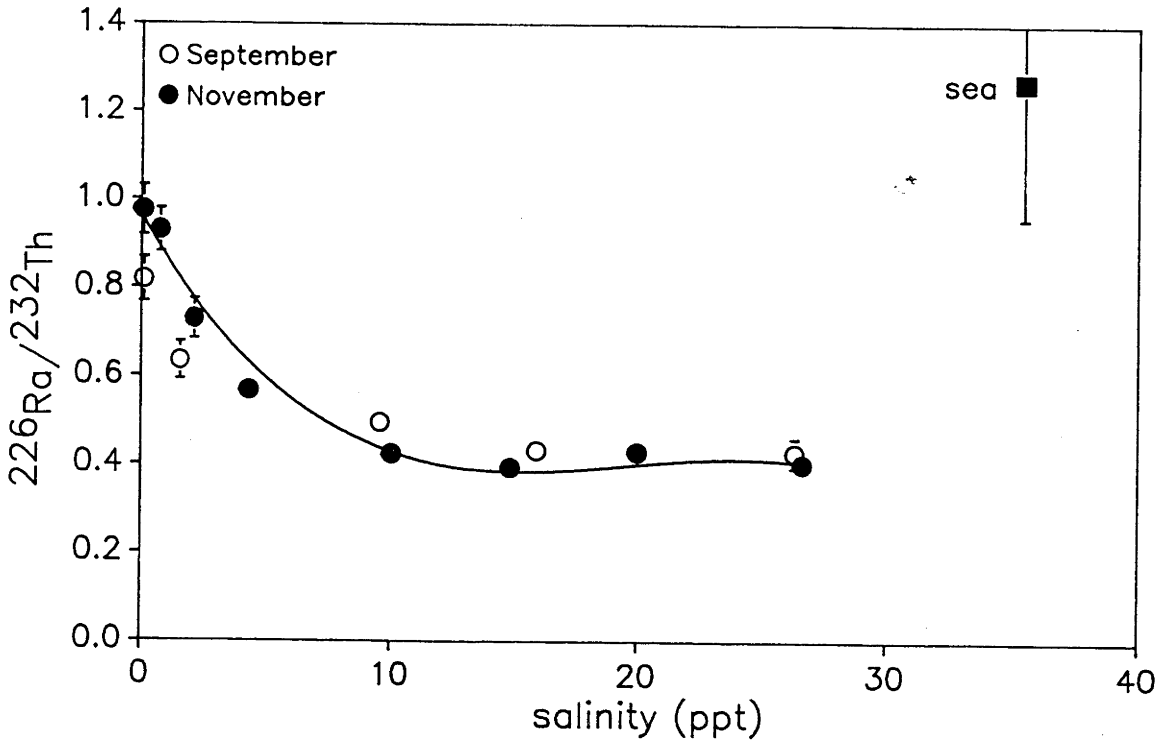

Figure 5.9 The suspended sediment $^{226}Ra/^{232}Th$ activity ratio and salinity.

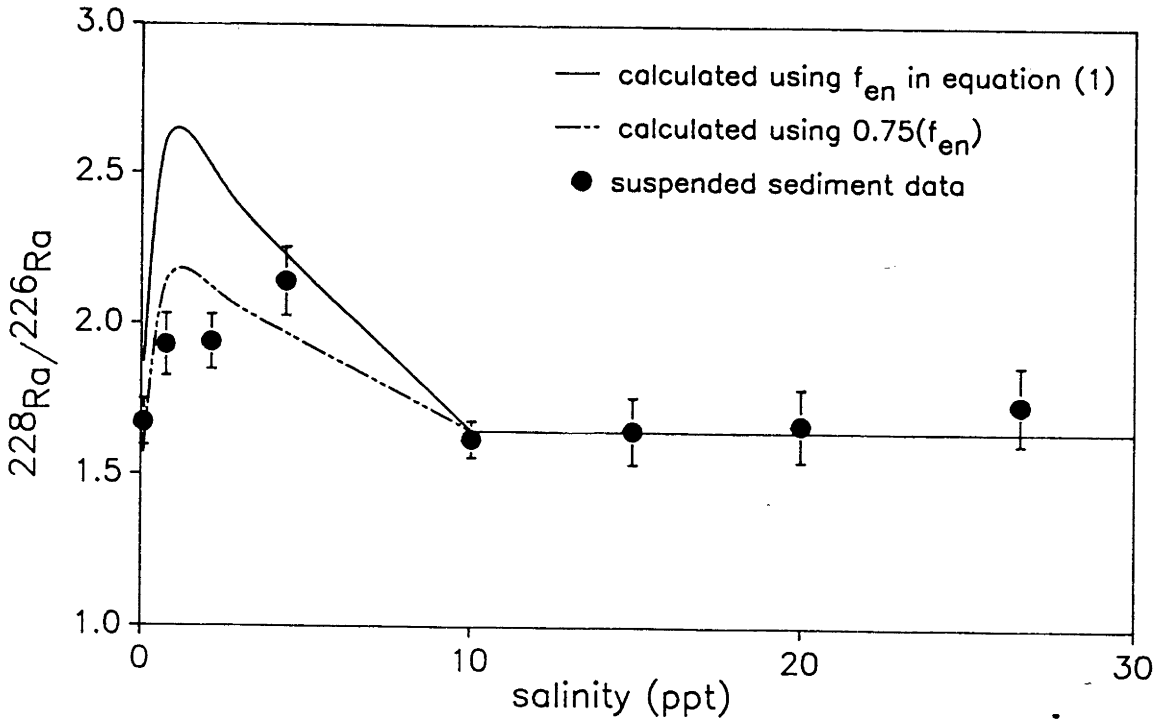

Figure 5.10 The $^{228}Ra/^{226}Ra$ activity ratio and salinity. The lines are fitted as described in section 5.6.3

increases in the dissolved $^{228}Ra/^{226}Ra$ AR will result in an increase in the AR of the associated suspended sediment (sites 1-3). The new suspended sediment AR will depend on the value of the dissolved $^{228}Ra/^{226}Ra$ AR and the fraction of the suspended sediment radium available for ion-exchange. As the salinity of the water continues to rise however, less radium is present on ion-exchange sites, and so the effect of a high dissolved $^{228}Ra/^{226}Ra$ AR is diminished. Consequently, after reaching a maximum the suspended sediment $^{228}Ra/^{226}Ra$ AR decreases to a value representing mainly the non-exchangeable radium fraction (sites 4-7).

It is possible to calculate the theoretical suspended sediment $^{228}Ra/^{226}Ra$ AR at each site using ^{226}Ra desorption information derived in section 5.6.2 above. Here the suspended sediment $^{226}Ra/^{232}Th$ AR at each site is used to derive a measure of the fraction of radium present in the exchangeable phase of the suspended sediment at that site. The fraction of exchangeable radium at site n (f_{en}) is

$$f_{en} = (RT_n - RT_I)/RT_n$$

where RT_n is the $^{226}Ra/^{232}Th$ AR at site n, and RT_I represents the $^{226}Ra/^{232}Th$ AR of suspended sediment which has lost all of its exchangeable radium, and so contains all of its radium in non-exchangeable or internal lattice sites. The value of RT_I is taken as the weighted mean of suspended sediment $^{226}Ra/^{232}Th$ AR's from sites 4 to 7 (Table 5.5, mean = 0.41 ±0.01). At site n, the fraction of ^{226}Ra in non-exchangeable sites (f_{In}) is therefore

$$f_{In} = 1 - f_{en}$$

If dissolved and exchangeable radium are in equilibrium, then the $^{228}Ra/^{226}Ra$ AR's of the dissolved and the exchangeable phases at site n (Rat_{dn} and Rat_{en} respectively) should be the same, i.e.

$$Rat_{dn} = Rat_{en}$$

The $^{228}Ra/^{226}Ra$ AR of the whole suspended sediment at each site can then be calculated from

$$Rat_{cn} = f_{In}.Rat_{I} + f_{en}.Rat_{dn} \qquad (1)$$

where Rat_I is the $^{228}Ra/^{226}Ra$ AR in non-exchangeable sites of the suspended sediment, taken as a weighted mean of the AR's of sites 4 to 7 (= 1.65 ±0.05).

When plotted, the $^{228}Ra/^{226}Ra$ AR's calculated using equation (1) (dashed line, Figure 5.10) show a similar trend to the measured values (filled circles), although the magnitude of the predicted increase at low salinities (sites 0-2) is greater. The discrepancy could be due to the fact that the fraction of ion-exchangeable radium on the suspended sediment (f_{en} in equation (1)), is derived from the extent of radium desorption at high salinities, and may overestimate the 'true' value of f_{en} at low salinities. If this is the case, the consequence will be an overestimate of the overall suspended sediment $^{228}Ra/^{226}Ra$ AR's, as the dissolved AR's (Rat_{wn}) are much higher than the estimate for the internal lattice sites (f_{In}). For example, if the values of f_{en} for sites 0-3 were decreased by a factor of 0.75, a better fit is obtained (solid curve, Figure 5.10). The possibility of a decrease in the mean suspended sediment particle size in the mid-estuary region was discussed in section 5.6.1. Because a large proportion of the ion-exchangeable radium is probably surface-sorbed, any change in the mean particle size, and hence mean surface area of the suspended particulates, would affect the fraction of radium available for ion-exchange. If the mean particle size is indeed greater at the low salinity end of the estuary, the predicted $^{228}Ra/^{226}Ra$ AR's in this region of the estuary would then be greater than the measured values.

5.6.4 Particulates >0.45 μm

The size fraction most commonly used to define the suspended sediment phase in surface waters is the >0.45 μm fraction. Murtz (1967) calculated that a CFC could extract suspended sediment down to a particle size of about 1 μm. Ongley and Blachford (1982) stated that the recovery efficiency of any CFC

apparatus was a function of input sediment concentration, particle size distribution, organic/inorganic ratio of the sediment, temperature and flow rate of water through the centrifuge. They indicated that the mineral sediment recovered could include significant quantities of material <1 μm. In most rivers, this size fraction would normally contain clay minerals whose sorption characteristics are not necessarily the same as coarser size fractions. For this reason, and because of the uncertainty associated with the mimimum particle size recovered by the CFC, the radium and thorium concentrations of the CFC sediment were compared with the concentrations of particulates >0.45 μm retained by the membrane filter after filtration of the total water sample (section 5.3.3). This was done in order to assess how well the sorption behaviour of radium and thorium in the CFC sediment represented the total suspended sediment >0.45 μm.

Only a small amount of sediment (10-20 mg) was able to be recovered by filtration, and long count times (7-8 d) were required to obtain an acceptable level of uncertainty in each measurement (± ~10%). Because the detector time available for counting was limited, the comparison included samples from only two sites. The samples selected were the November collection from site 0, representing the freshwater river input, and site 5, representing the mid-salinity region of the estuary. The results in Table 5.6 show that at site 0 all isotope concentrations in particles >0.45 μm are ~1.5 times higher than the CFC extractable sediment, implying that these nuclides are preferentially concentrated in the fraction of sediment not completely recovered by the CFC. Given the CFC is likely to recover coarse particles with greater efficiency than clay sized particles, and that clays contain higher concentrations of radionuclides, this result is not surprising. However at site 5 all isotope concentrations in the CFC extractable sediment are within error of their concentrations in the particulates >0.45 μm. This result indicates that at this site the CFC was able to recover a sample closely resembling suspended sediments >0.45 μm.

One possible explanation for the apparent difference in the ability of the CFC to recover particles <1 μm at the two sites is that the fine clays present at site 0 have aggregated in saline water to form larger heavier particles. Gibbs and Konwar (1986) observed that the mean suspended particle size of the Amazon River increased from 4 μm to >100 μm with

rising salinity. The aggregated clay particles should then be recovered with greater efficiency by the CFC. A general increase in ^{232}Th concentrations of CFC sediment in the mid-estuary region was noted in section 5.6.1. An increased presence of suspended clay aggregations in the mid-estuary region, whether they were formed 'in-situ' in the water column, or were resuspended older formations, would lead to a higher clay content and hence higher radionuclide concentrations of the CFC sediment.

Table 5.6 Comparison of thorium and radium isotope concentrations and activity ratios in particulates >0.45μm and CFC sediment, Bega River.

site	suspended sediment	^{232}Th	^{230}Th	^{228}Th	^{226}Ra
		mBq/g dry wt.			
0	>0.45 μm	97.4 ±6.1	67.2 ±5.4	116.0 ±9.1	93.9 ±6.4
	CFC	65.9 ±2.0	49.2 ±1.6	84.6 ±2.3	64.3 ±3.1
5	>0.45 μm	80.0 ±6.6	55.6 ±6.1	91.8 ±10.2	40.1 ±6.2
	CFC	91.6 ±3.4	62.3 ±2.6	83.7 ±3.1	36.1 ±1.9

site	suspended sediment	$^{226}Ra/^{232}Th$	$^{230}Th/^{232}Th$	$^{228}Th/^{232}Th$
0	>0.45 μm	0.96 ± 0.09	0.690 ±0.070	1.19 ±0.12
	CFC	0.98 ± 0.06	0.746 ±0.026	1.28 ±0.04
5	>0.45 μm	0.50 ± 0.09	0.695 ±0.095	1.15 ±0.16
	CFC	0.39 ± 0.03	0.680 ±0.028	0.91 ±0.03

Despite the fact that a significant fraction of clay sized particles appear to have been rejected by the CFC at site 0, the $^{226}Ra/^{232}Th$ and $^{230}Th/^{232}Th$ AR's of the particulate fraction >0.45 μm and the CFC extractable sediment are within error. This result is also true for site 5. For this study therefore, the above results are consistent with the premise that the CFC extractable sediment is able to characterise the sorption behaviour of radium and thorium in the total suspended sediment. Nevertheless the uncertainty in the measurement of the particulates >0.45 μm is large (±~10%). To define more precisely the sorption behaviour of radium and thorium in suspended clay particles, further study involving the collection of larger quantities of particles <1 μm is required.

5.7 Bottom sediments

In order to compare the behaviour of radium and thorium as a function of sediment particle size in fresh and saline waters, a suite of particle size fractions <250 μm from two bed sediment samples were analysed. One sediment sample was collected from site 0 representing freshwater sediment, and another was collected from the mid-estuary region (site 5). The water at site 5 had a salinity of 15 ppt at the time of collection, representing an approximate 60:40 mix of river and seawater. The beach sand grab samples from Tathra and Nelson beach were also particle sized. These samples were well sorted due to wave action, and no material <125 μm was recovered. Consequently, only the 125-250 μm size fraction was analysed. The radium and thorium isotope concentrations and AR's of the analysed size fractions are shown in Table 5.7.

5.7.1 Effect of particle size on radium desorption

As with the suspended sediment data, the $^{226}Ra/^{232}Th$ AR's in all bed sediment size fractions are substantially lower in the estuarine sediment compared with freshwater sediment. The difference is greatest in the <2 μm fraction, where the ^{226}Ra activity is lower by 48 ±10% (40 ±8 mBq/g). This value is within error of the corresponding decrease for the suspended sediment derived above. There is a general trend of increasing $^{226}Ra/^{232}Th$ AR with particle size in the estuarine sediment. This trend indicates that less ^{226}Ra has been desorbed from the coarser particles. For example, the $^{226}Ra/^{232}Th$ AR difference between the 125-250 μm size fractions of the fresh and estuarine sediments is only 15% ±9. The apparent high ^{226}Ra loss from smaller particles is probably due to their larger surface area per unit mass, allowing a relatively greater loss of surface sorbed radium.

5.7.2 Sourcing estuarine bed sediments using the $^{230}Th/^{232}Th$ AR

The $^{230}Th/^{232}Th$ AR's of the <2 μm (clay) and <20 μm (silt and clay) particle size fractions from site 0 and site 5 (Table 5.7) all have values which are within error of the mean of all estuarine and freshwater suspended sediment values (0.716 ±0.008). These results are consistent with the expected movement of sediment in the estuary, i.e. the downstream

transport of freshwater sediment particles towards the mouth of the estuary.

There is some evidence that the $^{230}Th/^{232}Th$ AR's of the 63-125 and 125-250 μm size fractions from both sites are lower than the silt and clay fractions, but again the AR's are consistent with downstream transport of these size fractions towards the mouth of estuary. The 125-250 μm size fraction of the beach sand samples (sites 8b and 8n) both have similar, but higher $^{230}Th/^{232}Th$ AR's than the corresponding size fraction of the two river sediment samples, suggesting a different source. The higher $^{230}Th/^{232}Th$ AR (0.77 $\pm$0.03) in the <63 μm fraction may represent a mixture of fluvial clays and fine coastal sand. However, no direct comparison of the <63 μm fraction is available for the beach sands, and it is not clear why coastal input should be significant in only one particle size fraction.

5.7.3 Sources of estuarine suspended sediment

As discussed above in section 5.6.1, resuspended 'older' bottom sediments are a likely source of at least a fraction of the estuarine suspended sediment downstream of site 3. Although the two smallest size fractions (<2 μm and <20 μm) of the estuarine bed sediment sample (site 5) had $^{228}Th/^{232}Th$ AR's somewhat lower than the corresponding fractions from the freshwater sample (site 0), they cannot account for $^{228}Th/^{232}Th$ AR's <1 in the suspended sediment from sites 4 to 7.

The <20 μm fraction from Blackfellows Lagoon however had an extremely low $^{228}Th/^{232}Th$ AR (0.59 $\pm$0.02). This result, together with the fact that all suspended sediment $^{228}Th/^{232}Th$ AR's are significantly lower downstream of the channel connecting the lagoon with the river (downstream of site 3, see Table 5.8), indicates that bottom sediments from Blackfellows Lagoon are a source of resuspended sediment to the estuary. As Blackfellows Lagoon is shallow (average depth ~1 m), and the surface layer of the bottom sediments consists almost entirely of fine mud, turbulence caused by tidal and wind action could easily result in the resuspension of bottom sediment. This sediment would then be carried into the river on an ebbing tide, increasing the suspended load of the river. If the sediment sample collected from site 3b is typical of the resuspended material in this lagoon, then a net lowering of the $^{228}Th/^{232}Th$ AR of the suspended sediment in the river would

Table 5.7 Thorium and radium isotope concentrations activity ratios in particle size fractions of bed sediments, Bega River.

site	particle size (μm)	^{232}Th	^{230}Th	^{228}Th	^{226}Ra	^{228}Ra
			(mBq/g dry wt.)			
0	<2	111 ±5	76.4 ±3.8	149 ±6	82.6 ±4.1	123 ±12
	<20	104 ±3	73.3 ±2.6	148 ±4	74.4 ±3.2	101 ±8
	<63	100 ±4	70.8 ±3.0	117 ±2	76.2 ±1.8	114 ±5
	63-125	63.4±2.0	44.5 ±1.6	48.9±1.7	41.9 ±2.4	58 ±4
	125-250	32.3±1.7	21.1 ±1.2	26.8±1.5	20.8 ±1.0	33 ±3
5	<2	107 ±5	74.5 ±3.8	120 ±5	42.0 ±2.4	69 ±9
	<20	102 ±3	70.4 ±2.6	107 ±3	51.0 ±2.1	95 ±8
	<63	101 ±3	78.2 ±3.1	105 ±4	51.4 ±1.8	91 ±6
	63-125	74.4±3.2	48.8 ±2.3	56.9±2.6	41.5 ±2.3	56 ±5
	125-250	33.7±1.1	22.4 ±0.9	28.8±0.6	18.4 ±1.0	28 ±2
3b	<20	131 ±5	96.0 ±4.2	77.6 ±3.5	41.0 ±1.4	57 ±1
8b	125-250	8.0±0.4	7.1 ±0.3	7.8±0.4	5.8 ±0.4	5.8 ±0.8
8n	125-250	7.1±0.4	6.4 ±0.3	6.1±0.3	4.8 ±0.4	5.8 ±1.1

site	particle size (μm)	$^{226}Ra/^{232}Th$	$^{230}Th/^{232}Th$	$^{228}Ra/^{226}Ra$	$^{228}Th/^{232}Th$
0	<2	0.745 ±0.049	0.689 ±0.036	1.49 ±0.12	1.35 ±0.06
	<20	0.715 ±0.039	0.702 ±0.020	1.35 ±0.09	1.24 ±0.03
	<63	0.764 ±0.034	0.710 ±0.028	1.49 ±0.04	1.17 ±0.05
	63-125	0.661 ±0.043	0.701 ±0.026	1.38 ±0.05	0.77 ±0.03
	125-250	0.644 ±0.046	0.654 ±0.035	1.57 ±0.11	0.83 ±0.04
5	<2	0.391 ±0.028	0.694 ±0.039	1.64 ±0.19	1.11 ±0.06
	<20	0.500 ±0.026	0.691 ±0.027	1.86 ±0.13	1.05 ±0.04
	<63	0.508 ±0.026	0.773 ±0.028	1.78 ±0.11	1.03 ±0.04
	63-125	0.557 ±0.030	0.656 ±0.027	1.34 ±0.08	0.77 ±0.03
	125-250	0.546 ±0.035	0.666 ±0.026	1.54 ±0.11	0.86 ±0.05
3b	<20	0.312 ±0.016	0.730 ±0.025	1.38 ±0.03	0.59 ±0.02
8b	125-250	0.730 ±0.061	0.887 ±0.054	1.00 ±0.11	0.97 ±0.06
8n	125-250	0.683 ±0.069	0.904 ±0.055	1.20 ±0.20	0.85 ±0.05

occur. It is probably significant that site 4, which is the downstream site closest to the channel connecting Blackfellows Lagoon to the Bega River, has both the highest suspended sediment concentration (5.2 mg/L) and the lowest $^{228}Th/^{232}Th$ AR.

If it is assumed that the suspended sediment at site 0 (1.7 mg/L) was representative of the river input, and the additional 3.5 mg/L present at at site 4 was entirely due to resuspended material from Blackfellows Lagoon (represented by the <20 μm fraction of the sediment collected from site 3b), then the theoretical $^{228}Th/^{232}Th$ AR at site 4 can be calculated using the data from Tables 5.1 and 5.5. The equation

$$Th_4 = (SS_oTh_o + SS_{BL}Th_{BL})/(SS_o + SS_{BL})$$

gives the theoretical ^{232}Th concentration in mBq/g at site 4 (Th_4). Here SS_o and SS_{BL} are the suspended sediment concentrations at site 0 and Blackfellows Lagoon, Th_o and Th_{BL} are the ^{232}Th suspended sediment concentrations. A similar calculation can be made for ^{228}Th, and the $^{228}Th/^{232}Th$ AR subsequently derived.

The calculated $^{228}Th/^{232}Th$ AR at site 4 is 0.73 ±0.04, compared to the measured value of 0.87 ±0.03. The lower calculated value may be due to a low estimate of the $^{228}Th/^{232}Th$ AR of resuspended sediment from Blackfellows Lagoon. Resuspended sediment is almost certain to come from the topmost layer of bed sediments, whereas the bed sediment sample from site 3b was collected using an Eckman grab sampler to a depth of about 10 cm. The deeper sediments are probably older than surface sediment, and are likely to contain a lower $^{228}Th/^{232}Th$ AR than recently deposited sediments.

Downstream of site 4 there is a gradual increase in the $^{228}Th/^{232}Th$ AR of the suspended sediment (Table 5.5, Figure 5.8), which may indicate a lower fraction of resuspended lagoon sediment at these sites. It may also be due to increased scavenging by the suspended sediment of dissolved ^{228}Th, which is produced at a greater rate in this part of the estuary as a result of higher dissolved ^{228}Ra concentrations (section 5.5.2 below).

5.8 Sources of Dissolved Radium to the Water Column

This section discusses the sources of all dissolved radium isotopes measured in the Bega estuary, and offers an interpretation of their relative concentrations.

5.8.1 Excess ^{226}Ra

In section 5.5.2 it was shown that there existed an additional source of dissolved ^{226}Ra to water in the Bega estuary. If this additional or 'excess' ^{226}Ra originates from sediments, then the relative amounts originating from suspended and bottom sediments can be estimated from mass balance calculations. The excess ^{226}Ra concentration at site n, i.e. the amount of ^{226}Ra exceeding the expected concentration assuming conservative mixing, Ra_{exn}, can be calculated from

$$Ra_{exn} = Ra_{obn} - (f_n.Ra_{sw} - (1-f_n)Ra_{rw})$$

where Ra_{obn} is the observed dissolved ^{226}Ra concentration at site n, Ra_{sw} and Ra_{rw} are the sea and river water concentrations, and f_n is the fraction of seawater at site n. The contribution of ^{226}Ra desorbed from suspended sediment at site n, Ra_{dn}, can estimated from

$$Ra_{dn} = SS_n(Ra_{so} - Ra_{sn})$$

where SS_n is the suspended sediment concentration at site n in g/L, and Ra_{so} and Ra_{sn} are the ^{226}Ra suspended sediment concentrations in mBq/g at sites 0 and n.

The fraction of excess ^{226}Ra coming from the suspended sediment at site n, F_{ssn}, is then

$$F_{ssn} = Ra_{dn}/Ra_{exn}$$

For the November data, the maximum excess occurs at site 6, and is 1.9 ±0.3 mBq/L. The loss of ^{226}Ra from the suspended sediment between

site 0 and the mid-estuary region was calculated in section 5.6.2 to be 38 ±3 mBq/g. The suspended sediment concentration at site 6 was 2.9 mg/L. A proportion of this is likely to be older resuspended bottom sediments (section 5.7.3) which have already lost their radium. However, even if all of the suspended sediment at site 6 is assumed to originate from the freshwater end, the amount of ^{226}Ra released to the water column by the suspended sediment at site 6 is still only 0.11 mBq/L. This is 6% ±1 of the observed excess. Previous estuarine studies (e.g. Li et al. 1977; Key et al. 1985; Elsinger and Moore 1980) have concluded that diffusion of radium from bottom sediments is the other major source of dissolved radium to estuarine surface water. Presumably this process is responsible for the remaining 94% of the excess ^{226}Ra in the Bega estuary.

The fact that dissolved ^{226}Ra concentrations in the estuary increase up to a salinity of 20 ppt means that bottom sediments in this region of the estuary must continue to supply radium to the water column. Given their long exposure time to saline water, net losses of radium from bottom sediments by the rapid desorption from surface ion-exchange sites ought to be zero. This should be so while the mean salinity of water contacting the sediments remains unchanged. However, if the mean salinity slowly increases, e.g. by migration of bottom sediments towards the mouth of the estuary into higher salinity waters, then a net desorption of radium from these sediments will result. Encroachment of seawater during low river flows onto bottom sediments deposited in relatively freshwater will also produce this effect (Elsinger and Moore 1980).

Another source of radium is in the pore water of bottom sediments. Moore and Scott (1986) pointed out that the diffusion of radium from bottom sediments into surface water must be preceded by its release into the pore water, although they did not consider this an important source of radium to the Mississippi River. The processes responsible for this release could include slow release desorption, dissolution of oxide coatings on sediment particles by anoxic conditions, or recoil ejection of ^{226}Ra generated by the decay of ^{230}Th.

5.8.2 Interpretation of dissolved radium isotope concentrations

Plots of the concentrations of each radium isotope against salinity for the November collection are shown in Figure 5.11. Radium-223 and ^{224}Ra were not determined on the September collection. A feature of the plots is the similarity in the shape of all the curves. All isotopes increase steadily up to a maximum in the mid-salinity region of the estuary (14 to 20 ppt) before stabilising, although ^{224}Ra may continue to increase up to site 7 (27 ppt). No data are available for the region between site 7 and the open sea, but presumably the activities of all isotopes decrease rapidly near the mouth of the estuary as a result of dilution with seawater.

In the low salinity region of the estuary the short-lived radium isotopes (^{224}Ra, ^{223}Ra, ^{228}Ra) increase at a much greater rate than ^{226}Ra, reaching concentrations many times greater than either end-member. For example, the ^{224}Ra concentration at site 5 is 11.9 ±2.4 times the concentration expected from conservative mixing. The corresponding values for the other isotopes are 17.3 ±5.3 for ^{223}Ra, 10.7 ±2.4 for ^{228}Ra, but only 3.2 ±0.4 for ^{226}Ra. This trend is reflected more clearly by the increase in the ^{223}Ra/^{226}Ra and ^{224}Ra/^{226}Ra AR's with salinity (Table 5.4). Although not as pronounced, the ^{228}Ra/^{226}Ra AR also increases significantly in the upper estuary region (sites 0-5). Previous studies have noted the enrichment of ^{228}Ra and ^{224}Ra relative to ^{226}Ra in estuarine waters (Elsinger and Moore 1983; Bollinger and Moore 1984; Levy and Moore 1985). Moore (1990) attributed this enrichment to their continued high activity production rate in sediments containing their thorium parents. Higher concentrations in near-bottom waters led Levy and Moore (1985) to suggest that bottom sediments were a source of ^{224}Ra to the water column.

In order to ascertain whether the pore water of the bottom sediments was a possible source of radium isotopes in the Bega River estuary, a pore water sample was collected near site 5 in July 1992. A cylinder, open at both ends, was placed in exposed bottom sediments at low tide to a depth of about 200 mm. The sediments inside the cylinder were removed, and the cylinder was allowed to fill with pore water. This water was filtered in the laboratory, and the concentrations of all radium isotopes determined.

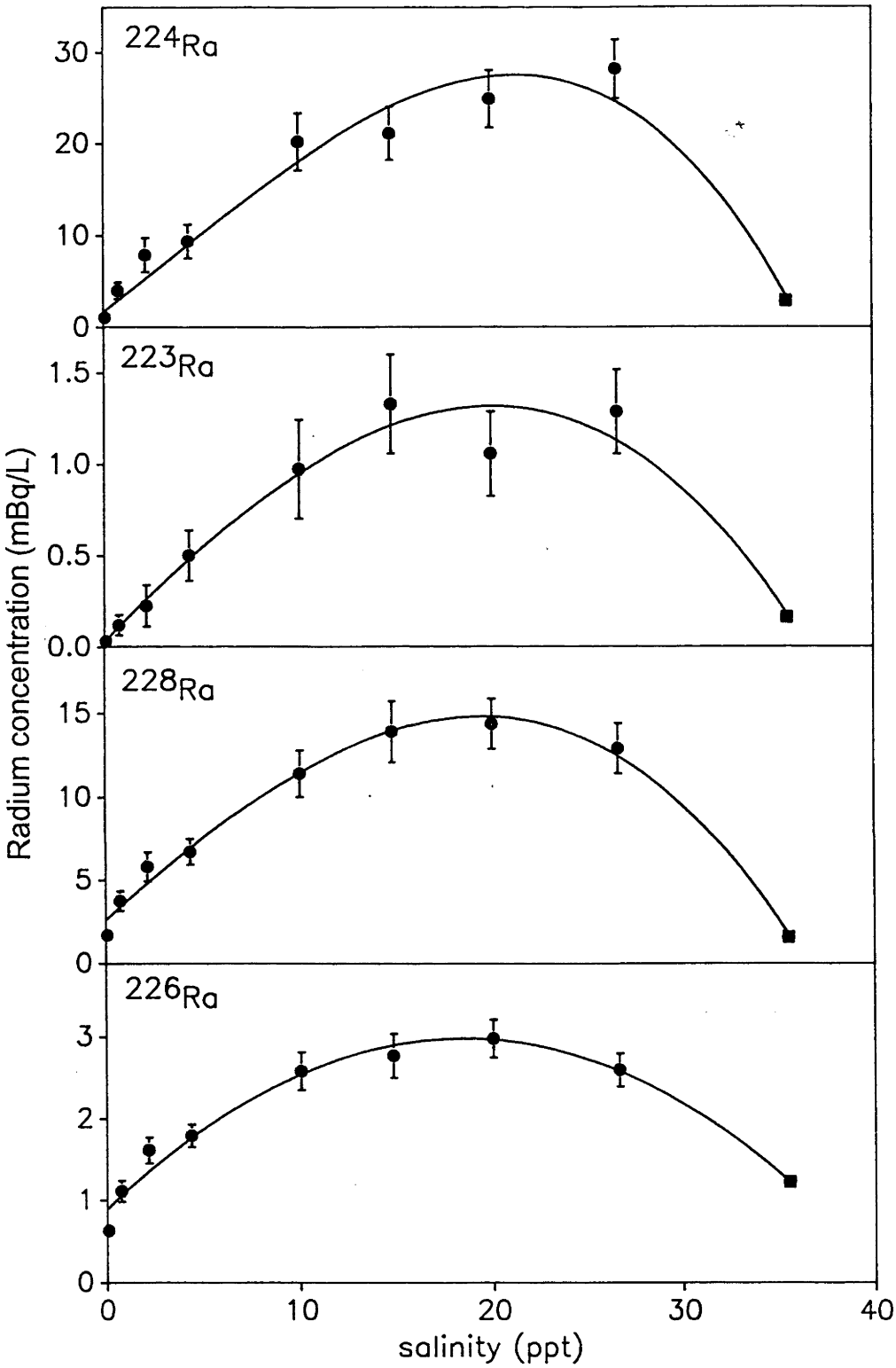

Figure 5.11 The dissolved concentrations of radium isotopes (circles). All curves have been forced through the seawater end-member (square).

The results have been included in Table 5.4, and show that the pore water concentrations of ^{223}Ra and ^{224}Ra are well in excess of the surface water sample collected in November 1991 from the same site. The $^{223}Ra/^{226}Ra$ and $^{224}Ra/^{226}Ra$ AR's are also extremely high, suggesting that pore water is a major source of ^{223}Ra and ^{224}Ra to surface water in the Bega estuary.

High concentrations of radium have been measured in deep-sea sediment pore water and near-bottom ocean water (Somayajulu and Church 1973; Cochran 1979), implying that pore water is a source of radium to the ocean. Bollinger and Moore (1984) concluded that interstitial water in marsh sediments supplied high fluxes of ^{224}Ra and ^{228}Ra to tidal creek waters. The results of this study indicate that the pore water in bottom sediments has mixed with or diffused into the water column, probably as a result of wave and/or tidal action. Wave action has been described as an important mechanism influencing the diffusion of pore water from bottom sediments (Webster and Taylor 1992), and tidal movements should be particularly significant in shallow estuaries such as the Bega estuary. The extent of enrichment of radium isotopes in the water column will depend on two factors; the salinity, and hence concentration of radium isotopes in the pore water, and the extent of surface-pore water mixing. Both of these factors will result in an increase in the radium concentrations of surface water as it moves towards the mouth of the estuary.

The ^{226}Ra and ^{228}Ra pore water concentrations are only slightly higher than their surface water concentrations, indicating that the half-life is a major factor governing the concentration of radium isotopes in pore water. Moore (1981) suggested that the enrichment of ^{228}Ra with respect to ^{226}Ra in estuaries is due to the shorter half-life of ^{228}Ra, and its higher activity generation in bottom sediments. The much higher activity generation of ^{223}Ra and ^{224}Ra therefore favours a proportionally greater increase in their pore water activities.

Production of ^{226}Ra and ^{228}Ra in bottom sediments and their subsequent release into pore water will also account for some of the excess dissolved ^{226}Ra and ^{228}Ra in the Bega River estuary. Without the analysis of more pore water samples from other regions of the estuary, it is not possible to ascertain what fraction of this excess is due to surface-pore water mixing,

and what fraction has simply been desorbed from surface bed sediments exposed to higher salinity waters. Nevertheless, the similarity in the shape of all curves in Figure 5.11 suggests that surface-pore water mixing is a major source of all radium isotopes to the water column.

5.8.3 The relationship between the $^{228}Ra/^{226}Ra$ AR and river flow

Figure 5.12 shows that two different curves can be generated from the September and November data when the dissolved $^{228}Ra/^{226}Ra$ AR (Table 5.4) is plotted against salinity. Although fewer measurements were made, the September values are significantly lower than the values for corresponding salinities in November. Elsinger and Moore (1983) noted that variations in the $^{228}Ra/^{226}Ra$ AR may correspond to the flushing time of an estuary, as the amount of ^{228}Ra generated and released to the water from sediments may be related to the water-sediment contact time.

The flow of the Bega River entering the estuary is not monitored. However daily flow rates of its major tributaries, the Bemboka River, Brogo River and Tantawanglo Creek show that the total flow of these tributaries during the September sampling period (~400 ML/d) was approximately 2.5 times higher than November (N.S.W. Department of Water Resources, Bega, unpublished data). No data is available for minor tributaries, but it would be reasonable to assume that the flow of Bega River water entering the estuary was lower during November. The lower flow rate would lead to a slower movement of surface water with respect to bottom sediments, a longer residence time of water in the estuary, and so a greater degree of mixing with pore water at a given site. Consequently, surface water in November would have contained a greater component of water derived from sediment pore spaces than September. If a high $^{228}Ra/^{226}Ra$ AR is generated in pore water, as has been suggested above, surface-pore water mixing can account for the higher surface water AR's in November.

5.8.4 The $^{224}Ra/^{223}Ra$ AR as a diffusion rate indicator

A plot of the dissolved $^{224}Ra/^{223}Ra$ AR and salinity (Table 5.4) is shown in Figure 5.13. Although the errors are large, the ratios in the mid-estuary region are consistently lower (weighted mean of sites 3-7 = 19 ±2) than the

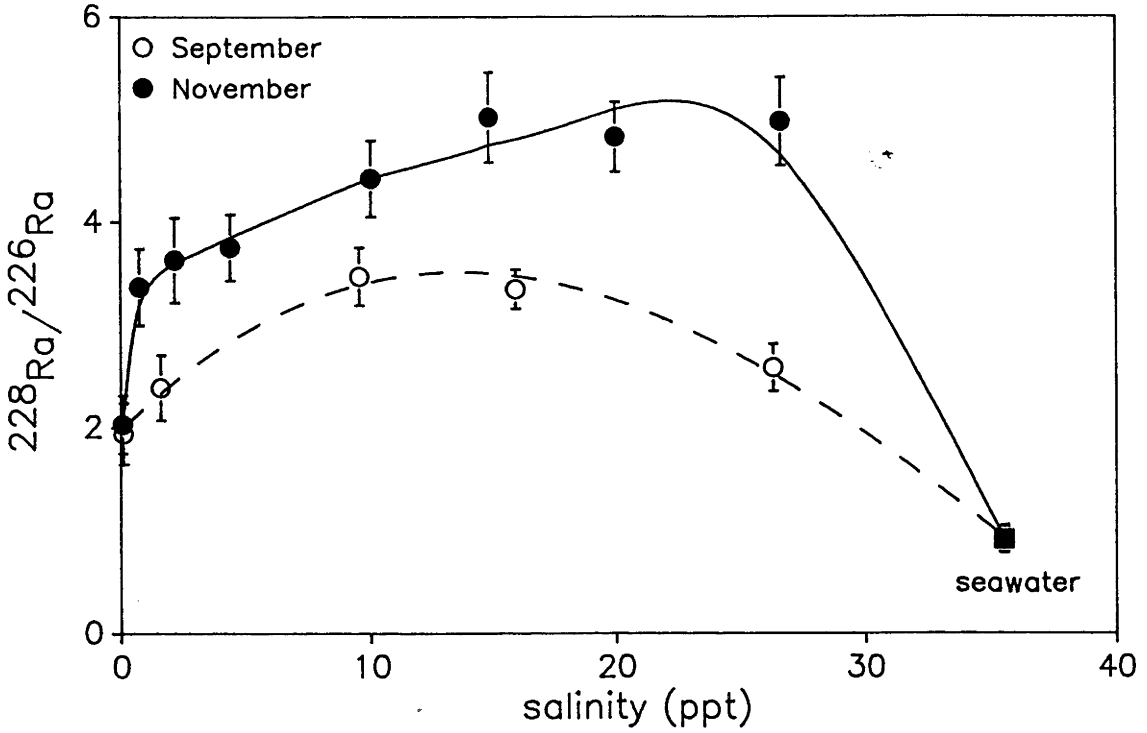

Figure 5.12 The dissolved $^{228}Ra/^{226}Ra$ activity ratio of samples collected in September and November 1991.

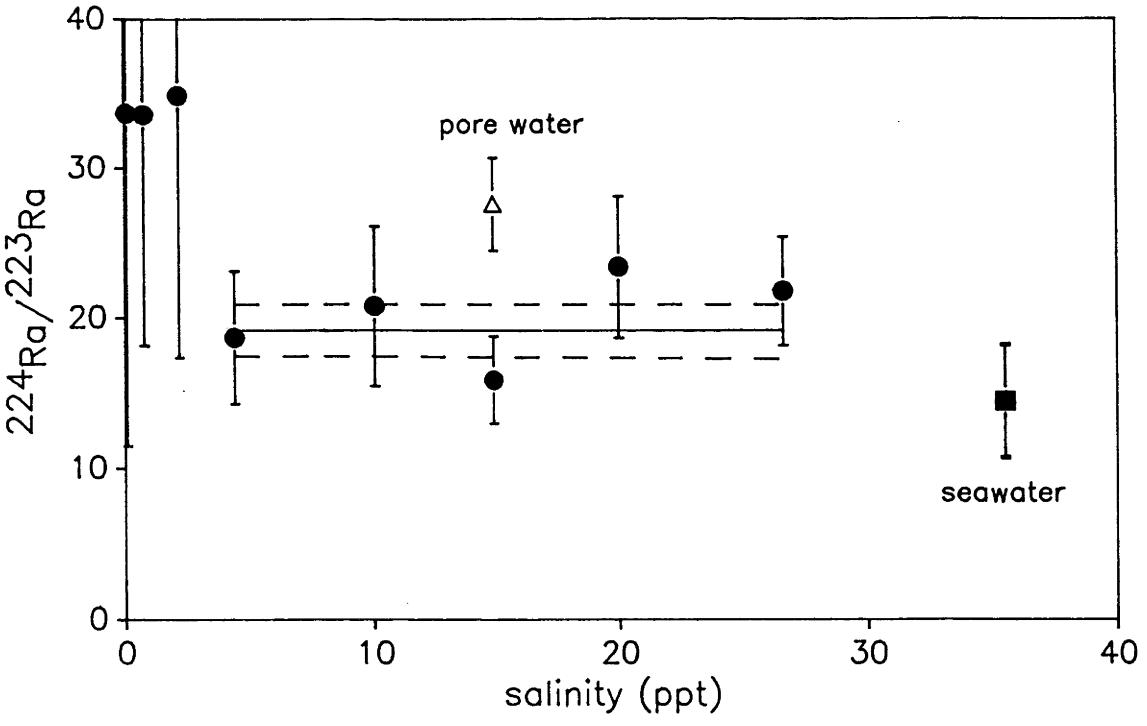

Figure 5.13 The dissolved $^{224}Ra/^{223}Ra$ activity ratio of surface water samples collected in November 1991. The solid line represents the weighted mean of estuarine samples from sites 3-7, and the dashed lines represent the uncertainty of the mean (1 standard deviation).

pore water value (28 ±3). The weighted mean is represented by the solid line in Figure 5.13, and its standard error by the dashed lines. The lower surface water $^{224}Ra/^{223}Ra$ AR's may be due to the different half-lives, and hence decay rates of the two isotopes. The dissolved concentrations of thorium isotopes are extremely low, and so dissolved ^{223}Ra and ^{224}Ra are essentially unsupported in the water column. As radium diffuses into the water column from bottom sediments, ^{224}Ra, having the shorter half-life, will decay to a proportionally lower concentration than ^{223}Ra after a given time. Consequently, the extent of the decrease in the surface water $^{224}Ra/^{223}Ra$ AR at a given site will then be affected by the residence time of pore water in the water column at that site.

Although the surface and pore water samples were collected on separate occasions and only one pore water measurement was made, the data in presented in Figure 5.13 are consistent with the expected lower water column AR's. It may be significant that the lowest measured $^{224}Ra/^{223}Ra$ AR (14 ±3) was the seawater value at site 8w, well away (~3 km) from the mouth of the estuary. Based on this data, a time constant of a few days is indicated for surface-pore water exchange in the mid-estuary region. However, because of the horizontal movement of surface water through the estuary, any calculations of this nature will be complicated by the fact that variable fluxes of ^{224}Ra and ^{223}Ra from bottom sediments in other regions of the estuary will affect their ratio at a particular site. These fluxes will need to be quantified before any time constants can be accurately determined. Nevertheless, ^{224}Ra and ^{223}Ra have the potential to yield information on the rates of surface-pore water mixing processes on time scales of days to weeks.

5.9 Summary

Radium behaves non-conservatively in the Bega River estuary. Approximately 58% of ^{226}Ra is desorbed from the freshwater suspended sediment as it is exposed to water of increasing salinity. Radium is probably lost from the suspended sediment as soon as salinity commences to increase, and it continues to be lost up to a salinity of about 10 ppt. The fraction of radium desorbed from saline bed sediments is a function of the particle

size of the sediment for particles up to 250 μm. Proportionally the greatest amount of radium was desorbed from particles <2 μm in size.

By contrast, there is no observable desorption of thorium from suspended sediments. The $^{226}Ra/^{232}Th$ AR decreases with increasing salinity and is therefore not a suitable sediment tracer in saline waters. The suspended sediment $^{230}Th/^{232}Th$ AR remains constant, within error, as a function of salinity, and appears to be a suitable tracer of fluvial sediments in an estuary. Resuspension of 'older' bottom lagoon sediments is the most likely explanation for decreases in the suspended sediment $^{228}Th/^{232}Th$ AR in the mid-estuary region. Variations in the suspended sediment $^{228}Ra/^{226}Ra$ AR with salinity are due to the equilibration of increasing concentrations of dissolved ^{228}Ra with radium in ion-exchangeable sites in the suspended sediment.

Dissolved ^{226}Ra concentrations increase up to 20 ppt salinity and are in excess of concentrations expected from the conservative mixing of river and seawater end-members. Mass balance calculations indicate that in the mid-estuary region about 94% of this excess originates from bottom sediments. High concentrations of short-lived dissolved radium isotopes in both surface water samples and a single pore water sample indicate that pore water is a major source of radium to the water column. Variations in the dissolved $^{228}Ra/^{226}Ra$ AR appear to be related to the flow of the river, and the extent of surface-pore water exchange. The different decay rates of ^{224}Ra and ^{223}Ra may be able to give information on the rates of surface-pore water mixing.

6. Laboratory Experiments

6.1 Introduction

The estuarine field study (chapter 5) identified a relationship between the extent of radium desorption from suspended sediment and salinity. However, due to limitations on the number of suspended sediment samples able to be collected, together with the uncertainties associated with analysis, the field study was unable to resolve the extent of radium desorption at low salinities (0.1-2 ppt), and so determine the salinity at which radium loss from the sediment becomes significant. Furthermore, the assessment of the extent of radium desorption at each salinity implicitly assumed that ion-exchange equilibrium had been attained between dissolved and surface sorbed radium. Because the salinity of the water carrying the suspended sediment was continually changing, together with the fact that the residence time of the water in the estuary was finite, the kinetics of radium desorption may have played a role in controlling the observed suspended sediment concentration of radium.

A detailed study of radium desorption from bed sediments as a function of salinity was not undertaken in the Bega River estuary because of the large variability in salinity at a particular site over a tidal cycle. In absolute terms, the loss of radium from bed sediments exposed to saline waters will not necessarily parallel suspended sediments. Factors such as particle size, mineralogy, and solid/liquid (S/L) ratio may differ significantly between bed and suspended sediments. It is known that in relatively fresh waters these factors can quantitatively affect radium sorption (see discussion in chapter 2).

6.1.1 Aims

This chapter presents and discusses the results of laboratory experiments which were carried out to investigate the importance of kinetics, S/L ratio and particle size on the sorption behaviour of radium in saline waters, and define more precisely its behaviour at low salinities. Specifically, the laboratory experiments were intended to investigate;

- the sensitivity of radium and thorium sorption to small increases in salinity;
- the effect of sediment concentration (S/L ratio) on radium sorption in saline water;
- the kinetics of radium desorption, and
- how sediment particle size affects radium desorption.

Two types of experiments were were undertaken; a) adsorption, and b) desorption experiments. They are summarised briefly below. The methods are presented in detail in section 6.2.

6.1.2 Adsorption experiments

A known amount of ^{226}Ra or ^{228}Th tracer was added to a water/sediment suspension and the quantity of tracer adsorbed by the sediment derived. Because the tracers were added in a soluble form, these experiments were able to focus exclusively on the sorption behaviour of radium and thorium, rather than the behaviour of radium and thorium in the sediment as a whole. The addition of high activities of tracer reduced counting errors, and enabled a more accurate determination of the response of radium and thorium sorption to small changes in salinities. Furthermore, this approach allowed the study of radium sorption behaviour at suspended sediment concentrations typically found in inland rivers (10-1000 mg/L). Although the concentrations of ^{226}Ra tracer were much higher than those normally present in surface waters, the sorption behaviour of radium in these experiments should not have been significantly affected. The sorption capacity of the sediment is many orders of magnitude greater than the quantity of available radium, and other studies (summarised by Benes 1990) have shown that the fraction of ^{226}Ra adsorbed by solids is independent of the initial ^{226}Ra solution concentration.

6.1.3 Desorption experiments

Three series of desorption experiments were run to investigate the effects of exposure time, salinity and S/L ratio on the desorption of radium. All desorption experiments utilized freshwater Bega River bed sediment which

had not been previously exposed to saline water. The sediments were equilibrated with saline water, and the activities of the naturally-occurring radium and thorium isotopes desorbed from the sediment were measured. By comparing the desorption behaviour of ^{226}Ra and the short-lived radium isotopes as a function of time, information was able to be gained on the possible mechanisms of sediment/water ion-exchange reactions.

6.2 Methods

Sediments from two different river systems were used in both the kinetic and salinity experiments. Preliminary experiments were performed on a sediment sample collected dry from the bank of the Murrumbidgee River at Balranald. These experiments were run to assess initial desorption rates, and gauge the extent of desorption losses from the sediment at various salinities. A second and more extensive series of experiments were performed on the <63 μm and the 125-500 μm size fractions of a freshwater bed sediment grab sample collected from the Bega River at site 0, upstream of the tidal limit (Figure 5.2). The <63 μm particle size fraction was used because it is the size fraction which was able to be recovered in sufficient quantities for use in these experiments, and because it is the fraction most likely to be transported by rivers in the suspended form. The 125-500 μm fraction represented the fine-medium sand size fraction, typical of bed sediments in the main channel of the Bega River.

6.2.1 Sample pre-treatment

Sediment: The dry Murrumbidgee River bank sediment was soaked in water for 7 days, and the sediment slurry thoroughly mixed. A sub-sample was taken, and the wet:dry weight determined by drying overnight at 50°C. The wet Bega River sediment was wet-sieved in fresh water, and the various size fractions retained. The wet:dry weight ratio was determined on the <63 μm and 125-500μm size fractions. These sediment slurries were retained for the desorption experiments.

A portion of the <63 μm fraction of the Bega sediment was suspended in river water, and placed in an ultra-sonic bath for 3 minutes. Sedimentation analysis (section 3.5) was then used to obtain a suspension

of particles <20 μm in size. An aliquot of this suspension was removed to determine the particulate mass concentration on a dry weight basis, and the remainder of the suspension retained for the adsorption experiments. All wet sediments were stored in sealed containers in a refrigerator at 4°C until required.

Water: The Murrumbidgee and Bega River water samples were collected from the same site as the sediment. A seawater sample collected from Tathra wharf (Figure 5.2) was used to vary the salinity of each experiment. All water samples were filtered through a 0.45 μm membrane filter and stored in a dark room at 15°C until required.

6.2.2 Adsorption experiments

Radium

A ^{226}Ra stock solution was prepared by adding a small quantity of a standard ^{226}Ra solution (supplied by Amersham) to filtered Bega River water in a polypropylene bottle. Filtered seawater (5% by volume) was added to limit adsorption of radium onto the walls of the bottle, and the pH adjusted to 7.0 by addition of a NaOH solution. The activity of the ^{226}Ra solution was ~140 Bq/mL.

All experiments were carried out in duplicate in capped 25 mL polypropylene bottles. Appropriate volumes of sediment suspension, river water and seawater were added (total volume ~20 mL). Salinities were varied from 0.2 ppt (river water only) to 35 ppt (98% seawater), and each series of experiments were performed at sediment concentrations of 10, 100 and 1000 mg/L. The bottle containing the sediment suspension was secured to a revolving wheel for 24 h. A weighed quantity (~200 mg) of ^{226}Ra stock solution was then added, and the suspension equilibrated for a further 24 h. At the end of the equilibration period, the suspension was drawn into a syringe and filtered through a 0.45 μm membrane filter directly into a 25 mL glass scintillation vial. The dissolved ^{226}Ra concentration was determined by liquid scintillation counting (section 3.3).

Procedural blanks containing only filtered water and ^{226}Ra tracer were determined at a range of salinities in order to assess the extent of sorption losses of radium onto the walls of the polypropylene bottle and the membrane filter. Losses were greatest from the blank of lowest salinity, with ~7% of the added ^{226}Ra lost from the 0.24 ppt solution. Losses decreased with increasing salinity, and were found to be negligible at salinities greater than 2 ppt.

The activity of ^{226}Ra adsorbed by the sediment (Ra_{sed}), was calculated at each salinity using the equation

$$Ra_{sed} = Ra_{tot} - (Ra_{sol}/(1-f_{ad})) \qquad (1)$$

where Ra_{tot} is the ^{226}Ra tracer activity added to the vial, Ra_{sol} is the measured ^{226}Ra activity in solution, and f_{ad} is the fraction of dissolved ^{226}Ra lost through sorption by the apparatus at that salinity, derived from the procedural blanks. The ^{226}Ra activity naturally present in the sediment suspension (~0.02-20 mBq) was many orders of magnitude lower than the activity of the added tracer (~30 Bq), and was ignored.

Because of the possible shielding of the vial walls by the suspended sediment, the value of f_{ad} derived from the procedural blanks may have been over-estimated, particularly for the 1000 mg/L experiments. Consequently, at low salinities sediment shielding may have resulted in an over-estimate of the values of Ra_{sed}, and hence K_d. However these errors will not exceed 0.5% for Ra_{sed}, and 7% for K_d.

Thorium

The ^{228}Th tracer used in the adsorption experiments was obtained from an ^{232}U solution, and was isolated using an anion exchange column (Martin and Hancock 1992). The preparation of the ^{228}Th stock solution and sediment suspensions were identical to the ^{226}Ra adsorption experiments described above, except that experiments were conducted at only one sediment suspension concentration (10 mg/L). Approximately 80 mBq of ^{228}Th tracer was added to each vial. The ^{228}Th filtrate concentrations were analysed using radiochemical and alpha-particle spectroscopy techniques described in

Chapter 4. Because of the time-consuming nature of these analyses, only single experiments were performed at each salinity.

Adsorption losses of ^{228}Th onto the walls of the apparatus, as determined by the procedural blanks, were much greater than ^{226}Ra losses, and varied from 46% of the filtrate activity at 0.2 ppt salinity, to 54% at 28 ppt salinity. The ^{228}Th activity adsorbed by the sediment was calculated in the same way as ^{226}Ra (equation (1) above).

6.2.4 Desorption experiments

For both the kinetic and salinity experiments, the wet sediment (~10 g dry wt.) was weighed into a polypropylene bottle, and ~800 g of a pre-mixed solution of river water and seawater of the appropriate salinity was added. Where different S/L ratios were used, the weights of solution and sediment were varied accordingly. The bottle containing the sediment suspension was placed in an ultra-sonic bath for 3 min, shaken vigorously for 30 min by mechanical shaker, and then attached to a revolving wheel for the duration of the experiment. After a suitable period of time had elapsed, the sediment suspension was centrifuged, and the supernatant filtered through a 0.45 μm membrane filter. The filtrate was weighed, and analysed for radium and thorium isotopes as described in Chapter 3.

The kinetics of radium and thorium desorption was studied by varying the equilibration time of freshwater sediments from 0.5 h to ~70 d. The salinity of the solution used was 17.8 ppt (50% seawater) which is close to the salinity of the NaCl solution used by Dickson (1985) in his kinetic experiments.

The salinity experiments involved the equilibration of river bed sediments at different salinities, ranging from 1.8 ppt (5% seawater) up to 35.6 ppt (100% seawater). Preliminary experiments indicated that radium desorption reached a maximum in less than 4 h of equilibration, and remained stable for at least 2-3 d. An equilibration time of 20 h was subsequently selected for all salinity experiments.

Both the kinetic and salinity experiments were run at high S/L ratios (12.5 g/L) so that the quantity of radium desorbed was sufficient to obtain a measurement of radium desorption with an acceptable level of uncertainty. This S/L ratio is the same as that used by Elsinger and Moore (1984) in radium desorption experiments on Pee Dee River sediment, allowing a direct comparison of the results of this work with those of sediments from another river.

The effect of S/L ratio on radium desorption was studied over a sediment suspension concentration range of 0.25-50 g/L, representing a 200 fold variation in sediment concentration.

6.3 Adsorption Experiments - Results and Discussion

6.3.1 Thorium adsorption K_d's and salinity

The results of ^{228}Th adsorption experiments, and the calculated K_d values are given in Table 6.1. The adsorption distribution coefficient (K_d) at each salinity was calculated from

$$K_d = \frac{\text{concentration of tracer in sediment (Bq/g)}}{\text{concentration of tracer in water (Bq/mL)}}$$

Table 6.1 ^{228}Th adsorption as a function of salinity; sediment concentration = 10 mg/L.

salinity (ppt)	f_{ad}*	Th_{sed} (Bq/g)	Th_{sol} (Bq/L)	K_d (x10^3) (mL/g)
0.24	0.53 ±0.02	252 ± 8	0.767 ±0.030	329 ±16
0.41	0.54 ±0.02	281 ± 8	0.628 ±0.035	448 ±28
0.59	0.51 ±0.02	325 ± 4	0.329 ±0.017	989 ±53
1.13	0.53 ±0.02	307 ± 5	0.427 ±0.021	720 ±38
2.01	0.51 ±0.02	326 ± 4	0.341 ±0.017	957 ±49
3.79	0.50 ±0.02	309 ± 6	0.420 ±0.025	735 ±46
7.35	0.48 ±0.02	333 ± 3	0.295 ±0.012	1129 ±47
14.5	0.51 ±0.02	324 ± 5	0.351 ±0.020	922 ±55
21.6	0.47 ±0.03	321 ± 6	0.328 ±0.020	978 ±63
28.4	0.46 ±0.03	321 ± 5	0.280 ±0.015	1148 ±63

* see section 6.2.2

When plotted against salinity (Figure 6.1), the thorium K_d initially increases rapidly in response to small increases in salinity. Although K_d's show some variability above 0.6 ppt salinity, they appear to have levelled off, and lie in the range 700-1150 x 10^3 mL/g. This variability is greater than that expected from counting statistics alone, and may be due to errors introduced by the large, and possibly variable losses of thorium onto the walls of the apparatus.

The higher affinity of thorium for the sediment phase at salinities >0.6 ppt may be due to the aggregation of fine clay particles and organic colloids <0.45 μm, previously discussed in chapters 2 and 5. This process could result in the net removal of thorium onto particulates >0.45 μm, thus increasing the K_d.

6.3.2 Radium adsorption K_d's and salinity

The results of the ^{226}Ra adsorption experiments are given in Table 6.2. Results of duplicate analyses have been averaged, and the quoted uncertainties are the standard errors on the mean. Due to the small fraction of ^{226}Ra adsorbed by the 10 mg/L sediment suspension, the errors on these determinations are large, particularly at high salinities.
A log-linear plot of K_d against salinity for each sediment suspension concentration is shown in Figure 6.2. To aid clarity only the K_d's for the 100 mg/L and 1000 mg/L suspensions have been plotted. The K_d's in Figure 6.2 decrease with increasing salinity before levelling off to more or less constant values of about 350 for the 1000 mg/L suspension, and ~3000 for the 100 mg/L suspension. These values are reached at a salinity of about 7 ppt for the 1000 mg/L sediment suspension, but at a lower salinity (~4 ppt) for the 100 mg/L sediment suspension. The variability in the 100 mg/L suspension at high salinities may be due variable radon loss from the vial (section 3.3).

When compared with the lowest salinity thorium K_d (determined at 10 mg/L), the corresponding radium K_d for the 10 mg/L sediment suspension is lower by at least an order of magnitude. At higher salinities meaningful radium K_d's for the 10 mg/L experiments are not available for comparison, but they

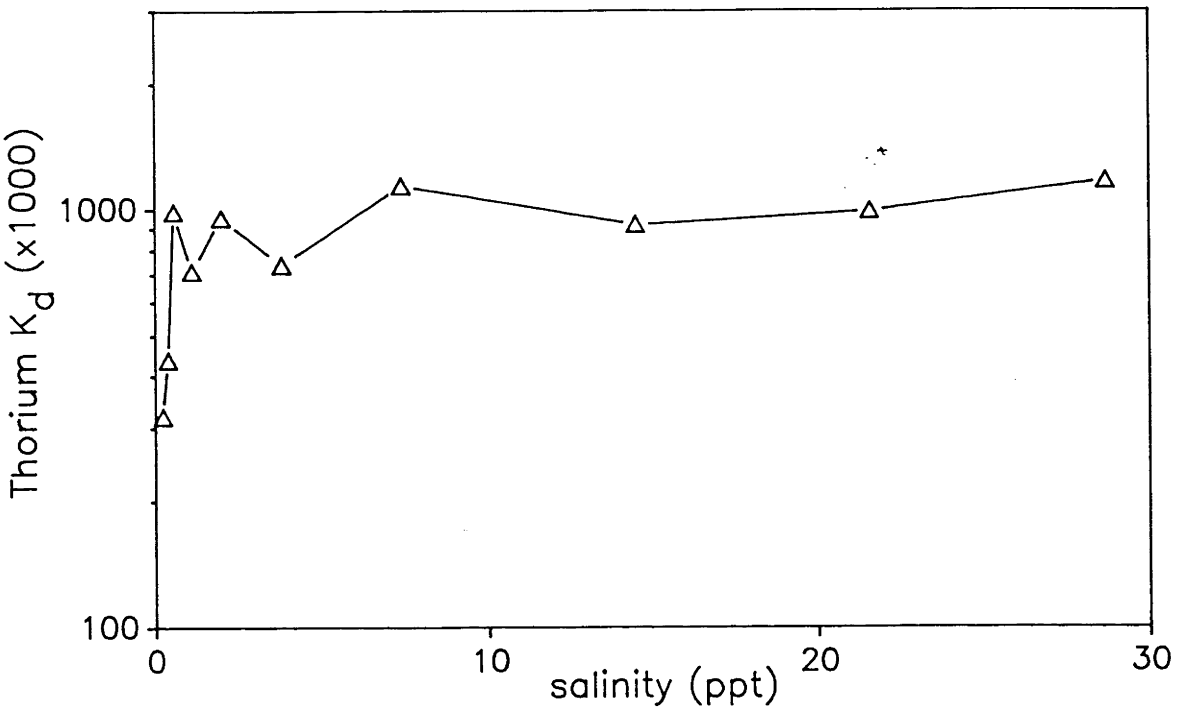

Figure 6.1 ^{228}Th distribution coefficient (K_d) as a function of salinity in adsorption experiments. The sediment concentration was 10 mg/L.

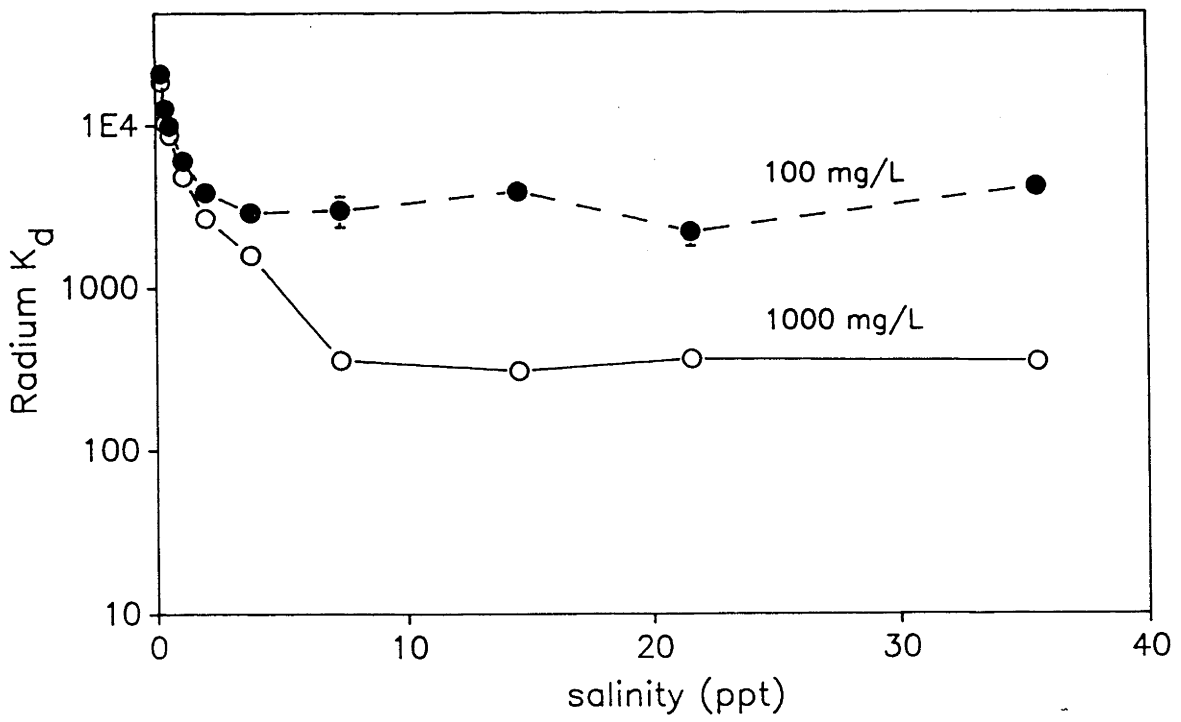

Figure 6.2 Radium distribution coefficient (K_d) as a function of salinity in adsorption experiments

are almost certainly lower than the corresponding thorium K_d's by at least two orders of magnitude.

6.3.3 Effect of S/L ratio

From Table 6.2 and Figure 6.2 it can be seen that K_d's for the 1000 mg/L sediment suspension are lower than the 100 mg/L suspension over the measured salinity range. A trend of decreasing K_d's with increasing S/L ratio has been noted previously for radium (Benes et al. 1984, 1985, 1986a) and other species (O'Connor and Connolly 1980; Li et al. 1984). Li et al. (1984) considered that one possible explanation for the enhancement of adsorption K_d's at low suspended particle concentrations is that a greater degree of particle aggregation occurs at high suspended particle concentrations. Aggregation may result in a net reduction in particle surface area, decreasing the concentration of potential sorption sites, and lowering K_d's. Further investigations into the effects of the S/L ratio were conducted using desorption experiments, and these results are discussed in sections 6.5 and 6.6.1 below.

6.3.4 Sediment sorption of radium

Although K_d's provide a sensitive way of assessing changes in ion-exchange equilibrium of radium between solid and solution, this study is primarily concerned with the change in the radium concentration of the sediment phase as a function of salinity. For this purpose the ^{226}Ra concentration of the sediment at each salinity (Ra_{sed}) has been normalised to the ^{226}Ra concentration of the sediment at the lowest salinity Ra_{sedo}, to obtain the parameter Ra_F, i.e.,

$$Ra_F = Ra_{sed}/Ra_{sedo}$$

The amount of ^{226}Ra tracer added to each vial was approximately the same, and so the values of Ra_{sed} can be used directly to gauge the effect of salinity on sediment adsorption of radium. The parameter Ra_F measures the decrease in radium adsorption at each salinity relative to radium adsorption in fresh water. Its values are given in Table 6.1, and have been plotted against salinity in Figure 6.3.a. Because of the large

Table 6.2 Results of ^{226}Ra adsorption experiments.

salinity (ppt)	f_{ad}[a]	Ra_{sed} (Bq/g)	Ra_{sol} (Bq/mL)	K_d (mL/g)	Ra_F[b]
1000 mg/L					
0.2	0.063	1696 ± 27	0.090 ±0.001	18832 ±353	1.00
0.4	0.050	1632 ± 26	0.156 ±0.001	10465 ±185	0.96 ±0.02
0.6	0.032	1595 ± 27	0.182 ±0.001	8753 ±157	0.94 ±0.02
1.1	0.022	1463 ± 34	0.303 ±0.002	4831 ±119	0.87 ±0.02
2.0	0	1282 ± 41	0.478 ±0.004	2684 ± 90	0.77 ±0.03
3.8	0	1067 ± 47	0.673 ±0.005	1586 ± 71	0.63 ±0.03
7.4	0	464 ± 75	1.301 ±0.010	357 ± 58	0.27 ±0.04
14.5	0	417 ± 81	1.351 ±0.011	309 ± 60	0.25 ±0.05
21.6	0	479 ± 88	1.304 ±0.012	367 ± 67	0.28 ±0.05
35.6	0	463 ± 93	1.316 ±0.013	351 ± 71	0.27 ±0.06
100 mg/L					
0.2	0.063	11845 ±407	0.561 ±0.005	21111 ± 748	1.00
0.4	0.050	9877 ±528	0.771 ±0.009	12803 ± 699	0.83 ±0.04
0.6	0.032	8779 ±523	0.876 ±0.008	10021 ± 605	0.74 ±0.05
1.1	0.022	6670 ±576	1.100 ±0.010	6064 ± 526	0.56 ±0.05
2.0	0	4997 ±441	1.293 ±0.005	3864 ± 341	0.42 ±0.04
3.8	0	3935 ±509	1.356 ±0.006	2903 ± 375	0.33 ±0.04
7.4	0	4042 ±861	1.355 ±0.012	2982 ± 636	0.34 ±0.07
14.5	0	5066 ±666	1.292 ±0.006	3921 ± 516	0.43 ±0.06
21.6	0	3205 ±588	1.440 ±0.005	2226 ± 408	0.27 ±0.05
35.6	0	5132 ±420	1.232 ±0.001	4167 ± 341	0.43 ±0.04
10 mg/L					
0.2	0.063	33600 ±5400	1.442 ±0.002	23300 ±3800	1.00
0.4	0.050	14400 ±4800	1.628 ±0.006	9000 ±3000	0.44 ±0.15
0.6	0.032	9100 ±6600	1.686 ±0.010	5390 ±3930	0.26 ±0.19
1.1	0.022	400 ±5500	1.761 ±0.011	200 ±3100	0.01 ±0.19
2.0	0	2700 ±6400	1.743 ±0.011	1600 ±3700	0.08 ±0.20
3.8	0	-1100 ±5000	1.780 ±0.007	-600 ±2800	-0.04 ±0.17
7.4	0	-12600 ±8000	1.899 ±0.011	-6600 ±4200	-0.39 ±0.25
14.5	0	300 ±10000	1.767 ±0.016	200 ±5600	0.01 ±0.32
21.6	0	2200 ±6000	1.752 ±0.006	1300 ±3400	0.07 ±0.18
35.6	0	-6300 ±6200	1.827 ±0.006	-3500 ±3400	-0.19 ±0.18

[a] see section 6.2.2
[b] see section 6.3.4

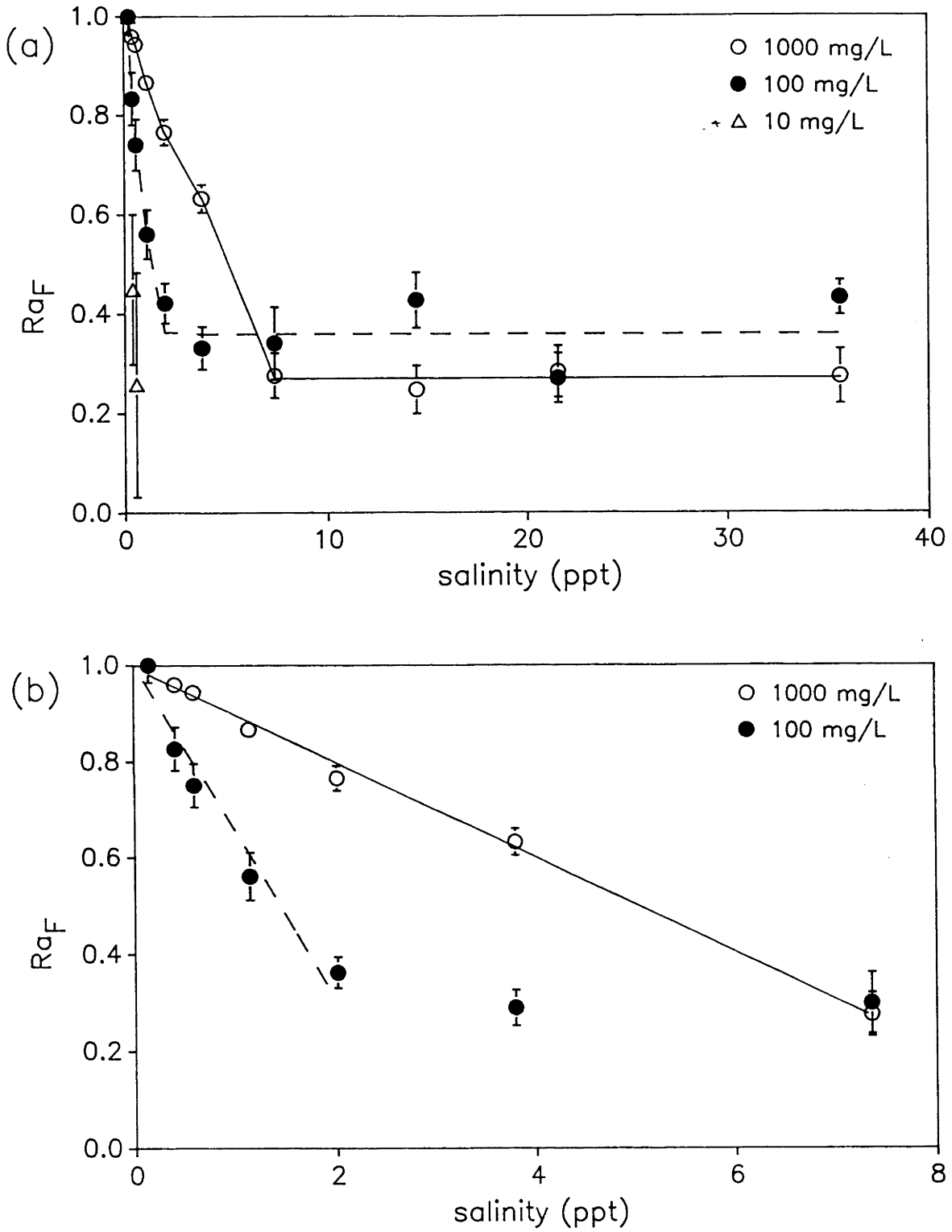

Figure 6.3 (a) Ra_F (see section 6.3.3) as a function of salinity. The sediment concentrations of sorbed radium in both the 100 mg/L and 1000 mg/L suspensions decrease to a more or less constant value as salinity increases.
(b) An expansion of (a). The relationship between sediment sorption of radium (Ra_F) and salinity is approximately linear at low salinities.

errors associated with the 10 mg/L suspension, only three values of Ra_F corresponding to salinities <0.6 ppt are plotted. Values of Ra_F for the 1000 mg/L (Ra_F^{1000}), 100 mg/L (Ra_F^{100}), and 10 mg/L (Ra_F^{10}) all show initial decreases as soon as salinity is increased. However, the extent of this reduction appears to be related to the sediment suspension concentration. Radium adsorption by the 10 mg/L suspension decreases at a greater rate than the 100 mg/L suspension, which in turn decreases more rapidly than the 1000 mg/L suspension. For example, at a salinity of 0.41 ppt the value of Ra_F^{10} has decreased by 55% ±15, whereas Ra_F^{1000} has decreased by only 4% ±2.

As salinity rises, Ra_F^{100} and Ra_F^{1000} both decrease to values of approximately 0.3, and remain relatively constant at higher salinities. If the extent of ^{226}Ra adsorption is controlled solely by the competing effects of other cations, and since ^{226}Ra was added in a soluble form, ^{226}Ra adsorption should continue to decrease with increasing salinity. The fact that ^{226}Ra adsorption reaches a constant value which appears to be independent of salinity suggests that a certain fraction of adsorption sites on the sediment selectively sorb radium at the expense of other cations in seawater. Benes et al. (1984, 1985, 1986a) showed that for some minerals, radium adsorbed from low salinity water could not be easily desorbed when equilibrated with water of a higher salinity. They suggested that radium in adsorption sites in these minerals is bound very strongly, and is not easily replaced by sodium ions. In this study it appears that the values of Ra_F at high salinities represent sorbed radium which is not available for ion-exchange with other major cations in seawater. In this context at least they may be termed 'irreversibly' bound.

The sorption behaviour of radium at low salinities can be seen more clearly by expanding Figure 6.3.a. The expansion (Figure 6.3.b) shows that in the salinity range 0.2-7 ppt there is a negative linear correlation between Ra_F^{1000} and salinity ($r^2 = 0.99$) The values of Ra_F^{100} are also consistent with a straight line in the salinity range 0.2-2 ppt ($r^2 = 0.95$). A linear decrease of sorbed radium with rising salinity suggests that at low salinities the sorption behaviour of radium is governed primarily by the number of competing cations in solution.

6.4 Desorption Experiments - Results and Discussion

The results of kinetic and salinity desorption experiments are discussed separately below. All measurements of thorium isotopes in the filtrate of the equilibrated sediment suspension were below detection, and are not shown. The extent of net thorium desorption from the sediment, if any, was less than 0.01% of the concentration of the sediment. Consequently, radium isotope data only is discussed in this section.

In all experiments radium isotopes in the filtrate were measured at the end of the equilibration period. The amount of radium initially present in the saline water was calculated from the known concentrations of river and seawater samples. This value was deducted from the filtrate concentration to obtain the amount of radium released from the sediment, which was then expressed as a percentage of the total sediment concentration. The radium isotope concentrations of the sediments used in these experiments are shown in Table 6.3.

6.4.1 Kinetic experiments - ^{226}Ra desorption

The results of radium desorption as a function of equilibration time are given for Murrumbidgee and Bega River sediments in Table 6.4. Figure 6.4 shows that radium desorption is rapid, with maximum desorption from (a) Murrumbidgee and (b) Bega River sediment reached between 1-4 h of equilibration. This rapid loss of radium is in agreement with previous published work, reviewed in chapter 2. The net radium desorption from the Bega sediment then decreases from an average value of 10.7 ±0.3% in the 0.5-4 h period, to 8.4 ±0.4% after an equilibration period of 456 h, a relative reduction of 22 ±5%. Net desorption then appears to remain unchanged for a period of up to 2184 h (91 d). Radium desorption from the Murrumbidgee sediment may have decreased slightly after an equilibration period of 240 h, although the evidence is weak.

The net decrease of ^{226}Ra desorption from the Bega sediment with time indicates that some radium initially released from the sediment has been re-adsorbed. Dickson (1985) also noticed a decrease in ^{226}Ra desorption from crushed U/Th ore with time, although in his experiments the decrease

Table 6.3 Radium isotope concentrations and CECs of sediments used in desorption experiments.

	CEC	^{226}Ra	^{228}Ra	^{224}Ra[a]	^{223}Ra[b]
	(meq/100g)	(mBq/g dry weight)			
Murrumbidgee River					
Unsieved bank sediment	23	36.6 ±0.8	52.7 ±0.7	52.3 ±1.2	2.2 ±0.2
Bega River bed sediment					
<63 μm	27	76.2 ±1.8	114 ±5	117 ±2	4.4 ±0.6
125-500 μm	3	14.6 ±0.3	15.5 ±0.7	17.3 ±0.5	0.8 ±0.2

[a] ^{224}Ra activity obtained by assuming secular equilibrium with ^{228}Th
[b] ^{223}Ra activity calculated from $^{235}U/^{238}U$ = 0.046, and assuming ^{223}Ra is in secular equilibrium with ^{235}U.

Table 6.4 The effect of equilibration time on the desorption of radium isotopes from Murrumbidgee and Bega River bed sediment (18 ppt salinity).

time (hours)	radium desorbed from sediment (%)				desorbed AR		
	^{226}Ra	^{228}Ra	^{224}Ra	^{223}Ra	$^{228}Ra/^{226}Ra$	$^{224}Ra/^{226}Ra$	$^{223}Ra/^{226}Ra$
Murrumbidgee River sediment							
0.5	9.6 ±0.5	8.5 ±0.6	19.6 ±1.3	16.3 ±4.0	1.28 ±0.07	2.94 ±0.15	0.08 ±0.01
1.15	11.6 ±0.7	10.1 ±1.1	25.1 ±1.8	21.5 ±5.4	1.25 ±0.12	3.10 ±0.16	0.09 ±0.02
2.7	11.8 ±0.6	10.0 ±0.8	22.2 ±1.5	21.0 ±4.9	1.22 ±0.09	2.72 ±0.15	0.09 ±0.01
5.5	11.5 ±0.6	11.8 ±1.1	25.1 ±1.8	13.6 ±3.7	1.48 ±0.11	3.15 ±0.17	0.06 ±0.01
20	11.6 ±0.5	12.2 ±0.7	21.8 ±1.6	17.1 ±4.3	1.55 ±0.05	2.71 ±0.16	0.07 ±0.01
240	10.5 ±0.5	10.1 ±0.9	19.4 ±1.1	19.6 ±4.1	1.38 ±0.08	2.66 ±0.11	0.09 ±0.01
Bega River sediment (<0.63 μm)							
0.5	10.4 ±0.6	11.9 ±0.8	20.2 ±1.3	14.2 ±2.9	1.75 ±0.08	2.97 ±0.12	0.08 ±0.01
1.25	10.4 ±0.5	12.4 ±0.9	20.2 ±1.3	11.1 ±2.4	1.83 ±0.09	2.99 ±0.12	0.06 ±0.01
4.25	11.4 ±0.6	14.3 ±1.0	22.9 ±1.5	13.7 ±3.1	1.92 ±0.10	3.09 ±0.14	0.07 ±0.01
20	9.8 ±0.5	12.0 ±0.9	17.4 ±1.1	11.0 ±2.5	1.88 ±0.11	2.72 ±0.11	0.07 ±0.01
96	9.0 ±0.4	11.2 ±0.8	18.8 ±1.2	13.6 ±2.8	1.93 ±0.11	3.22 ±0.14	0.09 ±0.01
456	8.4 ±0.4	10.0 ±0.8	18.4 ±1.2	13.4 ±2.7	1.83 ±0.11	3.35 ±0.14	0.09 ±0.01
2184	8.6 ±0.4	9.4 ±0.7	17.8 ±1.0	13.2 ±2.6	1.68 ±0.10	3.19 ±0.13	0.09 ±0.01

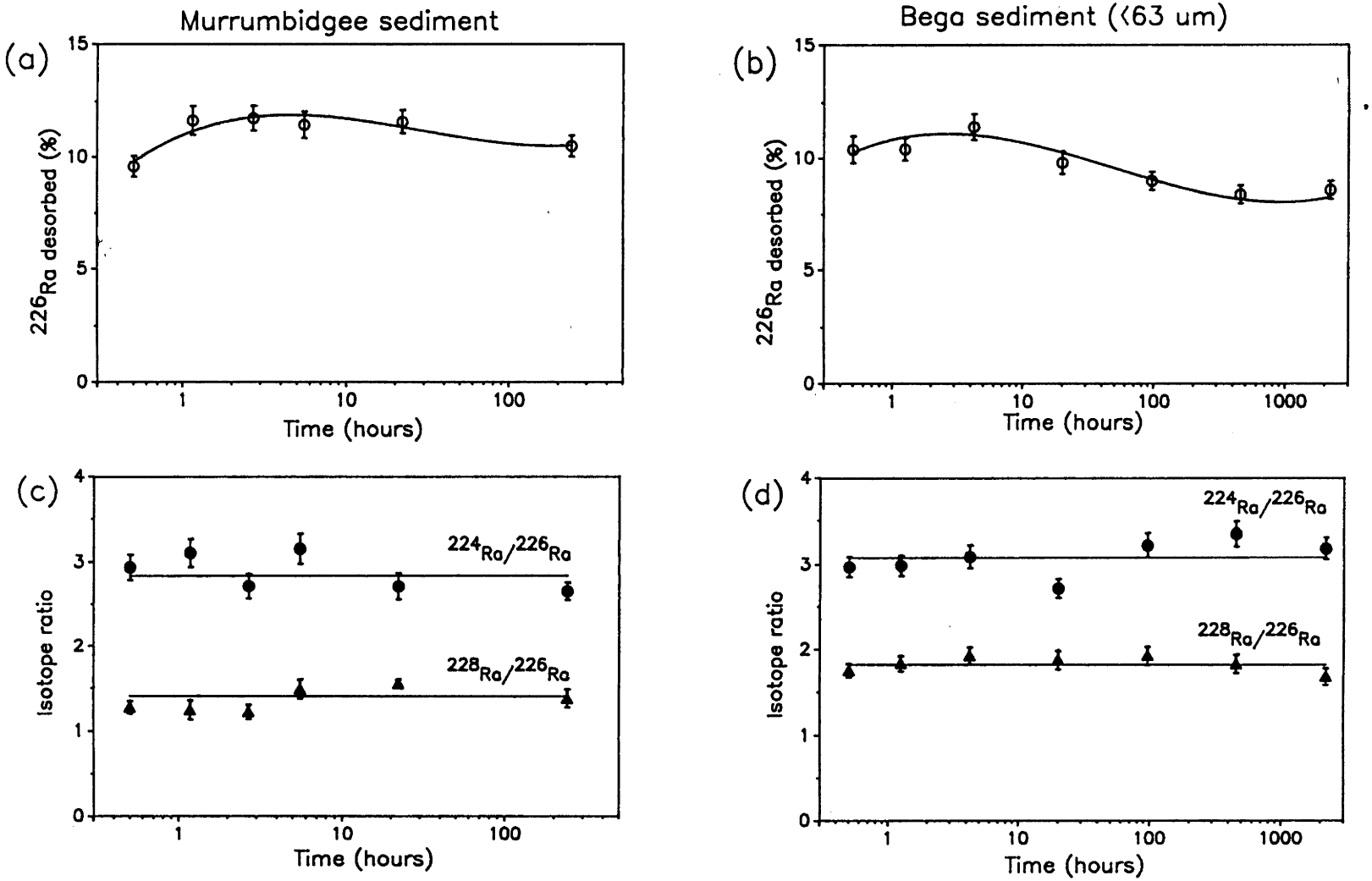

Figure 6.4 Desorption of ^{226}Ra and radium isotope activity ratios from Murrumbidgee sediment (a),(c), and <63 μm Bega River sediment (b),(d), as a function of time.

was much greater. He considered that the decrease may be due to a chemical reaction between the NaCl solution and the ore, resulting in the entrapment of radium. Such a reaction could include surface oxidation of the sediment particles. Surface oxidation would be expected to affect the sorption characteristics of the Bega sediment, which was collected from an aqueous and possibly reducing environment, more than the Murrumbidgee sediment which was collected as a dry exposed sediment.

6.4.2 Kinetic experiments - desorption of short-lived radium isotopes

The most useful way of interpreting the time dependence of the desorption of the short-lived radium isotopes (^{224}Ra,^{223}Ra and ^{228}Ra) is by the comparing the behaviour of each isotope with that of ^{226}Ra. Because the production and decay of the short-lived isotopes occurs at a much faster rate than ^{226}Ra, their net desorption relative to ^{226}Ra over a period of time may yield information on the kinetics and mechanisms of radium release from the sediment. This is particularly relevant for ^{224}Ra, whose half-life (3.7 d) is of a similar or much shorter time span than some of the equilibration experiments.

Plots of desorbed $^{228}Ra/^{226}Ra$ and $^{224}Ra/^{226}Ra$ AR's as a function of equilibration time are shown in Figure 6.4 for (c) the Murrumbidgee and (d) the Bega sediment. For clarity, the $^{223}Ra/^{226}Ra$ AR has not been plotted. Because of its low activity concentrations, the analytical uncertainties of ^{223}Ra determinations are high (±~25%), obscuring any possible trends in the $^{223}Ra/^{226}Ra$ AR. For both series of experiments there is no evidence for any long-term change with time for either the $^{228}Ra/^{226}Ra$ or $^{224}Ra/^{226}Ra$ AR.

Dickson (1985), in a similar series of experiments concluded that the continued presence of ^{223}Ra (half-life = 11.4 d) over a period of one year indicated that radium isotopes were in continual exchange between solid and solution. He also concluded that cation-exchange was the dominant method of release of radium into solution. The experiments in this study show that this also the case for ^{224}Ra. The fact that the $^{224}Ra/^{226}Ra$ AR desorbed from the Bega sediment remains more or less constant for up to 91 d, a period many times greater than the ^{224}Ra half-life, indicates that

the net amount of ^{224}Ra generated in the sediment via decay of its ^{228}Th parent and released into solution, balances the dissolved ^{224}Ra lost by decay. For this to occur, radium must be exchanging between solid and solution on a time scale short compared with the half-life of ^{224}Ra, in agreement with the results in section 6.4.1 above.

6.4.3 Salinity experiments - ^{226}Ra desorption

The results of desorption experiments performed at various salinities are shown in Table 6.5. Figure 6.5 shows that for the Murrumbidgee sediment (a), the ^{226}Ra desorption curve increases up to a salinity of about 18 ppt, and then flattens out to a relatively constant value up to 36 ppt (100% seawater). The maximum ^{226}Ra loss corresponded to 12.4% ±0.7 of total sediment activity. These results are similar to those of Elsinger and Moore (1984), who observed a maximum desorption of about 14% of ^{226}Ra from Pee Dee River sediment at a salinity of 20 ppt.

The desorption curves of the two particle size fractions of the Bega sediment (Figure 6.6) have significantly different shapes. The shape of the 125-500 μm desorption curve is similar to the Murrumbidgee curve, although the flattening of the curve occurs at a lower salinity (13 ppt). The <63 μm size fraction of the Bega sediment however shows evidence for the continued loss of ^{226}Ra throughout the measured salinity range. The desorption maximum is not defined by this data, but it appears to be at a much higher salinity than the 125-500 μm size fraction. The reason for this difference is not clear, but may be due to differences in the particle size distribution, mineralogy, and CEC of the two size fractions. The CEC of the <63 μm fraction (27 meq/100g, Table 6.3) is much greater than that of the 125-500μm fraction (3 meq/100g).

It is interesting to note that the maximum percentage loss of ^{226}Ra from the 125-500 μm fraction of the Bega sediment (13.2% ±0.9) is remarkably similar to that of the Murrumbidgee and Pee Dee Rivers. The <63 μm fraction of the Bega sediment also has a similar maximum loss (13.0% ±0.5). However, given the apparent continued increase in ^{226}Ra desorption from the <63 μm fraction with increasing salinity, its similarity to the other sediments is probably coincidental.

Table 6.5 The effect of salinity on the desorption of radium isotopes from Murrumbidgee and Bega River bed sediment (20 h equilibration).

salinity (ppt)	radium desorbed from sediment (%)				desorbed AR		
	^{226}Ra	^{228}Ra	^{224}Ra	^{223}Ra	$^{228}Ra/^{226}Ra$	$^{224}Ra/^{226}Ra$	$^{223}Ra/^{226}Ra$
Murrumbidgee River sediment							
1.8	1.9 ±0.1	2.7 ±0.3	3.7 ±0.4	3.2 ±1.1	1.42 ±0.15	2.77 ±0.24	0.08 ±0.02
3.7	2.6 ±0.2	2.9 ±0.3	5.4 ±0.7	4.0 ±1.6	1.52 ±0.16	3.00 ±0.31	0.07 ±0.03
5.3	4.2 ±0.2	3.7 ±0.3	8.8 ±0.7	9.2 ±2.4	1.27 ±0.08	3.02 ±0.17	0.11 ±0.02
8.9	6.1 ±0.4	5.8 ±0.4	13.2 ±1.1	11.7 ±3.2	1.36 ±0.06	3.10 ±0.16	0.10 ±0.02
12.8	7.4 ±0.4	n.d	15.6 ±1.2	14.7 ±3.5		3.12 ±0.16	0.10 ±0.02
17.8	11.3 ±0.5	12.2 ±0.7	23.8 ±1.1	18.9 ±4.0	1.55 ±0.05	2.97 ±0.11	0.08 ±0.01
26.7	12.4 ±0.7	12.5 ±0.9	26.8 ±2.1	29.2 ±6.9	1.46 ±0.06	3.11 ±0.18	0.11 ±0.02
35.6	12.1 ±.6	12.2 ±0.7	23.8 ±1.6	17.4 ±4.6	1.46 ±0.06	2.84 ±0.14	0.07 ±0.01
Bega River sediment							
<63μm							
1.8	1.2 ±0.1	1.6 ±0.2	2.4 ±0.3	1.9 ±0.6	1.97 ±0.22	3.07 ±0.27	0.10 ±0.03
3.7	2.0 ±0.2	2.8 ±0.3	4.9 ±0.5	2.6 ±0.8	1.95 ±0.19	3.74 ±0.27	0.08 ±0.02
7.4	4.4 ±0.2	5.3 ±0.4	8.7 ±0.6	6.0 ±1.3	1.81 ±0.10	3.03 ±0.16	0.08 ±0.01
12.8	7.1 ±0.3	9.2 ±0.7	14.8 ±0.9	11.3 ±2.3	1.94 ±0.12	3.22 ±0.15	0.09 ±0.01
17.8	9.8 ±0.5	12.4 ±0.9	18.6 ±1.2	13.7 ±3.0	1.88 ±0.11	2.91 ±0.13	0.08 ±0.01
17.8*	8.9 ±0.3	12.0 ±1.0	12.3 ±0.5	11.5 ±2.7	2.02 ±0.16	2.15 ±0.12	0.07 ±0.01
26.7	12.1 ±0.6	14.0 ±0.9	24.1 ±1.5	20.4 ±3.9	1.73 ±0.08	3.08 ±0.12	0.10 ±0.01
35.6	13.0 ±0.5	16.3 ±1.0	26.8 ±1.4	19.1 ±3.7	1.87 ±0.09	3.17 ±0.12	0.09 ±0.01
125-500μm							
3.7	6.7 ±0.8	13.2 ±1.3	n.d.	n.d.	2.08 ±0.06		
7.4	9.2 ±1.0	16.8 ±1.5	n.d.	n.d.	1.93 ±0.06		
12.8	12.1 ±0.8	23.7 ±2.0	n.d.	n.d.	2.08 ±0.11		
17.8	12.4 ±1.0	21.6 ±2.1	21.4 ±1.9	12.5 ±2.8	1.98 ±0.09	2.06 ±0.08	0.06 ±0.01
17.8*	12.6 ±1.1	23.8 ±2.5	15.9 ±1.5	10.6 ±2.8	2.01 ±0.13	1.50 ±0.08	0.05 ±0.01
26.7	13.2 ±0.9	24.8 ±2.2	n.d.	n.d.	1.99 ±0.11		
35.6	13.0 ±0.9	26.8 ±2.4	n.d.	n.d.	2.06 ±0.11		

n.d. not determined

* sediment dried at 60° C for 18 days prior to equilibration with saline water

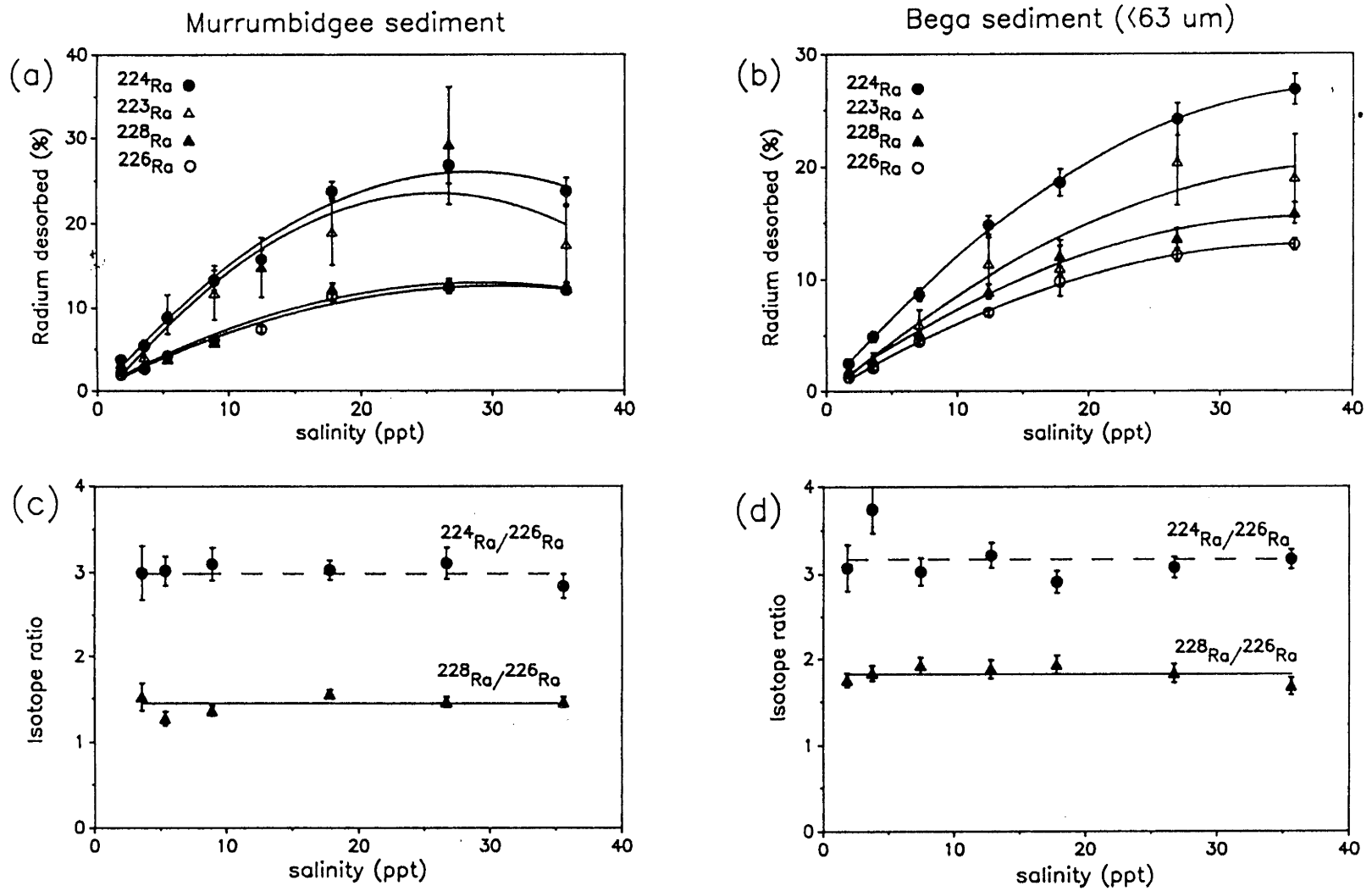

Figure 6.5 Desorption of radium isotopes and their activity ratios from Murrumbidgee sediment (a),(c), and <63 μm Bega River sediment (b),(d), as a function of salinity.

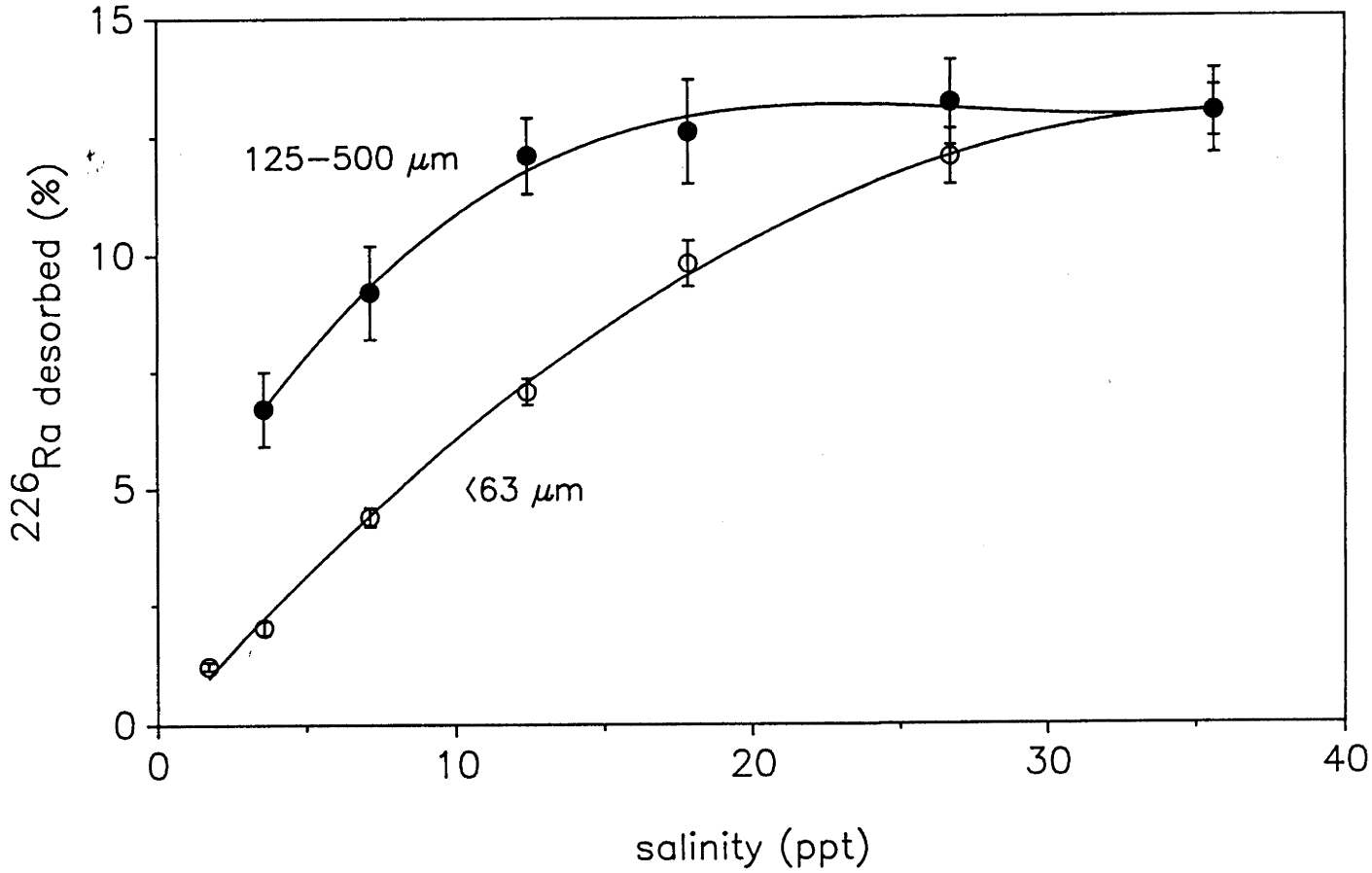

Figure 6.6 The desorption of ^{226}Ra as a function of salinity from two different size fractions of Bega River sediment.

6.4.4 Salinity experiments - the comparative desorption of radium isotopes

The desorption curves of the short-lived radium isotopes have the same shape as ^{226}Ra, as evidenced by the apparently unchanging $^{224}Ra/^{226}Ra$ and $^{228}Ra/^{226}Ra$ AR's (Figure 6.5, (b) and (d)). This is the case for both the Murrumbidgee and the <63 μm Bega River sediment. However, the percentage losses of each isotope vary (Table 6.5; Figure 6.5, (a) and (c)). Losses from the Bega sediment of the two shortest-lived isotopes, ^{224}Ra (max. 26.8% ±1.4) and ^{223}Ra (max. 20.4% ±3.9) are significantly greater than ^{226}Ra (max. 13.0% ±0.5). The Murrumbidgee results are similar. The percentage desorption of ^{228}Ra is also greater than that of ^{226}Ra for 125-500 μm size fraction, and to lesser extent, the <63 μm size fraction of the Bega River sediment. There is no difference in the percentage of ^{228}Ra and ^{226}Ra desorbed from the Murrumbidgee sediment.

If radium loss from the sediment in saline water is primarily by ion-exchange, these results indicate that short-lived radium isotopes must be preferentially concentrated in ion-exchange sites on the surface of the sediment particles. This situation could occur if their parent thorium isotopes were also preferentially concentrated near the surface of the sediment (Dickson 1985). Radium isotopes produced by the decay of surface-sorbed thorium would be more available for ion-exchange. Joshi et al. (1983) observed $^{228}Th/^{232}Th$ AR's of about 2 on the surface labile layers of estuarine sediments. The high AR was attributed to sorption of ^{228}Th produced in solution by the decay of ^{228}Ra. A $^{228}Th/^{232}Th$ AR of 2 on the surface layers of the Bega (<63 μm) and Murrumbidgee sediment used in these desorption experiments would account, almost exactly, for the greater desorption of ^{224}Ra compared to ^{226}Ra. A similar process may also explain the comparatively high ^{223}Ra desorption. Its parent (^{227}Th) may be preferentially concentrated on surface sites following its production in solution by the decay of dissolved ^{227}Ac.

Another process which could lead to an enrichment of ^{224}Ra and ^{223}Ra in surface sites of the sediment is that of alpha-recoil. This is a physical process whereby nuclei can be displaced across phase boundaries resulting in the 'ejection' into solution of radionuclides from sites within mineral grains (Osmond and Cowart 1982). Kigoshi (1971) estimated an alpha-recoil

range of about 900 angstroms in pelagic sediments. In an aqueous medium, the solution will act to bring the recoiling nucleus to rest. In fresh water where radium K_d's are high, a large fraction of ejected radium nuclei will then be rapidly sorbed onto surface sites of the sediment. Furthermore, recoil processes can preferentially locate radium at surface sorption sites via recoil emplacement and/or disruption of the crystal lattice of a mineral by an alpha-particle during radioactive decay (e.g. Fleischer 1982). In the short term (days-weeks), alpha-recoil followed by surface sorption will lead to an increase in the activities of surface-sorbed radium isotopes with short half-lives (^{224}Ra and ^{223}Ra), compared to the longer-lived ^{226}Ra and ^{228}Ra. All radium isotopes experience recoil when created, and so over longer periods (tens to thousands of years) the activities of surface-sorbed ^{228}Ra and ^{226}Ra would also increase. However, because ^{228}Ra and ^{226}Ra are much longer-lived, slow oxidation processes such as the formation of Fe/Mn oxide coatings on the surface of the sediment grains can be expected to reduce their availability for ion-exchange. Thus the half-life of a radium isotope could affect its net desorption in saline waters. The curves in Figure 6.5 (b) are consistent with this hypothesis, as there appears to be a relationship between the percentage desorption of an isotope and its half-life.

Fleischer (1982) noted that the presence of water increased the removal of alpha-recoil nuclei from minerals. Kigoshi (1971) observed that more alpha-recoil ^{234}Th was able to be dissolved from mineral powder after the powder had been kept in solution than when it had been kept in air or vacuum. In order to determine whether alpha-recoil played a significant role in the desorption of ^{224}Ra and ^{223}Ra, the <63 μm and 125-500 μm size fractions of the Bega River bed sediment were dried in an oven at 60° C for 18 d, and then equilibrated with saline water (18 ppt). The results of this experiment were then compared with the results of the desorption experiments at the same salinity using the wet sediment slurries. The absence of an aqueous medium surrounding the sediment grains prior to equilibration should result in less surface sorption of recoil ejected radium nuclei. Instead of losing their momentum in the water, a higher proportion of the nuclei may become deeply embedded in adjacent sediment grains, leaving them less accessible to ion-exchange processes. By keeping the sediment dry for a period of 18 d (about 5 half-lives of ^{224}Ra),

ion-exchangeable ^{224}Ra which had accumulated on the surface of the wet sediment particles due to alpha-recoil and sorption processes will have decayed to a small fraction its original activity.

The results of the experiment (denoted as * in Table 6.5) show that the desorption of ^{224}Ra relative to ^{226}Ra, as measured by the desorbed $^{224}Ra/^{226}Ra$ AR, is 26% ±5 lower from the <63 μm pre-dried sediment compared to the wet sediment. The corresponding reduction for the pre-dried 125-500 μm sediment is 28% ±9. The desorbed AR of the longer-lived radium isotopes, $^{228}Ra/^{226}Ra$, is relatively unchanged for both size fractions. The uncertainties of the ^{223}Ra results are too large to allow any conclusions to be drawn on its behaviour. These results are consistent with the hypothesis that alpha-recoil contributed, albeit indirectly, to the higher percentage losses of ^{224}Ra, and perhaps ^{223}Ra, reported above.

6.5 Effect of S/L ratio on ^{226}Ra desorption

The results of desorption experiments investigating the effect of the concentration of sediment (S/L ratio) on ^{226}Ra desorption are presented in Table 6.6. The experiments were conducted using <63 μm Bega sediment, at a salinity of 7 ppt. The fraction of ^{226}Ra desorbed from the sediment decreases with increasing S/L ratio. The highest ^{226}Ra loss (26% ±3) occurs at a sediment concentration of 0.25 g/L, whereas at a sediment concentration of 50 g/L only 1.2% is desorbed. These results verify the trend observed in the adsorption experiments (section 6.3.3), and show that the sediment concentration is a major factor affecting radium desorption in saline water.

Table 6.6 The effect of solid/liquid (S/L) ratio on the desorption of ^{226}Ra from <63μm Bega River sediment (7 ppt salinity).

S/L ratio (g/L)	% ^{226}Ra desorbed from sediment
0.25	26.1 ±2.7
1	13.8 ±1.2
4	6.9 ±0.5
12.5	3.4 ±0.2
50	1.2 ±0.2

6.6 The Fraction of Sediment-bound ^{226}Ra Available for Ion-exchange

Because of their design, the desorption experiments (section 6.4) did not quantify how much ^{226}Ra was able to be desorbed from freshwater sediment. The experiments only indicated how much radium could be desorbed under those experimental conditions. This section examines two methods of deriving an estimate of the fraction of ion-exchangeable radium in freshwater sediment, and compares the results.

6.6.1 An estimate using variable S/L ratios

The results of the variable S/L ratio experiments (section 6.5 above) indicate that at low sediment concentrations a large fraction of ion-exchangeable ^{226}Ra is desorbed in saline water. Figure 6.7 shows a plot of % ^{226}Ra desorption (from Table 6.6) against the inverse of the sediment concentration. The plot shows that as the sediment concentration becomes more dilute, ^{226}Ra desorption increases towards a maximum value. A curve fitted to the data approximates a saturating exponential of the form $y = A(1-e^{-bx})$, ($r^2 = 0.98$). The value of A is 26.8 $\pm$2.3, and can be used as an estimate of the % ^{226}Ra which could be desorbed from the sediment at an infinitely dilute sediment concentration.

6.6.2 An estimate obtained from repeated leaching of the sediment

All previous desorption experiments have been carried out in a closed system, with no addition or removal of solution or sediment during the course of the experiment. However, in a natural system bed sediments may be periodically flushed by new saline surface water as a result of agitation of the sediment particles, or by movement of surface water into and out of sediment pore spaces by tidal action. During this process radium will be desorbed from the sediment, increasing the concentration of radium in the water contacting the sediment. As this water is replaced with new surface water containing less radium, the result will be a net export of radium from the proximity of the sediment. Although the S/L ratio of bottom sediments may be high and the incremental loss of radium small, the continued flushing of the sediment may eventually result in the

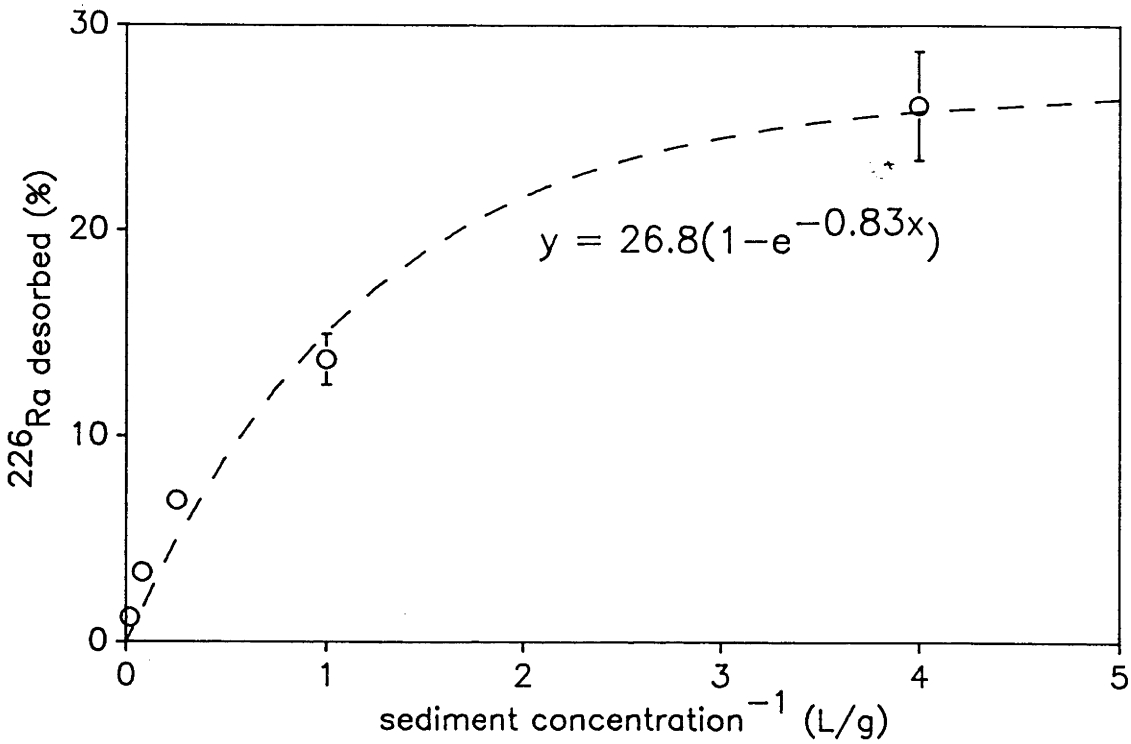

Figure 6.7 ^{226}Ra desorption (%) at 7 ppt salinity from <63 μm Bega River sediment plotted against the inverse of sediment concentration. The fitted curve increases towards a maximum value as the sediment concentration becomes more dilute.

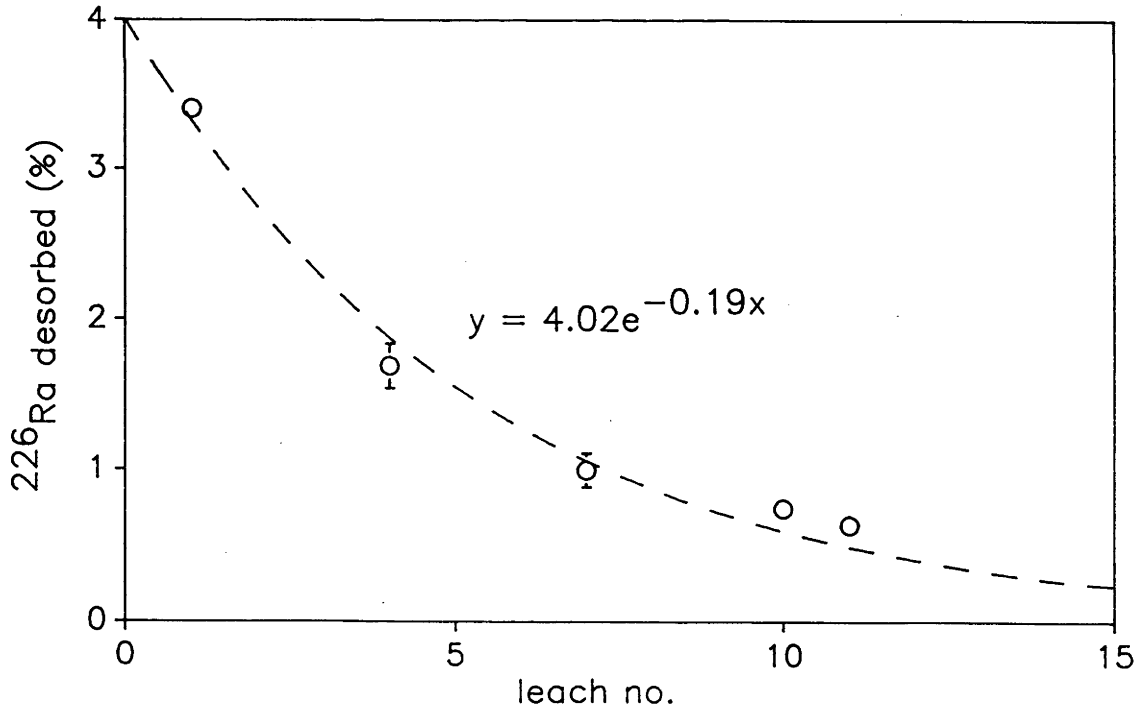

Figure 6.8 The effect of repeated leaching on the % ^{226}Ra desorbed from <63μm Bega River sediment. The cumulative ^{226}Ra loss can be estimated from the integral of the equation of the fitted curve.

desorption of most of the ion-exchangeable radium originally present in the freshwater sediment.

In order to simulate this process in the laboratory, and so quantify the fraction of ^{226}Ra able to be desorbed from freshwater sediment, a series of leachings were performed on the same sediment aliquot. Freshwater Bega River bed sediment (<63 μm, 12.5 g/L) was equilibrated (vigourously shaken) with saline water (7 ppt) for one hour. The sediment suspension was then centrifuged, the clear leachate decanted, and the sediment re-equilibrated with a new saline solution. This procedure was repeated 9 times, and every third leachate filtered (0.45 μm) and analysed for dissolved ^{226}Ra. The leached sediment was then stored for 20 d to allow for ^{224}Ra ingrowth (section 6.6.3 below), and an eleventh equilibration performed. The results are given in Table 6.7.

Table 6.7 Sequential leaching of radium from Bega River sediment (<63μm; 7 ppt salinity).

leach no.	^{226}Ra (% desorbed)	^{224}Ra	$^{224}Ra/^{226}Ra$
1	3.40 ±0.22	7.26 ±0.57	3.2 ±0.2
4	1.69 ±0.14		
7	1.00 ±0.11		
10	0.75 ±0.07		
11*	0.64 ±0.07	4.18 ±0.52	9.9 ±1.1

* Leach 11 was performed 20 days after leach 10 to allow ^{224}Ra in the sediment phase to attain secular equilibrium with its parent (^{228}Th).

A plot of % ^{226}Ra desorption from the sediment as a function of the number of leachings is shown in Figure 6.8. Radium loss from the sediment decreases exponentially with leach no., and approximates the curve Ae^{-bx}, ($r^2 = 0.98$) where A = 4.02 ±0.24 and b = 0.19 ±0.02. The amount of ^{226}Ra able to be desorbed from the sediment in saline water should be equal to the cumulative ^{226}Ra loss from the sediment after an infinite number of leachings. An estimate of this value can be obtained by integrating the

equation of the curve with respect to x. The integral, A/b, is equal to 21.1% ±2.3 of the original ^{226}Ra sediment concentration. This value is slightly lower than the fraction derived by varying the S/L ratio of the sediment suspension (section 6.6.1 above). The difference may be due to the repeated compaction and aggregation of the sediment particles during centrifugation, resulting in a gradual reduction in the effective surface area of the sediment particles.

It is interesting to compare these two experimentally derived values of ^{226}Ra loss with the estimate of ^{226}Ra desorption from the estuarine bed sediment sample of the same particle size. From the data in Table 5.7 the reduction in the $^{226}Ra/^{232}Th$ AR of the <63 μm size fraction of the bed sediment samples collected from site 5 (saline) relative to site 0 (freshwater) is calculated to be 33% ±4. Implicit in this calculation is the assumption that the particle size and mineralogical characteristics of the <0.63 μm fraction at both sites are similar. Given this assumption, and the different experimental methodologies used, the agreement between the experimentally derived ^{226}Ra losses and the observed loss is considered good.

6.6.3 Repeated sediment leachings - re-generation of exchangeable ^{224}Ra

Desorbed ^{224}Ra was determined on the first and eleventh sediment leachings (Table 6.7). The centrifuged sediment had been deliberately left for 20 d after the tenth leaching. During this time the sediment ^{224}Ra activity, which was deficient with respect to its parent ^{228}Th due to desorption losses, will have grown towards secular equilibrium with its parent again. The results show that although the activity of desorbed ^{226}Ra decreased by a factor of 5.3 from the first to the eleventh leaching, ^{224}Ra desorption decreased by a factor of only 1.7. As a result, the corresponding $^{224}Ra/^{226}Ra$ AR increased from 3.2 ±0.2 to 9.9 ±1.1. These results show that sediment which has had a substantial fraction of its ^{226}Ra leached, is capable of supplying high $^{224}Ra/^{226}Ra$ AR's to the surrounding water. They also provide experimental evidence for the process probably responsible for the high activities of short-lived radium isotopes relative to ^{226}Ra observed in the bed sediment pore water sample from the Bega River estuary (section 5.8.2, Table 5.4).

6.7 Summary

At low salinities there is a negative linear relationship between the adsorption by sediment of dissolved ^{226}Ra and the salinity, indicating that competition from other cations for ion-exchange sites is the major factor affecting sorption behaviour of ^{226}Ra. The results of adsorption experiments indicate that the sediment concentration of radium decreases to a constant value with increasing salinity. The salinity at which this constant value is reached appears to depend on the sediment concentration (S/L ratio).

The S/L ratio was shown to be a major factor affecting the extent of radium loss from sediment in a closed system. A proportionally greater loss of radium from the sediment occurs at low sediment concentrations, and may be due to solid-solid interactions such as particle aggregation.

As the sediment concentration decreases, radium loss appears to approach a maximum value. This observation, together with the results of sequential leaching experiments suggest that freshwater sediment contains a certain fraction of radium which is 'able to be desorbed' in saline water. This fraction probably corresponds to radium in sediment ion-exchange sites. The experimentally derived radium loss compares reasonably well with the calculated loss from an estuarine bed sediment sample.

Kinetic experiments show radium desorption is rapid, with maximum desorption from river sediment reached within 1 h of contact with saline water. Some of the released radium appears to have been re-adsorbed by the Bega River sediment over the next few days. The constancy of desorbed $^{224}Ra/^{226}Ra$ AR's over equilibration periods many times greater the half-life of ^{224}Ra is consistent with a continual rapid exchange of radium between solid and solution.

Desorption experiments with river bed sediments show that the shape of the desorption curve as a function of salinity may depend on the particle size of the sediment. Desorption maxima occur at lower salinities for coarser sized material.

The higher percentage losses of ^{224}Ra and ^{223}Ra relative to ^{226}Ra and ^{228}Ra indicates that short-lived radium isotopes are preferentially concentrated in ion-exchange sites in freshwater sediment. The repeated leaching of radium from sediment by saline water could enhance this situation. This process is probably responsible for the high activities of short-lived radium isotopes relative to ^{226}Ra in estuarine pore water.

7. Discussion and Conclusions

The aim of this study was to measure the effects of salinity on the sediment concentrations of radium and thorium, and assess whether radium and thorium AR's can be used successfully as sediment tracers in saline waters. The results of this study have shown that the sediment concentration of radium will be significantly reduced by salinity. In the process of quantifying the extent of radium loss, the study also examined other factors which, in conjunction with salinity, were expected to influence the sorption behaviour of radium.

In this chapter the significance of these factors is summarised, and the implications for sediment tracing discussed. Conclusions are then drawn on the suitability of some isotope AR's as sediment tracers in saline waters.

7.1 The Behaviour of Thorium in Saline Water

This study found there was no evidence of a net desorption loss of thorium from sediment with rising salinity. Indeed, laboratory adsorption experiments (section 6.3.1) indicated that thorium may be scavenged with increased efficiency by particulates in saline water. The dissolved and/or colloidal thorium activity concentrations of surface waters are usually extremely low (chapter 2), and so the net increase in sediment thorium concentrations is likely to be small. But if significant levels of thorium are present as clay particles <1 μm, or are complexed with dissolved organic species, aggregation of colloids in saline water could lead to a change in the thorium concentration of CFC extractable sediment (nominal particle size >1 μm). This process would be most significant in rivers where the concentrations of suspended sediment >1 μm are low.

7.2 The Behaviour of Radium in Saline Water

7.2.1 The rates and mechanism of radium release

Laboratory desorption experiments (chapter 6) showed that the kinetics of radium desorption is rapid, with maximum desorption from the sediment occurring within 1 h of contact with saline water (section 6.4.1). The

slight decrease in desorbed radium over the following days was probably due to a mineralogical or chemical change at the surface of the sediment.

The laboratory experiments also indicated that the mechanism of radium release from freshwater sediments is primarily that of cation exchange. At low salinities (<7 ppt) the relationship between radium sorption and salinity was approximately linear (section 6.3.4), suggesting that it is competition effects from other dissolved cations for sediment ion-exchange sites which results in the net loss of radium from freshwater sediment. There is some evidence that alpha recoil is indirectly responsible for radium desorption by providing a path by which radium can accumulate at the surface of freshwater sediments.

7.2.2 The extent of radium desorption from freshwater sediments

Both field and laboratory data show that the amount of ion-exchangeable radium desorbed from freshwater river sediment increases with salinity to a maximum value (sections 5.6 and 6.6). The fraction of radium which remains attached to sediment is presumably radium bound to non-exchangeable surface sites, and radium present in the internal lattice structure of the sediment grains. Adsorption experiments (section 6.3.4) show that the amount of sediment-sorbed radium decreases as soon as salinity rises, although the relationship between desorption and salinity appears to be influenced by other factors, such as the sediment concentration.

There is evidence that the suspended sediment samples from the Bega River estuary show a similar linear relationship between radium loss and salinity observed in the adsorption experiments (section 6.3.4). Figure 7.1 is an expanded version of Figure 5.9, and shows that a plot of the November suspended sediment $^{226}Ra/^{232}Th$ AR's against salinity approximates a straight line with a slope of -0.10 $\pm$0.01 (r^2 = 0.98) in the salinity range 0.15-4.4 ppt. The approximation of linearity enables an estimate of radium loss as a result of small increases in salinity. For salinities <4.4 ppt, the change (δ) in the $^{226}Ra/^{232}Th$ AR of the Bega River suspended sediment

as a result of an increase in salinity from S_1 to S_2 can be calculated from

$$\delta\ (^{226}Ra/^{232}Th\ AR) = -0.10 \times \delta S$$

where $\delta S = S_2 - S_1$ (ppt)

A calculation using this equation shows that a doubling of the salinity of the Bega River from its freshwater value of 0.12 ppt (EC = 220 μS/cm) to 0.24 ppt (440 μS/cm) would result in a decrease in the $^{226}Ra/^{232}Th$ AR of 0.012. This decrease corresponds to a desorption of 1.2 ±0.1% of the total ^{226}Ra bound to the freshwater suspended sediment.

The regression curve in Figure 7.1 intersects the line representing the minimum $^{226}Ra/^{232}Th$ AR reached by suspended sediment at a salinity of 6 ppt. This result suggests that all ion-exchangeable radium may have been desorbed from the suspended sediment at a salinity closer to 6 ppt than the original estimate of 10 ppt (section 5.6.2).

It is acknowledged that this study has only investigated the effects of water with the same ionic composition as seawater, and that some inland rivers may receive groundwater with high concentrations of dissolved ions in different proportions to that of seawater. Other studies (see chapter 2) have shown that the ionic composition of the water affects the extent of radium release from sediments. It is possible therefore that the relationship between radium desorption and salinity in an estuary may differ to that of an inland river system. Nevertheless, because the mechanism of radium release from sediment is primarily that of cation exchange, the same general trends should occur as those exhibited in seawater, i.e. an increase in radium desorption to a limiting value as the cation concentration of the water increases.

7.3 Other Factors Influencing Radium Desorption

Apart from salinity, this study has identified that two other factors, particle size and S/L ratio, can significantly affect the extent of radium loss from river sediments.

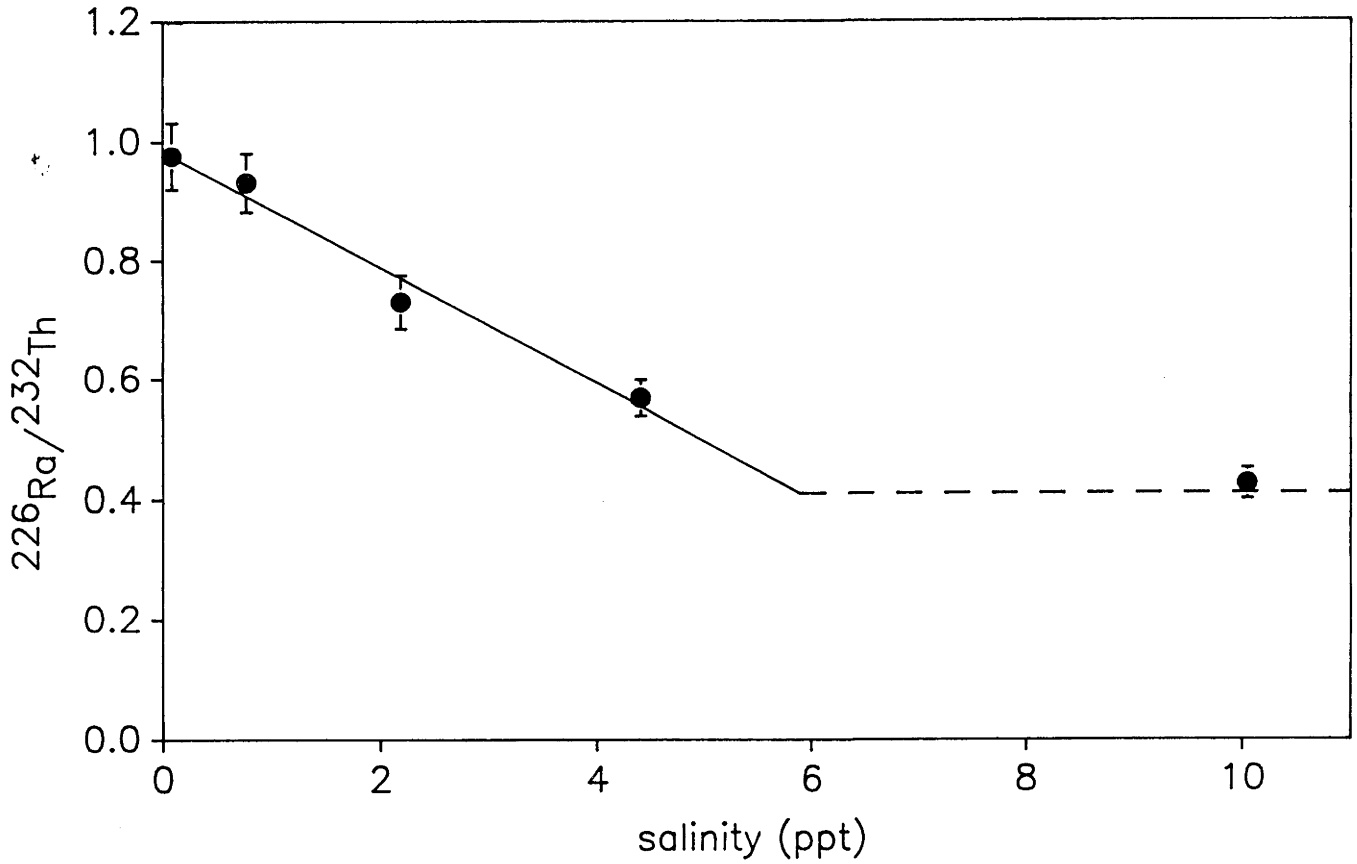

Figure 7.1 An expansion of Figure 5.9, illustrating the approximate linearity between the $^{226}Ra/^{232}Th$ activity ratio and salinity in the salinity range 0.2-4.4 ppt. The plot suggests that the minimum $^{226}Ra/^{232}Th$ activity ratio (dashed line) may have been reached at a salinity of about 6 ppt.

7.3.1 Particle size

Analysis of discrete particle size fractions of river and estuarine bed sediment samples indicated that a greater fraction of radium was able to be desorbed from smaller particles, probably due to their higher surface area per unit mass. However, desorption experiments indicated that radium was desorbed more easily from sand-sized sediment, with the maximum loss occurring at a lower salinity than the <63 μm fraction (section 6.4.3). Consequently, at low salinities the fraction of radium desorbed from coarse particles may actually be greater than that from fine particles.

Particle size effects are almost certainly associated with changes in mineralogy of the sediment. For example, the sorption behaviour of radium in particles <2 μm is probably dominated by the properties of clay minerals, whereas Bega River sediment sized >63 μm consisted mainly of quartz, feldspars and muscovite. The effect of mineralogy has not been determined in this study, but other studies have shown that the sorption behaviour of radium is related to factors associated with the crystal structure of a mineral, such as CEC (Ames et al. 1983) and the bond strength of sorbed radium (Benes et al. 1984, 1985, 1986a).

It should also be noted that the sorption behaviour of radium and thorium in the fine clay fraction (<1 μm) (section 5.6.4) was not examined in detail here because of low sample mass and poor counting statistics. The results of this study are based on the behaviour of suspended sediment recovered by the CFC, and river-bed sediments, and so are biased towards sediment with a particle size >1 μm.

7.3.2 Solid/liquid ratio

The S/L ratio of a sediment suspension also controls the sorption behaviour of radium (sections 6.3.3 and 6.5). In a closed system, proportionally more radium is desorbed from the sediment at low sediment concentrations. This conclusion implies that at the same total dissolved salt (TDS) concentration, suspended sediment will lose a greater proportion of its radium than bed sediments. However most river-bed sediments are not in a closed system, and their continued flushing by saline water could eventually result in the leaching of a large fraction of exchangeable

radium from the sediment (section 6.6.2). The flushing could occur as a result of the movement of surface water into and out of the pore spaces of estuarine bottom sediments by tidal and wave action, or by saline groundwater seepage through river-bed sediments. The extent of radium loss from bed sediments is therefore likely to be controlled by the extent of flushing, as well as by the TDS concentration of the surrounding water.

These factors will be important when assessing the radium loss from bed sediments recently transported and deposited during a flood event. Deposition is likely to have occurred in relatively fresh water, and the sediments may have had only a recent and limited exposure to water with a high salt content. Initially therefore, the bed sediments may have lost less radium than expected from TDS considerations alone. Only after continual flushing will the radium concentration of the sediments be reduced to a level consistent with the TDS concentration of the water.

The converse situation may exist in a river during a period of high flow and low TDS concentration. Even though the river water is relatively fresh at this time, the bed sediments may be apparently deficient in radium due to past regimes of high salt concentration. As discussed in chapter 4, this was the likely situation in the Loddon River-Barr Creek system in May 1992. If such sediments are continually exposed to fresh water without any intermittent rises in TDS concentration, it is possible that a gradual net adsorption of radium by the sediments would take place. The radium concentrations of the sediment would then increase towards their values prior to exposure to water with a higher salt content. The rate of this radium increase is not known, but it is likely to depend largely on the concentration of dissolved radium in the water, and in the case of bed sediments, the extent of flushing.

In summary therefore, the combined effects of both particle size and S/L ratio indicate that, when exposed to water with an increased salt content, the greatest radium loss from sediments will occur from clay particles when they are present in the water column at low concentrations. This appeared to be the situation in the Bega River estuary at the time of sampling. Consequently, the fraction of radium desorbed from suspended sediment in the Bega River estuary (50-58%) is probably close to the the maximum radium loss likely to be occur from river sediments. By contrast, it is expected

that coarse-grained bed sediments rich in quartz and feldspar are likely to lose proportionally less radium.

7.4 Implications for Sediment Tracing

In most cases, radium loss from sediments due to increases in TDS concentration will reduce the reliability of sediment sourcing using Ra/Th AR's, and thus the accuracy of sediment budget calculations. Because sediment tracing often relies on the difference between Ra/Th AR's from different sediment sources rather than their absolute values, an error introduced by an unquantified radium loss from one or more of the sediment sources will be magnified in sediment budget calculations. For example, calculations in the previous section indicate that an increase in the TDS concentration by only a few hundred EC units (μS/cm) may be enough to a cause reduction in the $^{226}Ra/^{232}Th$ AR of 1% or more in some river sediments. If the $^{226}Ra/^{232}Th$ AR's of the sediment sources differ by only a few percent in absolute terms, this reduction is significant. The magnitude of the error will then depend on the difference between the AR's of each sediment source, as well as the extent of the radium loss.

In chapter 4 the $^{228}Ra/^{226}Ra$ AR was identified as a potential sediment tracer because it eliminated differences in chemical behaviour inherent in Ra/Th AR's. However, this study has shown that it may not a reliable sediment tracer in rivers with a high salt content, particularly where the dissolved $^{228}Ra/^{226}Ra$ AR differs significantly from the bulk sediment value. In chapter 5 it was shown that variable suspended sediment $^{228}Ra/^{226}Ra$ AR's occurred in the Bega estuary in the 0-10 ppt salinity range. This variability was probably due to the equilibration of radium between two phases (sediment and water) with different $^{228}Ra/^{226}Ra$ AR's. Dissolved $^{228}Ra/^{226}Ra$ AR's are often high in estuaries (chapter 5, and other studies reviewed in chapter 2), and can vary considerably in groundwaters (Osmond and Cowart 1982; Dickson 1990). Outseepage of saline groundwater is the main source of dissolved salt to the Loddon River-Barr Creek system (Macumber 1991), and so the potential exists for the alteration of the $^{228}Ra/^{226}Ra$ AR of inland river sediments as well.

Furthermore, laboratory experiments showed that a higher percentage of ^{228}Ra than ^{226}Ra was desorbed from Bega River sediments in saline water

(section 6.4.4). Loss of this radium must therefore have altered the bulk sediment $^{228}Ra/^{226}Ra$ AR. However, the percentage ^{228}Ra and ^{226}Ra desorbed from Murrumbidgee sediment in saline water are the same, within error, indicating that there was no change in the bulk sediment $^{228}Ra/^{226}Ra$ AR. In the circumstance where the $^{228}Ra/^{226}Ra$ AR dissolved in the river water is close to the bulk sediment value, the $^{228}Ra/^{226}Ra$ AR should provide a stable signature for this sediment.

The $^{230}Th/^{232}Th$ AR appears to be a reliable tracer of sediment movement in an estuary (sections 5.6 and 5.7), and should also be suitable in inland saline rivers. The only situation where changes in TDS concentration could cause a significant change in the $^{230}Th/^{232}Th$ AR of sediment recovered by the CFC is outlined in section 7.1. The aggregation of material <1 μm with a $^{230}Th/^{232}Th$ AR different to that of the >1 μm phase could change the value of the suspended sediment recovered by the CFC.

It has also been shown that in some circumstances the $^{228}Th/^{232}Th$ AR can be used to give a characteristic signature to a sediment source where no difference could be discerned using other radium and thorium isotope tracers (sections 5.6 and 5.7). The characteristic signal was due to the 'estuarine age' of the sediment, coupled with disequilibrium in the thorium decay series caused by desorption of ^{228}Ra from the sediment.

7.5 Radium Isotopes as Tracers of Water Movement in an Estuary

This study has shown that in the estuary of a river containing low concentrations of suspended sediment, a large proportion of the observed increase of dissolved radium in the water column originated from bottom sediments (section 5.8). The dissolved concentrations of the short-lived radium isotopes (^{224}Ra, ^{223}Ra and ^{228}Ra) were particularly highly enriched. The most likely source of these isotopes was the pore water of bottom sediments. The analysis of a single pore water sample, together with the results of a sequential leaching experiment (section 6.6.3) indicated that estuarine pore water is characterized by high AR's of short-lived radium isotopes to ^{226}Ra. These high AR's occur as a result of salinity and the high rate of activity production of short-lived radium isotopes in the sediments. Radium isotopes have already been identified as potentially

powerful tracers of water mixing in estuaries and the continental shelf (Moore 1990). This work has shown that they may give information on the rates and extent of surface-pore water mixing, and act as tracers of pore water movement in an estuary. Recent modelling based on the work described in this thesis has shown that surface-pore water exchange can describe well the observed behaviour of dissolved radium isotopes in the Bega River estuary (Webster et al. 1993).

7.6 Conclusions

Radium is progressively desorbed from freshwater river sediment as salinity increases. The extent of radium loss depends on salinity, the solid/liquid ratio, and the particle size distribution of the sediment.

There is evidence that thorium is increasingly adsorbed in saline waters. In some circumstances, this behaviour could increase the sediment concentration of thorium.

It is concluded that the $^{226}Ra/^{232}Th$ AR is not a suitable sediment tracer in saline rivers. Nor is the the $^{228}Ra/^{226}Ra$ AR generally suitable, although it may be useful in specific cases. However the $^{230}Th/^{232}Th$ AR can provide a stable tracer of sediment movement in waters of varying salinity.

This work has also demonstrated that radium isotopes may provide a valuable tool in the investigation of water mixing and movement in an estuary.

References

Ames, L.L. and Rai, D. (1978) Radionuclide interactions with soil and rock media, Vol. 1, Processes influencing radionuclide mobility and retention, element chemistry and geochemistry, conclusions and evaluation. In "Radionuclide Interactions with Soil and Rock Media, Vol. 1, Section 3. pp 211-200. EPA 520/6-78-007A, U.S. Environmental Protection Agency.

Ames, L.L., McGarrah, J.E. and Walker, B.A. (1983). Sorption of trace constituents from aqueous solutions onto secondary minerals. II. Radium. Clays and Clay Minerals, **31**, No.5, pp 335-342.

Bacon, M.P. and Anderson, R.F. (1982). Distribution of thorium isotopes between dissolved and particulate forms in the deep sea. Journal of Geophysical Research, **87**, No. C3, pp 2045-2056.

Baes, C.F., and Mesmer, R.E. (1976). The hydrolysis of cations. 489 pp, Wiley-Interscience, New York.

Balistrieri, L.S. and Murray, J.W. (1984). Marine scavenging: Trace metal adsorption by interfacial sediment from MANOP site H. Geochimica et Cosmochimica Acta, **48**, pp 921-929.

Barney, G.S. (1984). "Radionuclide sorption and desorption reactions with interbed materials from the Columbia River basalt formation", Geochemical Behaviour of Disposed Radioactive Waste (Proc. Mtg Seattle), Symposium Series, No. 246, American Chemical Society, Washington DC, pp 3-22.

Benes, P. (1982). Physico-chemical forms and migration in continental waters of radium from uranium mining and milling. The Environmental Migration of Long-lived Radionuclides, (Proc. Int. Symp. Knoxville, TN, 1981), IAEA, Vienna, pp 3-23.

Benes, P. (1990). Radium in (continental) surface water. The Environmental Behaviour of Radium, Vol. 1, pp 373-418, IAEA, Vienna.

Benes, P., Obdrzalek, M. and Cejchanova, M. (1982). The physiochemical forms of traces of radium in aqueous solutions containing chlorides, sulphates and carbonates. Radiochemical and Radioanalytical Letters **50**, pp 227-242.

Benes, P., Strejc, P., and Lukavec, Z. (1984). Interaction of radium with freshwater sediments and their mineral components. I. Ferric hydroxide and quartz. Journal of Radioanalytical and Nuclear Chemistry Articles **82/2**, pp 275-285.

Benes, P., Borovec, Z., and Strejc, P., (1985). Interaction of radium with freshwater sediments and their mineral components. II. Kaolinite and montmorillonite. Journal of Radioanalytical and Nuclear Chemistry Articles **89/2**, pp 339-351.

Benes, P., Borovec, Z., and Strejc, P. (1986a). Interaction of radium with freshwater sediments and their mineral components. III. Muscovite and feldspar. Journal of Radioanalytical and Nuclear Chemistry Articles **98**, No. 1, pp 91-103.

Benes, P. and Strejc, P. (1986b). Interaction of radium with freshwater sediments and their mineral components. IV. Wastewater and riverbed sediments. Journal of Radioanalytical and Nuclear Chemistry Articles **99**, No. 2, pp 407-422.

Bollinger, M.S. and Moore, W.S. (1984). Radium fluxes from a salt marsh. Nature, **309**, pp 444-446.

Bondietti, E.A. (1974). Adsorption of plutonium(IV) and thorium(IV) by soil colloids. Agronomy Abstracts.

Choppin, G.R. (1987). Humics and radionuclide migration. Radiochimica Acta, **44/45**, pp 23-28.

Cochran, J.K. (1979). The flux of ^{226}Ra from deep-sea sediments. Earth and Planetary Science Letters, **49**, pp 381-392.

Cooper, M.B. and Wilkes, M.J. (1981). An analytical method for radium (^{226}Ra) in environmental samples by the use of liquid scintillation counting. Australian Radiation laboratory, Yallambie, Victoria. ARL/TR040.

Dickson, B.L. (1985). Radium isotopes in saline seepages, south-western Yilgarn, Western Australia. Geochimica et Cosmochimica Acta, **49**, pp 361-368.

Dickson, B.L. (1990). Radium in groundwater. The Environmental Behaviour of Radium, Vol. 1, pp 335-371, IAEA, Vienna.

Elsinger, R.J. and Moore, W.S. (1980). ^{226}Ra behaviour in the Pee Dee River-Winyah Bay estuary. Earth and Planetary Science Letters, **48**, pp 239-249.

Elsinger, R.J. and Moore, W.S. (1983). ^{224}Ra, ^{228}Ra and ^{226}Ra in Winyah Bay and Delaware Bay. Earth and Planetary Science Letters, **64**, pp 430-436.

Elsinger, R.J. and Moore, W.S. (1984). ^{226}Ra and ^{228}Ra in the mixing zones of the Pee Dee River-Winyah Bay, Yangtze River and Delaware Bay estuaries. Estuarine, Coastal and Shelf Science, **18**, pp 601-613.

Fleischer, R.L. (1982). Alpha-recoil damage and solution effects in minerals: uranium isotopic disequilibrium and radon release. Geochimica et Cosmochimica Acta, **46**, pp 2191-2201.

Gee, G.W. and Bauder, J.W. (1986). Particle size analysis. In "Methods of Soil Analysis." Part 1, Arnold Klute, Editor; pp 383-409. Madison, Winconsin, USA.

Gibbs, R.J. and Konwar, L. (1986). Coagulation and settling of Amazon River suspended sediment. Continental Shelf Research, **6**, No. 1/2, pp 127-149.

Gillman, G.P. (1979). A proposed method for the measurement of exchange properties of highly weathered soils. Australian Journal of Soil Research, **17**, pp 129-139.

Hancock, G.J. and Martin, P. (1991). The determination of radium in environmental samples by alpha-particle spectrometry. International Journal of Applied Radiation and Isotopes, **42**, No.1, pp 63-69.

Harmsen, K., and de Haan, F.A.M (1980). Occurrence and behaviour of uranium and thorium in soil and water. Netherlands Journal of Agricultural Science, **28**, pp 40-62.

Havlik, B., Nycova, B. and Grafova, J. (1967). Radium-226 liberation from uranium ore processing mill waste solids and uranium rocks into surface streams - I. The effect of different chemical compositions of surface waters. Health Physics, **14**, pp 423-430.

Helz, G.R., Setlock, G.H., Cantillo, A.Y. and Moore, W.S. (1985). Earth and Planetary Science Letters, **76**, pp 23-34.

Hunter, K.A., Hawke, D.J. and Lee Kwee Choo (1987). Equilibrium adsorption of thorium by metal oxides in marine electrolytes. Geochimica et Cosmochimica Acta, **52**, pp 627-636.

Ivanovich, M. and Harmon, R.S. (Eds) (1982). Uranium Series Disequilibrium: Applications to Environmental Problems, Clarendon, Oxford.

Joshi, L.U., Zingde, M.D. and Abidi, S.A.H. (1983). Thorium series disequilibrium and geochemical processes in estuarine sediments of Mandovi River. Journal of Radioanalytical Chemistry, **77**, No.1, pp 57-64.

Key, R.M., Stallard, R.F., Moore, W.S. and Sarmiento, J.L. (1985). Distribution and flux of ^{226}Ra and ^{228}Ra in the Amazon River estuary. Journal of Geophysical Research, **90**, No. C4, pp 6995-7004.

Kigoshi, K. (1971). Alpha-recoil ^{234}Th: dissolution into water and the $^{234}U/^{238}U$ disequilibrium in nature. Science, **173**, pp 47-48.

Knauss, K.G., Ku, T-L., Moore, W.S. (1978). Radium and thorium isotopes in the surface waters of the east Pacific and coastal southern California. Earth and Planetary Science Letters, **39**, pp 235-249.

LaFlamme and Murray (1987). Solid/solution interaction: The effect of carbonate alkalinity on adsorbed thorium. Geochimica et Cosmochimica Acta, **51**, pp 243-250.

Langmuir, D. and Herman, J.S. (1980). The mobility of thorium in natural waters at low temperatures. Geochimica et Cosmochimica Acta, **44**, pp 1753-1766.

Langmuir, D., and Riese, A.C (1985). The thermodynamic properties of radium. Geochimica et Cosmochimica Acta, **49**, pp 1593-1601.

Lesh, R.H. (1975). The geology and geochemistry of the Candelo-Bega Region New South Wales. Honours thesis, Department of Geology, Australian National University, 1975.

Levy, D.M. and Moore, W.S. (1985). ^{224}Ra in Continental Shelf waters. Earth and Planetary Science Letters, **73**, pp 226-230.

Li, Y.H. and Chan, L.H. (1979). Desorption of Ba and ^{226}Ra from river-borne sediments in the Hudson estuary. Earth and Planetary Science Letters, **43**, pp 343-350.

Li, Y.H., Mathieu, G., Biscaye, P. and Simpson, H.J. (1977). The flux of ^{226}Ra from estuarine and continental shelf sediments. Earth and Planetary Science Letters, **37**, pp 237-241.

Li, Y.H., Burkhardt, L., Buchholtz, M., O'Hara, P., and Santschi, P.H. (1984). Partition of radiotracers between suspended particles and seawater. Geochimica et Cosmochimica Acta, **48**, pp 2011-2019.

Mackay, N., Hillman, T. and Rolls, J. (1988). Water quality of the River Murray, review of monitoring 1978 to 1986. Water quality report No.1, Murray-Darling Basin Commission, Canberra, A.C.T. Australia, July 1988.

Macumber, P.G. (1991). Interactions between groundwater and surface water systems in northern Victoria. Department of Conservation and Environment, Victoria, Australia, 1991.

Martin, P. and Hancock, G. (1992). Routine analysis of naturally occurring radionuclides in environmental samples by alpha-particle spectrometry. Research Report 7, Supervising Scientist for the Alligator Rivers Region, AGPS, Canberra.

McKee, B.A., DeMaster, D.J. and Nittrouer, C.A. (1986). Temporal variability in the partitioning of thorium between dissolved and particulate phases on the Amazon shelf: implications for the scavenging of particle-reactive species. Continental Shelf Research, **6**, No.1/2, pp 87-106.

Megumi, K. and Mamuro, T. (1977). Concentration of uranium series nuclides in soil particles in relation to their size. Journal of Geophysical Research, **82**, No.2, pp 353-356.

Molinari, J. and Snodgrass, W.J. (1990). The chemistry and radiochemistry of radium and the other elements of the uranium and thorium natural decay series. In "The Environmental Behaviour of Radium", Vol.1, pp 11-55, IAEA, Vienna.

Moore, D.G., and Scott, M.R. (1986). Behaviour of ^{226}Ra in the Mississippi River mixing zone. Journal of Geophysical Research, **91**, No. C12, pp 14317-14329.

Moore, W.S. (1967). Amazon and Mississippi River concentrations of uranium, thorium and radium isotopes. Earth and Planetary Science Letters, **2**, pp 231-234.

Moore, W.S. (1981). Radium isotopes in Chesapeake Bay. Estuarine Coastal and Shelf Science, **12**, pp 713-723.

Moore, W.S. (1990). Radium isotopes in estuaries and coastal water. The Environmental Behaviour of Radium, Vol. 1, pp 419-428, IAEA, Vienna.

Moore, W.S. and Edmond, J.M. (1984). Radium and barium in the Amazon River system. Journal of Geophysical Research, **89**, No.C2, pp 2061-2065.

Murkes, J. (1967). The influence of different factors on the result obtained by centrifugal separation of mineral oils. Gas and Oil Power, July/August Issue.

Murray, A.S., Marten, R. Johnston, A. and Martin, P. (1987). Analysis of naturally occurring radionuclides at environmental concentrations by gamma spectrometry. Journal of Radioanalytical and Nuclear Chemistry Articles, **115**, pp 263-288.

Murray, A.S., Caitcheon, G., Olley, J.M. and Crockford, H. (1990). Methods for determining the sources of sediment reaching reservoirs: targeting soil conservation. ANCOLD Bulletin, **85**, pp 61-70.

Murray, A.S., Olley, J.M. and Wallbrink, P.J. (1991). Radionuclides for analysis of sediments in water supply catchments. Division of Water Resources, Consultancy Report 91/8, CSIRO, Canberra, Australia.

Murray, A.S., Johnston, A., Martin, P., Hancock, G., Marten, R. and Pfitzner, J. (1992a). Transport of naturally occurring radionuclides in the surface waters of the magela Creek and Flood plain, Northern Australia. Open File Record 93, Supervising Scientist for the Alligator Rivers Region, AGPS, Canberra.

Murray, A.S., Olley, J.M. and Wallbrink, P.J. (1992b). Natural radionuclide behaviour in the fluvial environment. Radiation Protection Dosimetry, **45**, pp 285-288.

Nishiwaki, Y., Honda, Y., Kimura, Y., Morishima, H., Koga, T., Miyaguchi, Y. and Kawai, H. (1972). Behaviour and distribution of radioactive substances in coastal and estuarine waters. In "Radioactive Contamination of the Marine Environment", IAEA-SM-158/11, IAEA, Vienna, 1973.

Nozarki, Y., Horibe, Y. and Tsubota, H. (1981). The water column distributions of thorium isotopes in the western North Pacific. Earth and Planetary Science Letters, **54**, pp 203-216.

O'Connor, D.J. and Connolly, J.P. (1980). The effect of concentration of adsorbing solids on the partition coefficient. Water Research, **14**, pp 1517-1523.

Olley, J.M., Murray, A.S., Wallbrink, P.J., Caitcheon, G. and Stanton, R. (1990). The use of fallout nuclides as chronometers. Paper presented at Workshop on Quaternary dating, pp 51-55, Australian National University, Canberra, November 1990.

Olley, J.M., Murray, A.S., Mackenzie, D.H. and Edwards, K. (1993). Identifying sediment sources in a gullied catchment using natural and anthropogenic radioactivity. Water Resources Research, **29**, No. 4, pp 1037-1043.

Ongley, E.D. and Blachford, D.P. (1982). Application of continuous flow centrifugation to contaminant analysis of suspended sediment in fluvial systems. Environmental Technology Letters., **3**, pp 219-228.

Osmond, J.K. and Cowart, J.B. (1982). Ground Water. In "Uranium Series Disequilibrium: Applications to Environmental Problems." Ivanovich, M. and Harmon, R.S. (Eds), Clarendon Press, Oxford.

Santschi, P.H., Li, Y.H. and Bell, J. (1979). Natural radionuclides in the water of Narragansett Bay. Earth and Planetary Science Letters, **45**, pp 201-213.

Sayles, F.L. and Mangelsdorf, P.C. (1977). The equilibration of clay minerals with seawater: exchange reactions. Geochimica and Cosmochimica Acta, **41**, pp 951-960.

Schell, W.R. and Sibley T.H. (1982). Distribution coefficients for radionuclides in aquatic environments, Final summary report, NUREG/CR-1869, 21 pp. U.S NRC Washington, D.C.

Scholkovitz, E.R., Boyle, E.A. and Price, N.B. (1978). The removal of dissolved humic acids and iron during estuarine mixing. Earth and Planetary Science Letters, **40**, pp 130-136.

Scott, M.R. (1968). Thorium and Uranium concentrations and isotope ratios in river sediments. Earth and Planetary Science Letters, **4**, pp 245-252.

Scott, M.R. (1982). The chemistry of U and Th series nuclides in rivers. In "Uranium Series Disequilibrium: Applications to Environmental Problems." Ivanovich, M. and Harmon, R.S. (Eds), Clarendon Press, Oxford.

Serne, R.J. and Relyea, J.F. (1981). The status of radionuclide sorption-desorption studies performed by the WRIT program. Rep. PNL-3977, Battele Pacific Northwest Laboratories, Richland, WA.

Somayajulu, B.L.K. and Church, T.M. (1973). Radium, thorium and uranium isotopes in the interstitial water from the Pacific Ocean sediment. Journal of Geophysical Research, **78**, No. 21, pp 4529-4531.

Wahlgren, M.A. and Orlandini, K.A. (1982). Comparison of the geochemical behaviour of plutonium, thorium and uranium in selected North American lakes. IAEA-SM-257/89.

Walling, D.E. and Kane, P. (1984). Suspended sediment particles and their geomorphological significance. In "Catchment Experiments in Fluvial Geomorphology", edited by T.P. Burt and D.E. Walling, pp 311-334, Geo Books, Norwich, 1984

Webster, I.T. and Taylor, J.H. (1992). Rotational dispersion in porous media due to fluctuating flows. Water Resources Research, **28**, No.1, pp 109-119.

Webster, I.T., Hancock, G.J. and Murray, A.S. (1993). On the use of radium isotopes to examine pore water exchange in an estuary. Submitted to Limnology and Oceanography.

Williams, A.R. (1985). Liquid scintillation counting of radon from a radium-226 sample digested in the vial. 'Measurement of Long-lived Environmental Radionuclides', Workshop proceedings, pp 60-73, Supervising Scientist for the Alligator Rivers Region, Sydney, Australia, 1985.